THE MECHANISM OF PRL-3 SIGNALLING UNDER CELLULAR STRESS

YE ZU

(BSc, Zhejiang University, P. R. China)

A THESIS SUBMITTED FOR THE DEGREE OF

DOCTOR OF PHILOSOPHY

DEPARTMENT OF PHYSIOLOGY

NATIONAL UNIVERSITY OF SINGAPORE

2015

DECLARATION

I hereby declare that this thesis is my original work and it has been written by me in its entirety. I have duly acknowledged all the sources of information which have been use in the thesis.

This thesis has also not been submitted for any degree in any university previously.

Ye Zu

18 Aug 2015

Acknowledgements

I would like to take this opportunity to express my most sincere and utmost appreciation to my supervisor in IMCB, Prof. Zeng Qi, for her unending encouragement, support, and professional guidance throughout these four years. Her enthusiasm and dedication to science have inspired me deeply, and left an indelible mark on my maturation process. I would also like to extend my deepest gratitude to my supervisor in NUS, A/Prof. Shen Han-Ming. His expertise in mTOR signalling, coupled with his willingness to always share research reagents, contributed invaluably to this work. Without question, my achievements would not have been possible without their excellent guidance and persistent help.

Special mention also goes to my thesis advisory committee members, Prof. Vinay Tergaonkar, and Prof. Philipp Kaldis, for their useful suggestions and continuous support on my study.

Over the past four years, I have forged special connections with my ZQ lab colleagues and must extend a well-deserved thanks to each. To our lab manager, Ms. Li Jie, for her ensuring a superb and efficient lab environment; to my mentors, Dr. Jung Eun Park, for all the useful techniques and helpful suggestions I learnt from her, and Dr. Abdul Qader Al-Aidaroos, for always providing instructive suggestions and criticism for my experimental results and scientific writing; to Dr. Thura Min, for the kind help and guidance on my mouse work; and to Dr. Sitaram Harihar, Dr. Lin You Bin, Dr. Huang Yun Han, Dr. Guo Ke, Dr. Yuen Hiu-Fung (Eric), Ms. PeiLing Chia, and Mr. Abhishek Gupta for being there for me when I needed any help or advice. Finally, to Dr. Low Kee Chung, thanks for the intellectual humor and razor-sharp wit which keeps me going when things might have looked bleak.

Beyond our lab, I sincerely extend my appreciation to the members from Prof. Shen's lab, including Dr. Shi Yin and Dr. Ng Shukie for the discussion, kind help, and support for my study. And to Dr. Yang Naidi, Mr. Ong Yeong Bing, Mr. Zhang Jianbin, Dr. Cui Jianzhou, Dr. Zhou Zhihong, Ms. Mo Xiaofan, Mr. Wang Limin and Mr. Renyi – they made the duration of my PhD term very enjoyable and unforgettable.

IMCB holds a special place in my heart and as a training grounds, has taught me the importance of making scientific connection with my peers, intellectual debates, and having access to the best tools for my research. Also, as a student with the Department of Physiology, Yong Loo Lin School of Medicine, NUS, I am indebted for Research Scholarship granted to me. I am also grateful to all of my friends and colleagues form GSS-SoM, PGSS, ZUAAS, and also my apartment-mates Dr. Yang Ming and Mr. Zhang Xiang. I will always cherish the days spent with them.

Lastly, I would like to dedicate this thesis to my parents, grandparents, and girlfriend, for their understanding, support, and endless love. They are my pillars of strength and resolve – without whom it will not be possible for me to accomplish this work.

List of publications:

Ye, Z., Al-aidaroos, A.Q.O., Park, J.E., Yuen, H.F., Zhang, S.D., Gupta, A., Lin, Y., Shen, H.-M., and Zeng, Q. (2015). PRL-3 activates mTORC1 in Cancer Progression. Scientific Reports 5, 17046.

Presentation at scientific conferences:

1. **Ye Z**, Park JE, Shen HM and Zeng Qi. PRL-3 activates mTOR signalling pathway in cancer progression. Singapore. 2014 (Oral presentation) (Best Presentation Award)
2. **Ye Z**, Park JE, Shen HM and Zeng Qi. PRL-3 activates mTOR signalling pathway in cancer cells, YLLSOM 4th Annual Graduate Scientific Congress. Singapore. 2014 (Selected as oral presentation)

Table of Contents

Summary

Phosphatase of regenerating liver 3 (PRL-3), an oncogenic phosphatase, is known to exhibit pleiotropic effects in cancer progression, including promoting cell proliferation, sustaining cell survival, inducing angiogenesis, and enhancing invasion and metastasis. However, the signalling mechanisms of PRL-3 remain largely unknown. Here, PRL-3 was identified as a novel activator of mTOR. PRL-3 induced an aberrant activation of mTOR signalling in cancer cells, as reflected by hyperphosphorylation of the direct substrates of mTORC1, 4E-BP1 and p70S6K. Despite growth-suppressing limitations, PRL-3 persistently activated mTORC1 in the presence of oxygen, serum, or amino acid deprivation. Functionally, PRL-3-mediated activation of mTORC1 resulted in increased cell motility, invasiveness, and MMP-2/9 production, suggesting a novel pathway for PRL-3-mediated cancer progression via mTORC1 activation. In the second part of the study, the mechanism underlying PRL-3-driven mTORC1 activation was characterised. PRL-3 was found to use a two-pronged approach in activating mTORC1: 1) increasing Rheb-GTP accumulation via activation of AKT-TSC2 signalling, and 2) enhancing Rag GTPases-mediated mTORC1 recruitment to lysosomes for Rheb-mediated activation. Thus, PRL-3 leads to sustained and efficient mTORC1 activation under both normal and stressed conditions. This novel mechanism might explain how PRL-3 promotes cancer progression through the mTOR pathway.

Finally, a protective effect of PRL-3 against $CoCl_2$-induced apoptosis was reported. This was p38 MAPK-dependent and mechanistically involved dephosphorylation of the pro-apoptotic kinase.

The findings presented contribute to our understanding of PRL-3 signalling and highlight potential targets for therapeutic intervention in PRL-3-driven cancers.

LIST OF FIGURES

List of tables

List of abbreviations

4E-BP1	eukaryotic translation initiation factor 4E (eIF4E)-binding protein 1
AA-	amino acid starvation
Arf1	ADP-ribosylation factor 1
AML	acute myeloid leukemia
AMPK	adenosine monophosphate-activated protein kinase
AktiVIII	Akt inhibitor VIII
AOM	asazoxymethane
BafA1	Bafilomycin A1
CHO	Chinese hamster ovary
CRCs	colorectal carcinomas
Csk	C-terminal Src kinase
CM-H_2DCFDA diacetate	5-(and-6)-chloromethyl-2',7'-dichlorodihydrofluorescein
DUSPs	dual-specific protein phosphatase
DSS	dextran sodium sulfate
DTT	dithiothreitol
EBSS	Earle's Balanced Salt Solution
ECM	cell-extracellular matrix
EF2	elongation factor 2
EGFR	epidermal growth factor receptor
EMT	epithelial-mesenchymal transition
ERKs	extracellular-signal-regulated kinases
FAT	two focal adhesion targeting domains
FKBP38	FK506-binding protein 38
FRB	FKPB12-rapamycin binding domain

GAP	GTPase-activating protein
HCC	hepatocellular carcinoma
HDAC4	Histone deacetylase 4
HMVEC	human microvascular endothelial cells
HUVEC	human umbilical vascular endothelial cells
Hx	hypoxia
IGFR	insulin-like growth factor receptor
IHC	immunohistochemistry
IL-4	interleukin-4
IP	immunoprecipitation
IR	insulin receptor
JNKs	c-Jun N-terminal kinases
KRT8	Keratin 8
LAMTOR	lysosomal adaptor and MAPK and mTOR activator/regulator
LMPTPs	low molecular weight PTPs
MEF2C	myocyte enhancer factor 2C
MAPK	mitogen-activated protein kinase
MAPKKs	MAPK kinases
MAPKKKs	MAPKK kinases
MKP-1	MAPK phosphatase-1
MMP	matrix metalloproteinase
MMTV	mouse mammary tumour virus
mTORC	the mechanistic target of rapamycin complex
MVD	micro-vessel density
NCL	nucleolin
NF-κB	nuclear factor-κB

NSA	necrosulfonamide
NSCLS	non-small cell lung cancer
p70S6K	p70 S6 kinase
PAF	RNA polymerase II–associated factor
PARP	poly(ADP-ribose) polymerase
PCBP1	poly(C)-binding protein 1
PDK1	phosphoinositide dependent protein kinase 1
PIKK	PI3K-related kinase
PIP2	phosphatidylinositol-(4,5)-bisphosphate
PIP3	phosphatidylinositol-(3,4,5)-trisphosphate
PMA	phorbol 12-myristate 13-acetate
PMSF	phenylmethylsulfonyl fluoride
PRL	phosphatase of Regenerating Liver
PSPs	protein serine/threonine phosphatases
PTEN	phosphatase and tensin homologue
PTMs	post-translational modifications
qRT-PCR	quantitative Real Time-PCR
Rag	Ras-relate GTPase
RAP1	Repressor/Activator Protein 1
Rapa	rapamycin
RFS	relapse-free survival
Rheb	Ras homolog enriched in brain
ROCK	Rho-coiled coil kinase
RT	room temperature
RTKs	receptor tyrosine kinases
RT-PCR	Semi-quantitative

PTPs	protein tyrosine phosphatases
PTyr	dephosphorylating phosphotyrosine residues
PyMT	polyomavirus middle T oncoprotein
SF	serum-free
shRNA	small hairpin RNA
siRNA	small-interfering RNA
STAT3	signal transducers and activators of transcription 3
TGFβ	transforming growth factor β
TRP32	thioredoxin-related Protein 32
TSC	tuberous sclerosis complex
UTR	untranslated region
VEGF	vascular endothelial growth factor

CHAPTER 1: INTRODUCTION

1.1. Protein Tyrosine Phosphatases

Protein phosphorylation is a reversible post-translational modification discovered in the 1950s (Burnett and Kennedy, 1954; Krebs and Fischer, 1955). It plays a pivotal role in the regulation of various biological processes, including metabolism, cell growth, proliferation, differentiation, migration, motility, organelle trafficking, immunity, and apoptosis (Ubersax and Ferrell, 2007; Zhang, 2005). It has been estimated that as many as 30% of the cellular proteins encoded in the human genome are regulated by phosphorylation (Cohen, 2002). The regulation of protein phosphorylation is coordinated by kinases and phosphatases (Hardie, 1990). Protein kinases catalyze the transfer of a phosphate group from ATP to its protein substrate while protein phosphatases catalyze the removal of the phosphate group from the phosphoprotein to a water molecule (**Figure 1.1**).

Protein phosphatases consist of two large families: protein serine/threonine phosphatases (PSPs) and protein tyrosine phosphatases (PTPs). The PSP family contains around 30 members (Shi, 2009) while the PTP superfamily is comprised of more than 100 members (Dewang et al., 2005). The first protein tyrosine phosphatase, PTP1B, was isolated and characterized in the late 1980s (Tonks et al., 1988). Subsequently, the family of PTPs grew extensively and 107 members were identified (Alonso et al., 2004). All these PTPs contain an active site motif $C(X)_5R$ (where X represents any amino acid) in the catalytic domain, which is termed the phosphate-binding loop (P-loop) or PTP signature motif. Despite high sequence variations in the $(X)_5$ segment, the consensus residues of cysteine and arginine result in a strictly conserved conformation of the P-loop (Tabernero et al., 2008). Besides the P-loop, the flexible general acid/base motif (known as WPD-loop) is another conserved feature of PTPs (Zhang and Bishop, 2008).

These two motifs are required for PTP-mediated catalysis. Generally, the enzymatic reaction of PTPs occurs in two distinct steps. In the first step, the cysteine of the P-loop carries out a nucleophilic attack on a phosphorous atom of the substrate, creating a cysteinyl-phosphate intermediate, while the catalytic aspartate in the WPD-loop functions as a general acid, donating a proton to the oxygen of the leaving group. In the second step, the same aspartate acts as a general base and facilitates the hydrolysis of the intermediate by deprotonating a water molecule, leading to a release of inorganic phosphate and the regeneration of the free enzyme (Zhang, 2003).

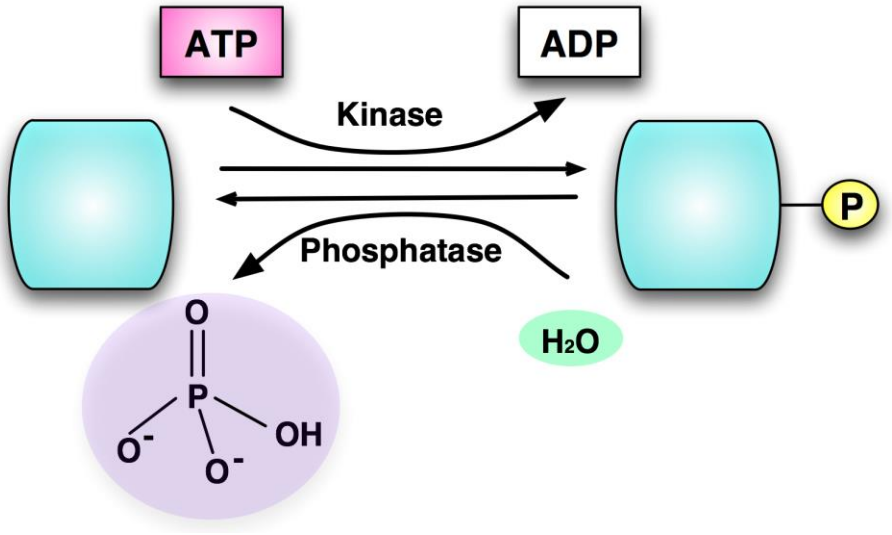

Figure 1. 1 PPs and PKs maintain homeostasis of protein phosphorylation

Based on the amino acid composition of catalytic domains and substrate specificity, PTPs can be classified into four separate subfamilies: class I cysteine-based PTPs, low molecular weight PTPs (LMPTPs), CDC25 phosphatases and Asp-Based PTPs (Alonso et al., 2004). Class I cysteine-based PTPs are the largest subfamily, consisting of about hundred PTPs, including 38 well-known classical PTPs that are tyrosine specific, and 61 dual-specific protein phosphatase (DUSPs) which exhibit high diversity in structure, function, and substrate specificity. Unlike classical PTPs which only dephosphorylate

phosphotyrosine residues (PTyr), DUSPs can also dephosphorylate phosphoserine/threonine residues (PSer/PThr), mRNAs, and phosphoinositides (Alonso et al., 2004).

1.2. Phosphatase of regenerating liver family

The Phosphatase of Regenerating Liver (PRL) family is a unique class of DUSPs. It consists of three members: PRL-1，PRL-2, and PRL-3 (also known as PTP4A1, PTP4A2, and PTP4A3 respectively). PRL-1 is the first member to be identified as an immediate-early gene highly upregulated in regenerating rat liver after partial hepatectomy (Diamond et al., 1994; Mohn et al., 1991). Subsequently, *in-vitro* prenylation screening and database search for PRL-1 homologues led to the identification of PRL-2 and PRL-3 (Cates et al., 1996; Zeng et al., 1998). In humans, PRL genes are located on different chromosomes, with *PRL-1*, *PRL-2*, and *PRL-3* localized on chromosomes 6q12, 1p35, and 8q24.3 respectively. They code for three small phosphatases of around 20kDa, 167 amino acid long for PRL-2, and 173 amino acid long for both PRL-1 and PRL-3 (Kozlov et al., 2004). These three PRLs exhibit significant amino acid sequence homology: 87% between PRL-1 and PRL-2, 79% between PRL-1 and PRL-3, and 76% between PRL-2 and PRL-3 (**Figure 1.2A**).

Besides primary sequence homology, PRLs also display a high similarity in structural and domain features (Rios et al., 2013) (**Figure 1.2B**). All of them contain the core PTP domain, which is made up of the WPD-loop and the P-loop in the N terminus. The WPD-loop of PRLs has the conserved sequence WPFDD, which is important for substrate recognition and binding. The P-loop of PRLs contains a CVAGLGR motif, which is responsible for enzymatic activity. Unlike other PTPs, PRLs have a prenylation motif (also known as the CAAX box) at the C terminus. The presence of this motif makes

them the only PTPs known to be prenylated (Zeng et al., 1998). Near the C terminus of PRLs, there is another motif called the polybasic region (K/R/K/R/R/K), which is thought to be involved in prenylation by supplying positive charges (Sun et al., 2007). Protein prenylation is a post-translational lipid modification involving the covalent addition of either farnesyl or geranylgeranyl isoprenoids to the cysteine residue(s) in the CAAX box. This modification is critical for proper function of the CAAX proteins, particularly for anchorage to the cellular membrane system (Gao et al., 2009).

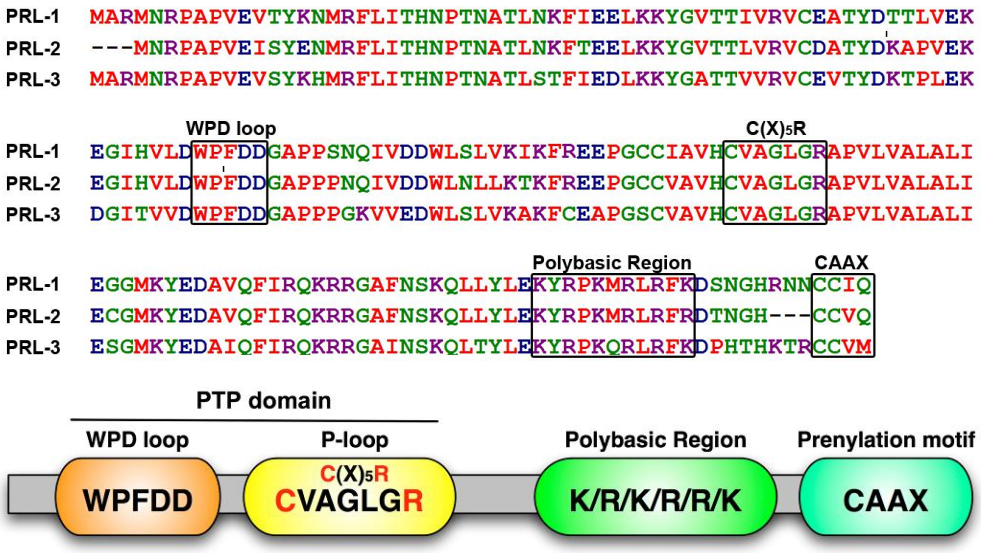

Figure 1. 2 Amino Acid Sequence Alignment and motifs of Human PRLs.

(A): Amino acid sequences of human PRLs. The WPD loop motif, $C(X)_5R$ motif, polybasic region and the CAAX prenylation motif are boxed in the amino acid sequences. (B): Structural model of human PRLs. Key motifs are marked.

In agreement with this finding, most PRLs localize to the intracellular membrane and early endosomes. Blocking prenylation by treatment with FTase inhibitors or deletion of the CAAX box leads to nuclear localization of the PRLs.(Zeng et al., 2000). Notably, PRL-1 and PRL-3 are expressed in the nucleus under specific conditions or in particular tissues (Bessette et al., 2008; Diamond et al., 1994; Fagerli et al., 2008; Kong et al., 2000; Liu et al., 2013). The localization of PRL1 and PRL-3 might be cell-cycle dependent.

Wang *et al* showed that in HeLa human cervical cancer cells, PRL-1 localizes to the endoplasmic reticulum in non-mitotic cells and to the centrosomes and spindle apparatus in mitotic cells (Wang et al., 2002). Similarly, a recent study in OH-2 human myeloma cells has also been reported that PRL-3 could shuttle between the nucleus and cytoplasm during cell cycle progression (Fagerli et al., 2008). In G0/G1 phase, overexpressed PRL-3 is mainly found in the nucleus, while in G2M phase, overexpressed PRL-3 is predominantly observed in the cytoplasm, implying the importance of PRL-3 in cell cycle progression.

In normal tissues, the PRLs have distinct expression patterns. *In situ* hybridization analysis reveals that PRL-1 mRNA is widely expressed in various human tissues, particularly in the small intestine, lung, oviduct, testis, gallbladder, T-lymphocytes, and adipocytes (Dumaual et al., 2006). Similarly, high levels of PRL-2 mRNA are nearly ubiquitous in human tissues, being absent only in taste buds and highly specialized fibrocartilage tissues (Dumaual et al., 2006). This widespread mRNA expression of PRL-1 and PRL-2 indicates that they may be implicated in basic processes common to most tissues and cell types. However, the protein expression patterns of PRL-1 and PRL-2 remain largely unknown due to the lack of highly sensitive antibodies. Unlike these two proteins, the expression of PRL-3 is much more restricted. Northern blot analysis demonstrated that PRL-3 mRNA expression is primarily observed in the heart, skeletal muscle, and pancreas (Matter et al., 2001). Intriguingly, PRL-3 protein is detected in the fetal heart, developing vasculature, and pre-erythrocytes, but not in their mature counterparts (Guo et al., 2006). These observations suggest a potential role for PRL-3 in cardiovascular development and a tissue and temporal specific regulation of PRL-3 expression.

1.3. Regulation of PRL-3

Despite being the last of the PRLs discovered, PRL-3, so far, is the most attractive and well-characterized PRL member. Several reports have shown PRL-3 expression is regulated at multiple levels, including DNA, RNA and protein levels **(Figure 1.3)**.

In most cases, the human *PRL-3* is a single-copy gene, which is located on the long arm of chromosome 8 and spans 9613 nucleotides. However, elevated copy numbers of *PRL-3* have also been reported in colorectal cancer with liver metastasis, and in some myeloma cell lines (Bardelli et al., 2003; Buffart et al., 2005; Fagerli et al., 2008). This copy number amplification was initially thought to be responsible for the high expression of PRL-3 in cancers. However, a recent study demonstrates that there is no significant correlation between PRL-3 gene amplification and mRNA expression, indicating PRL-3 expression may be strictly regulated at the transcriptional level (Fagerli et al., 2008).

The first evidence in support of this is the identification of p53 as a transcriptional regulator of PRL-3. p53 can directly bind to PRL-3 and activate its transcription in both human and mouse cell lines (Basak et al., 2008). Subsequently, several other transcription factors of PRL-3 as well as their corresponding functional promoter binding sites in *PRL-3* gene were identified (Park et al., 2013a; Xu et al., 2011; Zheng et al., 2011; Zhou et al., 2011). These factors include Snail, myocyte enhancer factor 2C (MEF2C), signal transducers and activators of transcription 3 (STAT3), and STAT5A. They show great specificity and ability to drive PRL-3 expression. In addition, extracellular stimuli transduced through growth factor signaling pathways can also affect PRL-3 transcription. Treating cells with conditioned media from carcinoma-associated fibroblasts or with mitogenic cytokines such as IL-6, TNF, and IL-21, lead to an increased expression of PRL-3 (Fagerli et al., 2008; Mollevi et al., 2009; Rouleau et al., 2006). On the other hand, suppression of PRL-3 mRNA expression has also been observed. Specifically,

transforming growth factor β (TGFβ) inhibits PRL-3 transcription by enhancing the binding of Smad transcription factors to PRL-3 promoter sequence, suggesting an important role of transcriptional regulation in the expression of PRL-3 (Jiang et al., 2011).

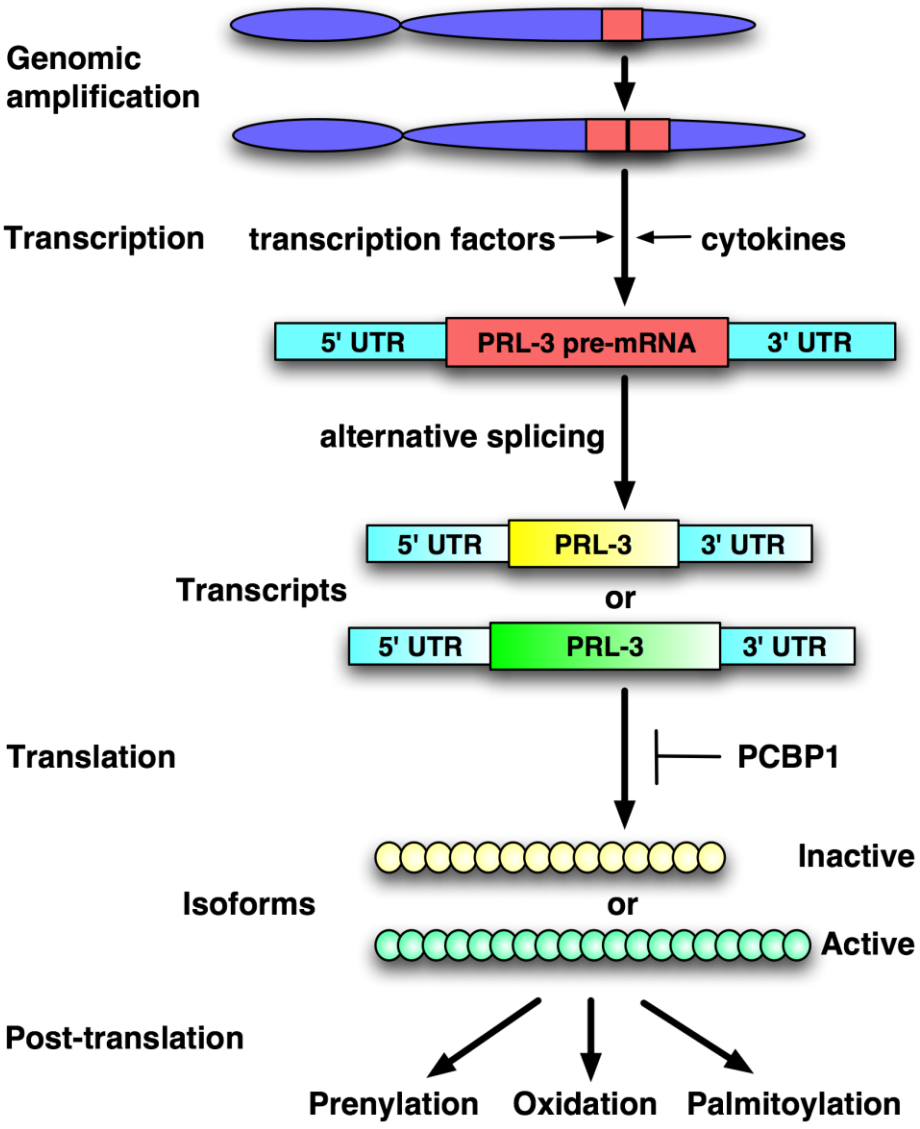

Figure 1. 3 The regulation of PRL-3 at multiple levels.

PRL-3 is regulated by genetic amplification, RNA transcription and splicing, protein translation, and post-translational mechanisms.

No strict correlation has been found between PRL-3 mRNA and protein levels in cancer cell lines, implying that the regulation of PRL-3 also occurs at the translational level (Wang et al., 2010). PRL-3 pre-mRNA has 5 exons and alternative splicing of exon 4 generates two different transcripts, resulting in two PRL-3 protein isoforms (Kozlov et al., 2002). Compared to the full-length PRL-3 protein, the spliced variant contains only 148 amino acids and showed no phosphatase activity (Kozlov et al., 2004). In the 5'-untranslated region (5'-UTR) of PRL-3 mRNA, there are three GC-motifs (GCCCAG), which can be recognized and bound by the poly(C)-binding protein 1 (PCBP1). PCBP1 is an RNA binding protein that has multiple functions, including mRNA stabilization and translational silencing (Choi et al., 2009). The binding of PCBP1 to the GC-motifs leads to the suppression of PRL-3 protein translation (Wang et al., 2010).

PRL-3 protein is also regulated by post-translational modifications (PTMs). PTMs refer to the covalent modification of proteins, which have a key role in determining protein structure, destination, activity, stability, and function (Wani et al., 2015). At present, three PTMs of PRL-3, prenylation, oxidation, and palmitoylation, have been characterized. As mentioned previously, the CAAX box of PRL-3 is subjected to prenylation. However, in contrast to other PRL members, PRL-3 can only be modified by farnesylation but not geranylgeranylation (Zeng et al., 2000). The former modification is necessary for proper localization and enzymatic activity of PRL-3 (Fiordalisi et al., 2006; Zeng et al., 2000). Additionally, just like the other PTPs, PRL-3 can also be oxidized. Upon oxidation, PRL-3 has been shown to lose its catalytic activity (Kozlov et al., 2004). Two possible mechanisms for the observed oxidative inactivation of PRL-3 have been proposed: i) the formation of a disulfide bond between the catalytically-active cysteine (Cys104) and conserved cysteine (Cys49), and ii) the conversion of the catalytically-active cysteine (Cys104) to catalytically-inactive glycine, resulting in the

loss of PRL-3 function (Orsatti et al., 2009). Besides these modifications, palmitoylation of PRL-3 has also been reported. However, the mechanism and function of PRL-3 palmitoylation needs to be further validated (Nishimura and Linder, 2013).

1.4. The implication of PRL-3 in cancer progression

Today, PRL-3 is best known for its involvement in cancer. Many types of cancer exhibit highly upregulated expression of PRL-3 and mounting evidence suggests this elevated PRL-3 expression is implicated in multiple processes of cancer progression, including promoting proliferation, resisting cell death, inducing angiogenesis, and inducing invasion and metastasis (**Figure 1.4**). In the following sections, the detailed biological roles of PRL-3 in cancer progression will be reviewed.

1.4.1. PRL-3 expression in human cancers

In 2001, PRL-3 was first identified as the only gene whose expression was dramatically upregulated in metastases from colorectal carcinomas (CRCs) while being undetectable in normal colon epithelia (Saha et al., 2001). Subsequently, this finding was confirmed by several groups who found that 11-45% of primary CRCs were PRL-3 positive and CRC metastases showed a high expression level of PRL-3 (Bardelli et al., 2003; Hatate et al., 2008; Kato et al., 2004; Li et al., 2005; Mollevi et al., 2008; Peng et al., 2004; Wang et al., 2007c). Later, the prevalence of PRL-3 in diverse types of cancers and metastases was reported, including gastric cancer (Bilici et al., 2012; Hu et al., 2013; Xing et al., 2013), breast cancer (Hao et al., 2010; Radke et al., 2006; Ustaalioglu et al., 2012; Wang et al., 2006), nasopharyngeal carcinoma (Zhou et al., 2009), liver carcinoma (Wu et al., 2004), ovarian cancer (Huang et al., 2014; Ren et al., 2009), uveal melanoma (Laurent et al., 2011), intrahepatic cholangiocarcinoma (Xu et al., 2010), esophageal

squamous cell carcinoma (Liu et al., 2008b; Ooki et al., 2010), oral squamous cell carcinoma (Hassan et al., 2011), and endometrioid cancer (Guzinska-Ustymowicz et al., 2013). These reports revealed that PRL-3 can promote advanced stage disease and/or metastasis in cancer and its expression correlated with poor overall survival in a number of examined cancers, indicating PRL-3 may be highly involved in tumour progression.

1.4.2. PRL-3 promotes cell proliferation

The ability to chronically proliferate is an important characteristic of cancer cell malignancy (Hanahan and Weinberg, 2011). Following the discovery of the role for PRL-1 in liver cell proliferation (Diamond et al., 1996), PRL-3 was also found to be involved in sustaining proliferation in HEK293 human embryonic kidney cells (Matter et al., 2001). HEK293 cells expressing PRL-3 grew at a faster rate compared to the cells expressing vector control or inactive PRL-3 mutant (C104S). This growth rate could be reduced by inhibition of PRL-3 with PTPase inhibitors, confirming the requirement of phosphatase activity for PRL-3 mediated enhancement of cell proliferation. Furthermore, in vivo xenograft mouse models injected with B16 melanoma cells overexpressing PRL-3 showed almost a 3-fold increase in tumour volume compared to control cells (Wu et al., 2004). Similarly, ectopic PRL-3 expression in SW480 human colon adenocarcinoma, TE5 human esophageal squamous carcinoma, LoVo human colorectal adenocarcinoma, TF1 human acute myeloid leukemia, and A2780 human ovarian carcinoma cells, enhanced their proliferative ability (Huang et al., 2014; Lai et al., 2011; Ooki et al., 2010; Park et al., 2013a; Semba et al., 2010). Conversely, suppression of endogenous PRL-3 by RNA interference severely impaired cell proliferation in various human ovarian, lung, gastric, esophageal, colorectal, and leukemia cancer cell lines (Matsukawa et al., 2010; Ming et al., 2009; Ooki et al., 2010; Park et al., 2013a; Polato et al., 2005; Semba et al., 2010; Wang et al., 2008; Zhou et al., 2012a).

However, our understanding of the precise mechanism(s) by which PRL-3 promotes cell proliferation is still limited. It has been reported that overexpression of PRL-3 in HEK293 cells activated Src kinase via suppression of C-terminal Src kinase (Csk), a negative regulator of Src (Liang et al., 2008). Furthermore, these observations were also confirmed in SW480 colon cancer cells in comparison with their SW620 counterparts that possess low PRL-3 levels; SW480 had increased Src activity and low Csk expression. Activation of Src initiates a number of downstream signaling pathways that enhance cell proliferation (Liang et al., 2007). One of these pathways involves the STAT3 signaling cascade. STAT3, a transcription factor widely implicated in cell proliferation, migration and invasion, is activated upon PRL-3 expression (Yu et al., 2014). Upon activation, STAT3 induces the expression of several microRNAs, such as miR-21, miR-17, and miR-19a, which contribute to increased cell proliferation (Zhang et al., 2012b). Another downstream signaling pathway involved in PRL-3-mediated upregulation of cell proliferation is the nuclear factor-κB (NF-κB) pathway. NF-κB is a protein complex found in a vast majority of animal cell types and controls DNA transcription (Jing and Lee, 2014). PRL-3 overexpression in LoVo colon cancer cells upregulates the expression of KCNN4 in a NF-κB-dependent manner, thereby enhancing cellular proliferative ability. Furthermore, PRL-3-induced cell proliferation in LoVo cells was significantly reduced upon treatment with specific KCNN4 inhibitor (Lai et al., 2011). Recently, PRL-3 was reported to drive cell proliferation in an autophagy dependent manner. Blocking autophagy by the knockdown of critical autophagy regulators or treatment with chloroquine reduces the ability of PRL-3 to drive cell proliferation in A2780 ovarian cancer cells, implying PRL-3 requires a functional autophagy pathway to promote cancer proliferation (Huang et al., 2014).

A few reports have also surfaced showing no significant role for PRL-3 in cellular proliferation. In DLD-1 human colorectal adenocarcinoma and A431 human epithelial carcinoma cells, no significant differences in cell proliferation were observed upon PRL-3 overexpression (Al-Aidaroos et al., 2013; Rouleau et al., 2006). Furthermore, in B16-BL6 mouse melanoma , HCT116 human colon carcinoma, INA-6 human myeloma, 5-8F, and HONE1 human nasopharyngeal carcinoma cells**,** knockdown of PRL-3 failed to have any obvious effect on their proliferative ability (Fagerli et al., 2008; Polato et al., 2005; Qian et al., 2007; Zhou et al., 2009). Moreover, in SGC-7901 human gastric cancer cells, contrasting data on the role of PRL-3 in regulating cell proliferation further cloud our understanding (Li et al., 2006; Sun and Bu, 2012; Wang et al., 2008).

Taken collectively, although there is mounting evidence that PRL-3 promotes cell proliferation, there is still controversy over whether that role is cell type-specific.

1.4.3. PRL-3 resists cell death

A distinguishing trait of cancer cells is its innate ability to resist cell death and survive in harsh conditions. Apoptosis, a well-known programmed cell death, is essential for normal biological development and for maintenance of tissue homeostasis. It serves as a natural barrier to cancer development (Hanahan and Weinberg, 2011). Physiological stress or internal genomic instability results in apoptosis of the normal cell. However, apoptosis can be disrupted when there is an abnormal expression of oncogenic proteins, leading to tumour initiation and progression (Lowe and Lin, 2000).

As an oncoprotein, PRL-3 plays an important role in inhibiting apoptosis of cancer cells. PRL-3 was firstly reported to attenuate 5-FU-induced apoptosis in HeLa human epithelial carcinoma cells. In this study, PRL-3 was shown to reduce p53 stability by upregulating

MDM2 and PIRH2, thereby inhibiting p53-mediated apoptosis (Min et al., 2010). Furthermore, depletion of endogenous PRL-3 with siRNA significantly enhances 5-FU-induced apoptosis in TE8, TE10, TE11, and TE14 human esophageal cancer cells (Ooki et al., 2010). Treatment with the PRL-3 inhibitor1-4-bromo-2-benzylidene rhodanine induced apoptosis in GCIY, AZ521, SH10, and MKN74 human gastric cancer cells. However, in normal skeletal muscle C2C12 cells, which highly express PRL-3, no effect was observed (Ooki et al., 2011). This implies PRL-3 expression levels alone are not responsible for the observed sensitivity to PRL-3 inhibitor treatment in normal cells, and the anti-apoptotic function of PRL-3 may be specific to tumour cells (Ooki et al., 2011). In line with this, treatment of SCG-7901 gastric carcinoma cells with another PRL-3 inhibitor, emodin, downregulated PRL-3 activity with a commensurate increase in apoptosis (Sun and Bu, 2012). Besides drug-induced apoptosis, apoptosis induced by other stresses, such as UV radiation and growth factor deprivation, was also attenuated in PRL-3 expressing FET and GEO human colon carcinoma cells. These cells maintained a high activated AKT level, which is believed to be associated with resistance to stress-induced apoptosis (Jiang et al., 2011). Similarly, an anti-apoptotic effect of PRL-3 was also detected in H1299 human lung cancer, TF-1, U937, and ML-1 human acute myeloid leukemia (AML) cells (Lian et al., 2012; Park et al., 2013a; Qu et al., 2014). TF-1 is a cytokine dependent leukemia cell line requiring additional supplementation of cytokines in culture media to sustain cell growth and survival. Lack of cytokine supplementation triggers apoptosis in TF-1 cells (Lin et al., 2007). Overexpression of PRL-3 was shown to promote cell growth and abrogate apoptosis in TF-1 cells upon cytokine deprivation, suggesting an anti-apoptotic role of PRL-3 in AML cells (Park et al., 2013a). This process is thought to be mediated by Leo1, a component of RNA polymerase II–associated factor (PAF) complex, which is induced upon ectopic PRL-3 expression. Abrogation of Leo1 removed the protective effect of PRL-3 toward cytokine

deprivation in TF-1 cells (Chong et al., 2014). Recently, it was reported that PRL-3 causes drug resistance, preventing the cancer cell from dying by apoptosis. Ectopic PRL-3 expression enhanced the anti-apoptotic machinery to prevent drug cytotoxicity, mainly resulting from the activation of STAT5 and AKT, indicating their involvement in PRL-3-mediated apoptosis evasion (Qu et al., 2014).

So far, our understanding of the mechanism involved in PRL-3-abrogated apoptosis is minimal. Several key signaling cascades involved in cell growth and survival, such as the p53 pathway, PI3K/AKT pathway, and STAT pathway have been reported to be aberrantly regulated upon PRL-3 overexpression. Interestingly, PRL-3 has also been reported to drive autophagy under starvation conditions in A2780 human ovarian cells (Huang et al., 2014). Autophagy is a self-degradation process that occurs in nutrient demanding conditions. It leads to increased stress tolerance and protects the cell from apoptosis via nutrient recycling (He and Levine, 2010). Thus, this PRL-3-mediated autophagy might be critical for its role in apoptosis abrogation. Collectively, PRL-3 inhibits apoptosis in a number of cancer cells, despite the lack of a precise molecular mechanism.

1.4.4. PRL-3 induces angiogenesis

During their growth, tumours require an excess amount of nutrients and oxygen, and they also need to eliminate metabolic wastes and carbon dioxide. These requirements are met by a process known as angiogenesis, an ability to form new blood vessels (Mittal et al., 2014). It is a normal and vital natural process in growth and development. In normal adult tissues, angiogenesis is largely quiescent or only transiently turned-on. However, during tumour progression, angiogenesis is constitutively activated, leading to a constant sprouting of new vessels. This provides the sustenance factors for expanding neoplastic growth (Hanahan and Weinberg, 2011).

Numerous studies have revealed a potential role of PRL-3 in the promotion of tumour angiogenesis. In human colorectal cancer patients, high PRL-3 levels were detected in the tumour vasculature, including the epithelium and smooth muscle cells, but not in normal tissues (Bardelli et al., 2003; Kato et al., 2004). Similarly, breast tumour vasculature also shows strikingly higher PRL-3 expression levels (Parker et al., 2004). In line with these observations, clinical statistical data reveal a significant association between PRL-3 mRNA expression and micro-vessel density (MVD) in human hepatocellular carcinoma (HCC) and non-small cell lung cancer (NSCLS), raising an intriguing question about the role of PRL-3 in tumour angiogenesis (Ming et al., 2009; Zhao et al., 2008). Interestingly, high PRL-3 protein levels were detected only in developing blood vessels, but not in mature ones, implying that PRL-3 may be involved in the early development of the vascular system (Guo et al., 2006). Moreover, PRL-3 expression was shown to be dramatically upregulated in human microvascular endothelial cells (HMVEC) and human umbilical vascular endothelial cells (HUVEC) exposed to phorbol 12-myristate 13-acetate (PMA). In addition, these cells were shown to exhibit increased level of tube formation, a phenotype associated with angiogenesis (Rouleau et al., 2006). Conversely, reduced RPL-3 expression or activity using genetic or pharmacological means led to suppression of tube formation, indicating that PRl-3 may play an important role in tumour angiogenesis (Xu et al., 2011).

Angiogenesis is a process controlled by opposing factors, with some promoting and others suppressing the development of new vessels (Casey and Li, 1997). In an *in vitro* co-culture system, Chinese hamster ovary (CHO) or DLD-1 cells overexpressing PRL-3 could redirect the migration of HUVECs towards them, thereby enhancing HUVEC vascular formation. Similarly, subcutaneous injection of PRL-3-expressing CHO cells into nude mouse leads to a recruitment of host endothelial cells towards the tumour mass,

thereby initiating angiogenesis. This pro-angiogenic process can be partially attributed to PRL-3-mediated suppression of interleukin-4 (IL-4), a well-known modulator of the immune system, which also acts as an inhibitor of angiogenesis (Guo et al., 2006; Volpert et al., 1998). Vascular endothelial growth factor (VEGF) is another cytokine that can stimulate angiogenesis, and its expression levels significantly correlate with that of PRL-3 in NSCLC and endometrial adenocarcinoma (Ming et al., 2014; Ming et al., 2009). In A549 lung cancer cells, blocking PRL-3 expression resulted in a decrease in VEGF expression (Ming et al., 2009). On the other hand, overexpression of PRL-3 induces VEGF expression through upregulation of the ERK signaling pathway, thereby facilitating microvascular vessel formation and angiogenesis (Ming et al., 2014). Furthermore, *in vivo* studies have also reported similar results, with VEGF-mediated vascular permeability largely attenuated in PRL-3 knockout mice compared to wild type mice. Colon tumour tissues derived from PRL-3-deficient mice also showed a reduction in tumour microvessel density, suggesting that loss of PRL-3 decreases tumour-driven angiogenesis (Zimmerman et al., 2014).

Collectively, both *in vitro* and *in vivo* studies have shown a role for PRL-3 in promoting tumour angiogenesis to aid in cancer progression. This PRL-3-triggered angiogenesis requires the involvement of the cytokines IL-4 and VEGF. Due to the importance of angiogenesis in cancer progression, inhibiting angiogenesis has long been proposed for cancer therapy (Noonan et al., 2007). The implication of PRL-3 in angiogenesis provides a novel attractive target for cancer treatment through inhibition of angiogenesis.

1.4.5. PRL-3 enhances cancer invasion and metastasis

In general, most cells remain confined to their organ of origin where they perform their specialized activities. However, cancer cells have acquired the ability to disseminate from

their organ of origin to other parts of the body in a process called metastasis (Hanahan and Weinberg, 2011). The metastatic cascade involves several steps, including invasion, migration, implantation and colonization (Scanlon and Murthy, 1991). The acquisition of invasive and motile behavior is the primary step and requires reversible changes in cell-cell and cell-extracellular matrix (ECM) adherence (Sahai, 2007). After penetrating through the tissue barriers, cancer cells enter the circulatory system and lymphatic system, and infiltrate other organs. These disseminated cells that travel through the body are capable of establishing new tumours at locations distant from the site of the original tumour. Hence, once metastasized, it is difficult to target tumour cells by chemotherapy or surgery. This is a significant challenge for cancer therapy, as more than 90% of all cancer mortality and morbidity are associated with metastasis (Gupta and Massague, 2006).

During the past few years, many studies have shown a correlation between elevated PRL-3 expression and increased cancer severity and metastasis. In 2001, PRL-3 was found to be the only gene expressed at high levels in all CRC liver metastases examined, and at low levels in matched non-metastatic tumours and normal colorectal epithelium (Saha et al., 2001). Subsequently, various groups confirmed PRL-3 was dramatically elevated in CRC metastases in liver, and also in secondary CRC lesions found in the lung, brain, ovary, peritoneum, and lymph nodes (Bardelli et al., 2003; Kato et al., 2004; Peng et al., 2004; Wang et al., 2007c). Moreover, clinical statistical analysis revealed that high PRL-3 expression is associated with increased liver and lung metastasis in colorectal cancer, implying that PRL-3 expression might be important for CRC metastasis (Kato et al., 2004; Peng et al., 2004). Similarly, in human gastric carcinoma, PRL-3 expression levels are much higher in metastatic lesions compared to their corresponding primary tumours (Miskad et al., 2004). This increased PRL-3 expression is correlated with

increased lymphatic and venous invasion, lymph node and peritoneal metastasis, as well as increased tumour stage (Li et al., 2007; Miskad et al., 2007). In addition to CRC and gastric carcinoma, breast, lung, esophageal cancers and melanoma also exhibit a strong correlation between high PRL-3 expression levels and distant metastasis (Hao et al., 2010; Laurent et al., 2011; Lou et al., 2012; Ming et al., 2009; Ooki et al., 2010; Radke et al., 2006). Notably, analysis of the global gene expression profiles comparing uveal melanoma patients with and without liver metastases identified PRL-3 as the only gene specifically upregulated in tumours from patients who developed liver metastasis (Laurent et al., 2011). These observations strongly indicate the involvement of PRL-3 in metastasis.

To understand the significance of PRL-3 in metastasis, several cell lines and mouse models have been employed. In CHO cells, stable expression of PRL-3 enhanced cell migration, as detected by wound healing and trans-well assays; and increased cell invasion as determined in matrigel trans-well assays. Additionally, *in vivo* metastasis assays revealed that overexpression of PRL-3 in CHO cells induced metastatic tumour formation in mice, with the development of lung and liver metastases (Zeng et al., 2003). Furthermore, PRL-3 catalytic activity was found to be essential for tumour progression and metastasis (Guo et al., 2004). In good agreement with this, overexpression of PRL-3 in B16 melanoma cells was shown to enhance their migration, adhesion, invasion, and *in vivo* metastatic tumour formation abilities (Wu et al., 2004). Conversely, ablation of the expression or activity of PRL-3 reduces metastasis-associated properties in melanoma, gastric carcinoma, colon carcinoma, and breast carcinoma cells, indicating specific targeting of PRL-3 as a potential effective treatment option for PRL-3 positive human cancers (Fagerli et al., 2008; Kato et al., 2004; Li et al., 2006; Qian et al., 2007; Rouleau et al., 2006; Wu et al., 2004). Notably, compared with wild type mice, PRL-3 deficient

mice developed 50% fewer colon tumours when treated with mutagens such asazoxymethane (AOM) and dextran sodium sulfate (DSS); this strongly supports the critical role of PRL-3 in tumour formation (Zimmerman et al., 2013). Collectively, these studies indicate that specific targeting of PRL-3 may be an effective therapeutic strategy for treating PRL-3 positive human cancers.

The molecular mechanism behind PRL-3 enhanced metastasis is largely unknown. However, PI3K/Akt, integrin/Src and Rho family GTPases signaling pathways have been reported to mediate some pro-metastasis effects of PRL-3. The PI3K/Akt pathway is an important oncogenic pathway that is frequently hyper-activated in human cancers, contributing to tumour development, including cell survival, proliferation, invasion, migration, and metastasis (Zhang et al., 2015). Overexpression of PRL-3 has been shown to activate the PI3K/Akt signaling pathway (Jiang et al., 2011; Lee et al., 2012; Wang et al., 2007a). Concomitant with Akt activation, PRL-3 also promotes epithelial-mesenchymal transition (EMT) (Wang et al., 2007a). EMT is a process by which epithelial cells transform to a more mesenchymal phenotype over a period of time, a crucial step in the initiation of the metastasis cascade (van Zijl et al., 2011). Generally, it is characterized by loss of adhesion of epithelial cells through disruption of the assembly and stability of the adherens junction complexes, thus promoting migratory capacity and invasiveness of the cells (Kalluri and Weinberg, 2009). In DLD-1 colorectal cancer cells, overexpression of PRL-3 reduces the expression of epithelial marker proteins E-cadherin, γ-catenin, and integrin β3, and increases the expression of mesenchymal marker proteins Snail and fibronectin, strongly indicating a role for PRL-3 in triggering EMT (Wang et al., 2007a). In line with this, PRL-3 was also shown to induce EMT in SW480 cells both *in vivo* and *in vitro* (Liu et al., 2009). Furthermore, treating PRL-3 overexpressing cells with the PI3K inhibitor LY294002 mitigates the

EMT process, strongly suggesting that PRL-3-induced EMT requires PI3K/Akt activation (Wang et al., 2007a).

Another PRL-3 effector pathway in metastasis is the integrin/Src pathway, a key regulator in EMT and focal adhesions (Playford and Schaller, 2004). Focal adhesions are dynamic sub-cellular structures composed of multi-protein complexes that mediate the attachment of cells to the ECM. The regulation of their formation and disruption is a requisite for mestastasis (Campbell, 2008). In mammalian cells, PRL-3 can interact with integrin α1 and integrin β1 (Peng et al., 2006; Peng et al., 2009). These two proteins are transmembrane receptors considered as bridges for cell-cell and cell-ECM interactions. Activation of integrins leads to the recruitment of a plethora of adaptors, kinases, and other signaling proteins to focal adhesion complexes, all aiding in cellular migration (Eke and Cordes, 2015). In LoVo cells, expression of PRL-3 enhanced Erk1/2 and matrix metalloproteinase (MMP2) activities, leading to an increase in cell migration, invasion, and metastasis. Furthermore, depletion of integrin β1 abrogates these PRL-3-induced phenotypic changes, suggesting the involvement of integrin β1 in PRL-3-mediated cell motility and metastasis (Peng et al., 2009). In addition, PRL-3 was shown to regulate the activity of Src protein, a key downstream effector of integrin signaling (Mitra and Schlaepfer, 2006). In HEK-293 cells, overexpression of PRL-3 activated Src through downregulation of Csk, a negative regulator of Src, leading to an increase in cell invasion and proliferation (Liang et al., 2007). Some of the direct substrates of Src, such as STAT3 and $p130^{Cas}$, were also activated in PRL-3 expressing cells (Liang et al., 2007). $p130^{Cas}$ is a scaffold protein that plays a critical role in focal adhesion formation (Nakamoto et al., 1997). Overexpression of PRL-3 induced phosphorylation of $p130^{Cas}$ resulting in the establishment of an interaction between $p130^{Cas}$ and the focal adhesion protein vinculin (Nakamoto et al., 1997). This PRL-3 mediated enhancement of focal

adhesions and cell motility was eliminated upon introduction of Csk in PRL-3 expressing HEK 293 cells, indicating that PRL-3-mediated promotion of focal adhesions required the activation of the Src pathway (Liang et al., 2007). However, in contrast to this finding, expression of PRl-3 reduced paxillin and vinculin levels in HeLa and CHO cells (Wang et al., 2007a). These two proteins are components of focal adhesions, suggesting a role for PRL-3 in reducing focal adhesions in HeLa and CHO cells. The contrast in behavior of PRL-3 from these two reports might be a result of cell type differences or dynamic focal adhesion turnover, as both focal adhesion formation and disassembly are important for cell spreading and migration.

Besides the involvement of Akt and integrin/Src pathways, Rho family GTPases have also been reported to regulate PRL-3-induced metastasis. Rho GTPase, such as Rho, Rac, and Cdc42, are critical regulators of actin polymerization, stress fiber assembly, focal adhesion formation, and cell motility (Parsons et al., 2010). In SW480 colorectal carcinoma cells, ectopic PRL-3 expression induced a robust activation of the Rho family GTPases RhoA and RhoC by over 4- to 6-fold, and reduced Rac activity by 70% (Fiordalisi et al., 2006). Consistent with these results, the observed increase in cell migration and invasion upon ectopic PRL-3 expression was reversed with pharmacological inhibition of Rho-coiled coil kinase (ROCK), a key Rho effector (Fiordalisi et al., 2006). Furthermore, depletion of PRL-3 levels in A549 lung cancer cells reduced RhoA activity and mDia1 expression, leading to inhibition of cell migration and invasion (Jian et al., 2012). Blocking RhoA or mDia1 showed a reduction in migration and invasion, which was alsoobserved on inhibiting PRL-3, suggesting an involvement of RhoA, RhoC, and mDia1 in mediating PRL-3-promoted cell migration and invasion. However, in contrast to these observations, it was also reported in CHO and DLD-1 cells that RhoA and Rac1 expressions were reduced upon PRL-3 expression (Wang et al.,

2007a). As discussed above, the distinct observations of these two groups may reflect the role of enhanced dynamic focal adhesion turnover in promoting cell migration and invasion.

Recent reports have shown that PRL-3 also affects Arf1 protein, microRNAs, and calcium channels to regulate metastasis. Arf1 is a member of Arf family GTPases. Together with the Rho family GTPases, the Arf family GTPases play a key role in actin cytoskeleton remodeling and cell migration (D'Souza-Schorey and Chavrier, 2006). In HeLa cells, PRL-3 overexpression increased Arf1 activity, leading to increased cell migration. Blocking the expression or activity of Arf1 completely abrogated the pro-migratory effect of PRL-3, suggesting that PRL-3-mediated migration requires Arf1 activation (Krndija et al., 2012). Additionally, PRL-3 elevated the expression levels of miR-17, miR-19a, and miR-21 in CRC cells, resulting in an enhancement of metastasis (Zhang et al., 2012b). In LoVo colon cancer cells, PRL-3 upregulated the expression of KCNN4 channels to increase the expression of Snail and downregulate the expression of E-cadherin, leading to EMT. The EMT process was reversed on suppression of KCNN4 expression or activity, indicating KCCN4 might be implicated in mediating PRL-3-induction of EMT and promotion of cancer metastasis (Lai et al., 2013).

Taken together, PRL-3 promotion of tumour metastasis is quite dynamic and complex. Many signaling pathways are involved in this process, which requires activation of different effector proteins. Despite these advances in our understanding of PRL-3 function, the detailed mechanisms and direct substrates are still an open area to be explored for further investigation.

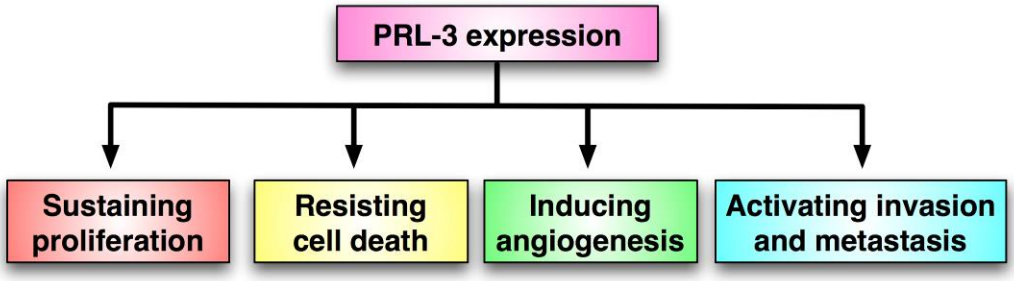

Figure 1. 4 The implication of PRL-3 in cancer progression

1.5 Proposed substrates of PRL-3

Despite achievements in elucidating the role of PRL-3 in cancer progression and in identifying its associated signaling pathways, a gap remains in our understanding of its molecular mechanism(s) of action. This is compounded by the lack of well-characterized substrates. To date, a number of PRL-3 binding partners have been reported (**Table 1.1**). However, only a few of them have been confirmed as putative PRL-3 substrates.

The first suggested substrate of PRL-3 is Ezrin, a linker protein between the plasma membrane and the actin cytoskeleton (Forte et al., 2008). In HCT116 colon cancer cells, PRL-3 overexpression reduces Ezrin phosphorylation at the Tyr145, Tyr353, and Thr567 residues. However, knockdown of PRL-3 only affects Ezrin phosphorylation at position Thr567. In line with this observation, an *in vitro* phosphatase activity assay also suggests Ezrin as a direct substrate of PRL-3, and Thr567 as the primary site for PRL-3 activity (Forte et al., 2008; Orsatti et al., 2009). In addition to Ezrin, elongation factor 2 (EF2) was also identified as another potential substrate of PRL-3 (Orsatti et al., 2009). EF2 is a protein synthesis regulator that promotes the GTP-dependent translocation of ribosomes (Kaul et al., 2011). PRL-3 expression has been shown to suppress EF2 phosphorylation (Orsatti et al., 2009). In addition, Keratin 8 (KRT8), Nucleolin (NCL), Integrin β1, and

phosphatidylinositol-(4,5)-bisphosphate (PIP2) have also been suggested as possible substrates of PRL-3. KRT8 is a member of the intermediate filament family, which plays an important role in maintaining cellular structural integrity (Khapare et al., 2012). In SW480 colon cancer cells, PRL-3 interacts and dephosphorylates KRT8 at the Ser73 and Ser431 residues, resulting in dysregulation of intermediate filament disassembly (Mizuuchi et al., 2009). Similarly, NCL protein, a phosphoprotein involved in rRNA synthesis and ribosome biogenesis, could also be dephosphorylated by PRL-3, leading to its accumulation in the nucleolus (Semba et al., 2010; Tajrishi et al., 2011). Interestingly, *in vitro* phosphatase activity assays also reveals that PRL-3 is active towards phosphoinositide PI(4,5)P2, indicating a lipid phosphatase role for PRL-3 (McParland et al., 2011). Another putative substrate for PRL-3 is the Integrin β1. In BGC823 and SW480 cancer cells, Tyr783 amino acid residue of Integrin β1 was shown to be dephosphorylated by PRL-3 both *in vivo* and *in vitro* (Tian et al., 2012).

Additionally, other proteins, such as Integrin α1, Cadherin-22, Stathmin, FK506-binding protein 38 (FKBP38), Histone deacetylase 4 (HDAC4), ADP-ribosylation factor 1 (Arf1), Thioredoxin-related Protein 32 (TRP32), Repressor/Activator Protein 1 (RAP1), and Leo1, have also been demonstrated to interact with PRL-3 physically. However, whether PRL-3- shows any phosphatase activity towards these proteins is still unknown. Further validation of these substrates is necessary to completely understand the function of PRL-3.

TABLE 1. 1 Putative substrates and Binding partners of PRL-3

Substrate	Interacting protein	Outcome	Cell line(s)	Validation method(s)	Refs.
Ezrin		Ezrin dephosphorylation	HCT116	MS, PA	(Forte et al., 2008)
EF2		EF-2 dephosphorylation	HCT116	MS	(Orsatti et al., 2009)
KRT8		KRT8 dephosphorylation	SW480	IP, MS	(Mizuuchi et al., 2009)
NCL		NCL dephosphorylation	SW480	IP, MS	(Semba et al., 2010)
PI(4,5)P2		PI(4,5)P2 dephosphorylation	HEK293	IP, PA	(McParland et al., 2011)
Integrin β1		Integrin β1 dephosphorylation	BGC823, SW480	IP, PD	(Tian et al., 2012)
	Integrin α1	N.D.	COS-7	IP, PD, Y2H	(Peng et al., 2006)
	Cadherin-22	PRL-3 suppresses the expression of CDH22	SW480, SW620, HEK-293	IP, PD, Y2H	(Liu et al., 2009)
	Stathmin	N.D.	SW480, LoVo	IP, MS	(Zheng et al., 2010)
	FKBP38	FKBP8 reduces the stability of PRL-3	HeLa HEK293A	IP, Y2H	(Choi et al., 2011)
	HDAC4	N.D.	MOLM-14 DLD-1	IP	(Zhou et al., 2011)
	Arf1	PRL-3 activates Arf1	HeLa	IP, PD	(Krndija et al., 2012)
	TRP32	TRP32 reduces oxidized PRL-3	HEK293	PD	(Ishii et al., 2013)
	RAP1	PRL-3 induces cytosolic localization of RAP1	HCT116 BGC823	IP, PD	(Lian et al., 2013)
	Leo1	PRL-3 induces expression of Leo1	SW480	IP, PD	(Chong et al., 2014)

MS, mass spectrometry; *PA*, phosphatase activity assays; *IP*, immunoprecipitation; *PD*, GST pull-down; *Y2H*, yeast 2-hybrid assay; *N.D*, not determined.

1.6 PRL-3-based cancer therapy

Due to a critical role of PRL-3 in tumour progression, it has long been considered a potential target for cancer therapy, attracting the attention of many scientists in the past few years. To date, different groups are focusing on two major methods of PRL-3 targeted therapy: PRL-3-based chemotherapy and PRL-3-based immunotherapy.

1.6.1 PRL-3-based chemotherapy

Chemotherapy is the use of drugs to suppress cancer cells by inhibiting cell growth and division (Liu et al., 2015). As PRL-3 is involved in cancer progression, several small molecule inhibitors of PRL-3 have been screened and identified that block PRL-3 activity in cells. Pentamidine, an anti-protozoan drug for leishmaniasis treatment, was the first reported inhibitor of PRL-3. It can block PRL-3 activity as well as the *in vitro* growth of PRL-3-positive human cancer cells. Besides PRL-3, Pentamidine could also inhibit several other PTPs, including PTP1B, mitogen-activated protein kinase (MAPK) phosphatase-1 (MKP-1), PRL-1, and PRL-2. Therefore, it remains elusive whether the suppression of cell growth is due to the specific inhibition of PRL-3 or a general inhibition of all these phosphatases (Pathak et al., 2002).

Subsequently, it was found that some natural chemicals from plants, such as bioflavonoids, anthraquinones, and curcumin, could also act as PRL-3 inhibitors (Choi et al., 2006; Moon et al., 2010; Wang et al., 2009). Two bioflavonoids, ginkgetin and sciadopitysin, which are extracted from *Taxus cuspidate*, are the first known natural inhibitors of PRL-3 to be discovered. Similar to pentamidine, they strongly inhibit all three PRL members (Choi et al., 2006). Certain anthraquinones, such as emodin, were also shown to effectively block PRL-3 phosphatase activity, leading to an inhibition in

PRL-3-induced cancer cell migration and invasion (Han et al., 2012). Another natural inhibitor of PRL-3, curcumin, a polyphenol derived from the spice turmeric, was shown to selectively suppress PRL-3 expression and reduce PRL-3-mediated cell proliferation, migration and adhesion (Wang et al., 2009).

Furthermore, modern high throughput screenings of chemical libraries have identified rhodanine derivatives as PRL-3 inhibitors (Ahn et al., 2006). Two of these derivatives, BR-1 and G-707, selectively inhibit PRL-3 phosphatase activity without affecting the activity of the other 10 PTPs. Moreover, they exhibit anti-tumour activity in both cell culture models and mouse xenograft models (Min et al., 2013). These findings have encouraged scientists to screen for other rhodanine derivatives as inhibitors of PRL-3. Recently, 12 novel potent inhibitors of PRL-3 were identified by structure-based virtual screening and *in vitro* enzymatic assays (Park et al., 2008). Some of these 12 lead compounds are rhodanine derivatives. However, in spite of a promising activity profile of the rhodanine derivatives, additional screening of these compounds is required for identification of true lead candidates.

At present, thienopyridone (7-amino-2-phenyl-5H-thieno[3,2-c]pyridin-4-one) might be the most promising inhibitor of PRL-3 as it is the most characterized. It selectively inhibits PRLs, but not 11 other known PTPs (Daouti et al., 2008). Inhibition of PRLs by thienopyridone resulted in significant suppression of tumour cell anchorage-independent growth, anoikis, and an inhibition in cell migration through p130Cas cleavage (Daouti et al., 2008).

Despite the recent successes in the identification of new PRL-3 inhibitors, the specificity, stability and solubility of these compounds could be improved further. In addition, since chemical compounds could have potential adverse side effects and toxicity, further

investigation of these drugs would be required before PRL-3-targeted inhibitors could be used in clinical cancer therapy.

1.6.2 PRL-3-based immunotherapy

Immunotherapy is a form of treatment that employs or enhances the function of the immune system to eliminate cancer cells. Normally, the immune system would detect and destroy abnormal cells to prevent disease occurrence. However, some cancer cells are able to avoid immune detection and destruction by undergoing mutations that help them escape immune surveillance, thus making it harder for the immune system to recognize and kill them. Hence, one approach to circumvent this problem is to mobilize the immune system by employing antibody-directed recognition of cancer cell makers to specifically target cancer cells. In comparison to chemotherapy, immunotherapy offers more specificity with less side effects (Makkouk and Weiner, 2015) .

As discussed earlier, PRL-3 is a prenylated protein localized to the intracellular portion of the cell membrane. Based on this fact, it does not seem a promising candidate for antibody-directed cancer therapy as traditional dogma dictates that the cell membrane serves as a barrier to prevent antibodies from entering cells and therefore antibodies could only target external surface makers (Baker, 2005). However, an increasing body of evidence show that antibodies could enter cells and bind to intracellular antigens, leading to apoptosis (Hazin et al., 2015). Our lab was the first to demonstrate that anti-PRL-3 monoclonal antibodies could dramatically reduce PRL-3-expressing metastatic lung tumour growth in nude mouse (Guo et al., 2008). Furthermore, a monoclonal antibody directed against PRL-1 also exhibited a strong inhibitory effect towards PRL-1-expressing metastatic lung tumours in nude mice. Notably, although both PRL-1 and PRL-3 share significant amino acid sequence identity, PRL-3 monoclonal antibody

could not inhibit PRL-1 metastatic tumours. Similarly, PRL-1 monoclonal antibody specifically inhibited only PRL-1 but not PRL-3 metastatic tumours, suggesting a high specificity for antibody therapy against PRLs (Guo et al., 2008). In another experiment, mice primed for PRL-3 antibody production exhibited reduced metastatic tumour formation when injected with cancer cells in comparison to the unimmunized control mice (Guo et al., 2011). Moreover, chimeric monoclonal antibody directed against PRL-3 also selectively inhibited the formation of PRL-3-expressing metastatic tumours, implying that cancer therapy targeting intracellular proteins with antibodies is feasible (Guo et al., 2012).

However, the mechanism(s) behind this antibody targeted therapy is still largely unknown. A role for B-cells has been speculated for an effective immune response to PRL-3, as no therapeutic effect of PRL-3 antibody treatment was observed in B-cell deficient mouse models (Guo et al., 2012). Hence, further study of the mechanism is warranted to refine our understanding of PRL-3 based immunotherapy.

CHAPTER 2. MATERIALS AND METHODS

2.1. Reagents and antibodies

2.1.1 Reagents

The chemicals used in this study were as follows: Rapamycin (100 nM final; LC Laboratories, #R-5000); Akt Inhibitor VIII (5 μM; Santa Cruz Biotechnology, #sc-202048), U0126 monoethanolate (U0126) (10 μM, Sigma-Aldrich, #U120); bafilomycin A1 (50 nM; Sigma-Aldrich, #B1793), LY29400 (10 μM, Cell Signaling Technologies, #9901), PP2 (10 μM, Sigma-Aldrich, #P0042), Tyrphostin AG 490 (10 μM, Sigma-Aldrich, #UT3434), SB203580 (10 μM, Sigma-Aldrich, #S8307), SP600125 (10 μM, Sigma-Aldrich, #S5567), Cobalt(II) chloride ($CoCl_2$) (5 μM, Sigma-Aldrich, #U60818)

2.1.2 Antibodies

The Antibodies used in this study were obtained as indicated in the following: Antibodies against mTOR (#2983), p-mTOR S2448 (#2971), 4E-BP1 (#9644), p-4E-BP1 T37/46 (#2855), p-p70S6K T389 (#9234), TSC2 (#4308), and p-TSC2 S939 (#3615), Erk1/2 (#4695), p-Erk1/2 (#4370), AMPKα (#2603), p-AMPKα T172 (#2535), Akt (#4691), p-Akt S473 (#4060), raptor (#2280), p-JNK (#9251), JNK (#9252), p-p38 MAPK (#4511), p38 MAPK (#9212), Cleaved PARP (#9544), ASK1 (#8662), p-ASK1 T845 (#3765), MKK4 (#9152), p-MKK4 S257 (#4514), p-MKK4 T261 (#9151), MKK3 (#8535), p-MKK3/6 (#9236) were purchased from Cell Signaling Technologies (Danvers, MA, USA). Anti-p70S6K (#611260) antibody was purchased from BD Biosciences (San Jose, CA, USA). Anti-LAMP2 (#ab25631) antibody was purchased from Abcam (Cambridge, England, UK). Antibodies against GST (#sc-138) and GFP (#sc-9996) were purchased from Santa Cruz Biotechnology (Dallas, TX, USA). HRP-conjugated sheep

anti-mouse (#515-035-062) and goat anti-rabbit (#111-035-045) antibodies were purchased from Jackson ImmunoResearch Laboratories Inc. (West Grove, PA, USA), whilst AlexaFluor568-conjugated goat anti-mouse (#A-11004) and AlexaFluor633-conjugated goat anti-rabbit (#A-21071) antibodies were from Life Technologies (Grand Island, NY, USA). Anti-PRL3 antibody was generated by our own lab previously (Li et al., 2005).

2.2. Plasmids and siRNA

2.2.1 Plasmids

The pEGFP-PRL-3 and catalytically-inactive pEGFP-PRL-3-C104S constructs were generated by our own lab previously (Wang et al., 2007a). The pRK5-HA-GST-RagB-WT (#19301), pRK5-HA-GST-RagC-WT (#19304), pRK5-HA-GST-RagD-WT (#19307), pRK5-HA GST RagB 54L (#19302), and pRK5-HA GST RagD 121L (#19309) constructs were gifts from David Sabatini and sourced from Addgene (Cambridge, MA, USA). The pCDNA3-Flag-p38a construct was a gift from Roger Davis and sourced from Addgene (# 20352). Human PRL-3-targeting shRNA (5'-TTCTCGGCACCTTAAATTATT-3') have been reported previously (Al-Aidaroos et al., 2013). Expression vectors encoding PRL-3–directed (5′-TTCTCGGCACCTTAAATTATT-3′) or non-targeting scrambled shRNA sequences were purchased from OriGene (Rockville, MD, USA).

2.2.2 siRNA

Human *AKT*-targeting (# 6211) and control siRNA (# 6568) were purchased from Cell Signaling Technologies.

2.3. Cell lines and derivatives

2.3.1. Cell lines

Human colon cancer cell lines (HCT116, HCT15, LoVo, SW620, DLD-1), human cervical cancer cells (HeLa), human melanoma cells (G361), and human breast cancer cells (MCF7) were purchased from ATCC (Manassas, VA, USA). Human ovarian cancer cells (A2780) were purchased from ECACC (Salisbury, England, United Kingdom).

2.3.2. Generation of stable cancer cell lines with expression of EGFP, EGFP-PRL-3 or EGFP-PRL-3-C104S

HCT116, DLD-1 and MCF-7 cells were seeded in their respective antibiotic-free media in a 12-well culture plate (1 x 10^5 cells/well). Lipofectamine2000, a cationic lipid-based transfection reagent (Invitrogen, USA), was used according to manufacturer's protocol. 1 µg of pEGFP-C1, pEGFP-PRL-3 or pEGFP-PRL-3-C104S plasmid DNA were mixed with 2 µL Lipofectamine2000 and diluted in 200 µL OptiMEM media for 20 min before transfecting cells, to form DNA-lipid complexes. Then, the DNA-lipid complexes were added evenly over the cells. After overnight incubation, cells were reseeded to a 150 mm tissue culture dish with their respective growth media supplemented with 1 mg/mL neomycin. And the selection sustained for 2 weeks to obtain cell populations with at least 90% GFP positivity. The GFP signal was confirmed using an Eclipse TE2000-U inverted fluorescence microscope (Nikon, Japan). While all the mock-transfected cells were died after 2 weeks of neomycin selection. Stable cell pools were thereafter grown in normal complete media without neomycin selection. Early passage stocks were kept in growth media supplemented with additional FBS (20% v/v final) and DMSO (10% v/v) and stored in -80°C or liquid nitrogen.

2.3.3. Generation of HCT116 cancer cell lines with stable PRL-3 knockdown

SureSilencing shRNA plasmids (Origene, USA) encoding either a non-targeting scrambled or human PRL-3-targeting shRNA (5'-TTCTCGGCACCTTAAATTATT-3') were transfected as described above in HCT116 cells. After 2 weeks of puromycin selection (1 μg/mL), individual colonies were picked and expanded. And the cells showing ≥75% knockdown of PRL-3 expression were stored and used for subsequent experiments. Viable cells were not found in mock-transfected cells after 2 weeks of puromycin selection.

2.3.4. Cell culture and Treatments

Cells were grown in RPMI-1640 media supplemented with 10% FBS (HyClone, Carlsbad, CA, USA) and 1% (v/v) penicillin/streptomycin in a humidified incubator at 37°C with 5% CO_2. For serum depletion (serum-free; SF) experiments, cells were washed twice in PBS and changed to RPMI-1640 media without FBS, supplemented with 1% (v/v) penicillin/streptomycin. For hypoxia experiments, cells were placed in a GasPak EZ Gas Pouch (BD Biosciences, Sparks, MD, USA) containing ≤ 1% O_2. For amino acid starvation (AA-) experiments, cells were washed twice in PBS, once with Earle's Balanced Salt Solution (EBSS), and finally incubated with EBSS media without FBS for 1 h. For conditioned media analysis, cells were washed thrice in PBS and cultured in RPMI-1640 media without FBS for 24 h. Then media was collected and condensed using centrifugal concentrators. Where indicated, cells were treated with rapamycin (100 nM final; LC Laboratories, #R-5000), Akt Inhibitor VIII (5 μM final; Santa Cruz Biotechnology, #sc-202048), U0126 monoethanolate (U0126) (10 μM, Sigma-Aldrich, #U120); bafilomycin A1 (50 nM; Sigma-Aldrich, #B1793), LY29400 (10 μM, Cell Signaling Technologies, #9901), PP2 (10 μM, Sigma-Aldrich, #P0042), Tyrphostin AG

490 (10 μM, Sigma-Aldrich, #UT3434), SB203580 (10 μM, Sigma-Aldrich, #S8307), SP600125 (10 μM, Sigma-Aldrich, #S5567), Cobalt(II) chloride ($CoCl_2$) (2 μM - 10 μM, Sigma-Aldrich, #U60818), or DMSO alone (0.1% final).

2.3.5. Transit Small-interfering RNA (siRNA) and plasmids transfection

For siRNA, human AKT-targeting (catalogue number 6211S) and control siRNA were from Cell Signaling Technologies. siRNA (100 nM final) was transiently transfected using jetPRIME (Polyplus-transfection SA, Illkirch, France) following the manufacturer's recommended protocol. Briefly, cells cultured in 6-well plate were transfected with the siRNA for 48 h, then subjected to the designated treatments. For plasmids transfection, the plasmids were also transfected using jetPRIME reagents. After 24 h transfection, cells were subjected to following treatments.

2.4. RNA extraction

The RNeasy kit (Qiagen, USA) was utilized for cellular RNA extraction according to the manufacturer's protocol. Briefly, sub-confluent cell monolayers cultured in 6-well plates (~80%; $1x10^6$ cells) were harvested, washed by PBS, and lysed in 350 μL of Buffer RLT containing 1% β-mercaptoethanol (v/v). Then, the lysates were passed through a QIAshredder spin column once (Qiagen, USA) to homogenize cells. 350 μL of 70% ethanol (v/v) was subsequently mixed with homogenates, and transferred into an RNeasy spin column. After the initial spin, the column containing membrane-bound RNA was washed once with 700 μL Buffer RW1, twice with 500 μL Buffer RPE, and spun completely dry. 30 μL of RNase-free water was used for RNA elution. Purified RNA was analyzed and quantified using a Nanodrop spectrophotometer (Thermo Fisher Scientific).

2.5. Semi-quantitative (RT-PCR)

SuperScript III First Strand Synthesis System (Invitrogen, USA) were used for reverse transcription according to manufacturer's protocol. Then, for RT-PCR, HotStarTaq Master Mix Kit (QIAGEN, USA) was utilized following manufacturer's protocol. The primer set sequences used are as follows: human β-actin forward (5'-TCA CTC ATG AAG ATC CTC-3'), human β-actin reverse (5'-TTC GTG GAT GCC ACA GGA C-3'), human MMP2 forward (5'-CAC TTT CCT GGG CAA AT-3'), human MMP2 reverse (5'-TGA TGT CAT CCT GGG ACA GA-3'), human MMP9 forward (5'-GAG ACC GGT GAG CTG GAT AG-3'), human MMP9 reverse (5'-TAC ACG CGA GTG AAG GTG AG-3'). Then, PCR products were detected by agarose gel electrophoresis and imaged in a UV trans-illumination chamber equipped with a CCD camera.

2.6. Immunoprecipitation

All immunoprecipitation (IP) assays were performed in spin columns (Thermo Scientific, USA). Before IP assay, 20 µL equilibirated Protein-A/G beads were first bound to the designated antibodies (4 µL each) by 1 hour incubation with IP-Wash buffer (10 mM sodium phosphate, 150 mM NaCl; pH 7.2) at room temperature (RT) on an end-over-end rotator. Then, three volumes of IP-Wash Buffer were used to wash away the unbound antibodies (three times). For crosslinking, 450 µM disuccinimidyl suberate (DSS) was used to crosslink these antibodies to Protein-A/G beads in IP-Wash buffer for 45 min at RT. The termination of crosslinking reaction was performed by using two volumes of Elution buffer (0.1 M glycine; pH 2.8) to wash the antibody-bead conjugates twice, followed by four volumes of Lysis buffer (25 mM Tris, 150 mM NaCl, 1% NP-40, supplemented with a protease inhibitor cocktail and phosphatase inhibitor cocktail; pH 7.3) twice.

For each IP reaction, cells cultured in 60 mm culture dishes were collected with 300 µL Lysis buffer. After a 10 min incubation (on ice), lysates were centrifuged for 10 min at 16,000 x *g* at 4°C. Supernatants were collected, quantitated, and normalized to similar protein amounts. Then 30 µL supernatants were saved as an input control for each IP reaction. The antibody-bead conjugates described above were added to the remaining supernatants. After 16 h incubation at 4°C, immunoprecipitates were subsequently washed with Lysis buffer four times. Finally, 40 µL Elution buffer was used to collect immunoprecipitates. Lysates aliquots and eluted immunoprecipitates were stored at -80°C until use.

2.7. Western Blotting

Western blots were performed as described (Li et al., 2005). Briefly, cells were washed with ice-cold PBS and lysed in RIPA buffer containing a cocktail of EDTA-free protease inhibitors (Roche, Mannheim, Germany) and phosphatase inhibitors (Nacalai Tesque, Kyoto, Japan). Lysates were subjected to western blotting with indicated primary antibodies at 1:1,000 dilutions. Species-specific secondary antibodies were used at 1:2,000 dilutions. Protein-antibody conjugates were visualized using a chemiluminescent detection kit (Thermo Scientific, Waltham, MA, USA), and quantification of band intensities was done using ImageJ software. The ratio of phosphorylated/total protein was calculated and normalized as described in the figure legends.

2.8. Production of GST fusion proteins for cytosolic pull-down assays

After expansion of glycerol stocks of BL21 *E.coli* cells carrying either pGST-KG or pGST-PRL-3 plasmids by incubating the cells in 3 mL LB-ampicillin overnight, all 3 mL of bacteria culture was transferred into 500 mL LB-ampicillin and incubated till an OD_{600}

of ~0.6. Then, 0.25 mM IPTG were added for 3 h at 37°C. Bacteria cells were spun down and resuspended in Bac-Lysis buffer [20 mM Tris pH 7.5, 500 mM NaCl, 1 mg/mL lysozyme, 2 mM dithiothreitol (DTT), 2 mM benzamidine, 0.1 mM phenylmethylsulfonyl fluoride (PMSF)]. The homogenization was performed on ice by using a sonicator (large tip; 1 min, 3 times) with 1 min cooling between pulses. Then after clarification of these resulting lysates by centrifugation, the pre-cleared glutathione sepharose beads (Amersham, USA) were added to clarified lysates and incubated for 3 h on a rotator at 4°C. Protein-bound beads were washed by Bac-Lysis buffer (trice), low-salt buffer (20 mM Tris pH 7.5, 200 mM NaCl, 2 mM DTT, 2 mM benzamidine, 0.1 mM PMSF, twice), and immediately quantified and utilized for GST-pulldown assays.

2.9. Immunoflurescence Analysis

Immunofluorescence analysis was carried out as previously described (Li et al., 2005). Briefly, cells grown on glass coverslips were subjected to various treatments as indicated before rinsing with PBS and fixation for 15 min with 4% paraformaldehyde in PBS. After rinsing twice with PBS, cells were blocked for 1 h in 5% BSA blocking buffer containing 0.1% Triton-X 100, and incubated with mouse anti-LAMP2 (1:100) and rabbit anti-mTOR (1:100) antibodies overnight at 4°C. Coverslips were then rinsed three times with PBS and subsequently incubated with secondary antibodies (1:200) for 1 h at RT followed by a further three washes in PBS. Coverslips were mounted on glass slides using DAPI-containing mounting media and analysed using an LSM700 confocal microscope (Carl Zeiss AG, Jena, Germany).

2.10. Cell MTS Assay

For MTS (3-(4,5-dimethylthiazol-2-yl)-5-(3-carboxymethoxyphenyl)-2-(4-sulfophenyl)--2H-tetrazolium) assays, 2 x 10^3 cells were seeded in 10% FBS media into triplicate wells of a 96-well plate and allowed to attach overnight. Then the cells were subjected to designated treatments, and left to incubate for 24 or 48 h. The media was subsequently aspirated, and replaced with 150 uL 0.5% FBS media containing MTS (Promega) and formazan development was done for 2 h at 37° at 5% CO_2 before measuring absorbance at 490 nm (formazan product) and 630 nm (reference wavelength) in a spectrophotometer.

2.11. Wound Healing Assay

3.5 x 10^4 HCT116-Vec or HCT116-PRL-3 cells were seeded into μ-dishes (Ibidi, Martinsried, Germany) and cultured under normal conditions until they reached confluence. Subsequently, inserts were removed to yield standardized 500 μm-wide gaps. 'Wounded' cell monolayers were washed in PBS and subsequently cultured in low-serum media (0.5% FBS) with 100 nM rapamycin or 0.1% DMSO for 48 h. Images were acquired sequentially every 24 h using an Axiovert 200M inverted microscope (Carl Zeiss AG).

2.12. Invasion assay

1 x 10^4 HCT116-EGFP or HCT116-EGFP-PRL-3 cells were suspended in complete media containing 100 nM rapamycin or 0.1% DMSO and seeded into BioCoat Matrigel invasion chambers with 8.0 μm PET membranes (Corning, MA, USA). After incubation for 24 h at 37°C, non-invading cells were removed from the upper surface of the membrane by a cotton swab, and membrane inserts were washed three times with PBS

and fixed in 4% paraformaldehyde for 15 min. Subsequently, membranes were cut, mounted inverted on glass slides, and observed for EGFP fluorescence under an LSM700 confocal microscope (Carl Zeiss AG). The numbers of invaded cells in four ramdomly-chosen fields were counted. Data were presented as mean ± SE of cell number/field and statistically analyzed using the Student's t-test.

2.13. *in vitro* Rag GTPase binding assay

GST-RagB and GST-RagC vectors were co-transfected into HCT116-EGFP or HCT116-EGFP-PRL-3 stable cells. The next day, culture media was replenished before placing cells under normoxia, hypoxia, or serum-free conditions for a further 24 h. Lysates were harvested, clarified by high speed centrifugation (14 000 × g, 15 min), and incubated with glutathione beads overnight at 4°C with rotation. The beads were washed three times with lysis buffer and finally eluted with reduced glutathione (25 mM). Elutes were subjected to western blotting with the indicated antibodies.

2.14. Analysis of human gastric tissues

Human gastric tissue samples were obtained with patient consent from the National University Hospital-National University of Singapore (NUH-NUS) Tissue Repository. Experimental procedures were approved by the Institutional Review Board (IRB) of NUH-NUS for research use and conducted in accordance with approved guidelines and regulations.

2.15. Analysis of mouse mammary tissues

For the isolation of mammary tissue lysates, the uppermost pair of mammary glands from wild-type FVB/N mice or MMTV-PyMT mice (at 6, 9, 12, and 15 weeks) were

surgically removed, rinsed in PBS, and homogenised in RIPA lysis buffer using a Polytron homogenizer (Luzern) prior to western blot analysis. All animal studies were approved by an Institutional Animal Care and Use Committee (IACUC) and were performed in accordance with approved guidelines and regulations of the Biological Resource Centre, A*STAR, Singapore.

2.16. *In vitro* malachite green phosphate assay

The *in-vitro* malachite green phosphate assay was performed by using Malachite Green Phosphate Assay Kit (Bioassay systems, #POMG-25H) following the manufacturer's protocol. Briefly, working reagent was prepared by mixing 100 vol of Reagent A and 1 vol of Reagent B at RT. Then 20 µL of working reagent was incubated with 80 µL of the sample solution containing GST-PRL-3 and Flag-p38, GST-PRL-3 and Flag-ctrl, GST-Ctrl and Flag-p38, or GST-Ctrl and Flag-Ctrl proteins in a 96-well plate for 30 min at RT for color development. The absorbance at 600 nm - 660nm (620 nm) were measured by a plate reader (BD Biosciences, USA). The phosphate standard curve was also established by following the same protocol above (1 mM phosphate was provided in the kit) at the same time. Finally, the amount of free phosphate was analyzed and determined by using Excel software (Microsoft, USA).

2.17. Detection of Reactive Oxygen Species (ROS)

The ROS level was detected by CM-H_2DCFDA (Thermo Fisher Scientific, #C6827). Briefly, cells were cultured in 24-well plate, and followed with the designated treatments. Then after incubation with PBS containing 10 µM CM-H_2DCFDA for 10 min, cells were trypsinized, washed, and examined by fluorescence microscope (Nikon) or BD FACS

cytometer (BD Biosciences). The quantitative data were presented as Means±SE and analysed using Student's t test.

2.18. Rheb activation assay

Analysis of intracellular Rheb-GTP levels was done using a Rheb activation assay kit (Abcam), according to the manufacturer's instructions. Briefly, 2.5×10^6 cells, grown under the indicated culture conditions, were washed with ice-cold PBS and lysed in kit-supplied lysis buffer containing a cocktail of EDTA-free protease inhibitors (Roche). Lysates were clarified by centrifugation (16,000 × g, 10 min) before equivalent amounts of lysates (2 mg) were subjected to immunoprecipitation with a configuration-specific monoclonal antibody that specifically recognizes RheB-GTP, but not RheB-GDP. Western blotting and densitometry analysis was subsequently used to characterize the proportion of active Rheb (as reflected by the Rheb-GTP/Rheb ratio) present in cellular extracts.

2.19. Statistical Analysis

For the proliferation assays, the Student's *t*-test was used to test for significant differences. Statistical analyses of the colon cancer patient dataset GSE40967 (n = 566) were performed using SPSS 19.0 software (IBM, NY, USA). Correlation between PRL-3 and MMP-2, MMP-7, or MMP-9 gene expression was analysed by Spearman Correlation. The association between PRL-3 expression and relapse-free survival (RFS) was analysed by Kaplan-Meier analysis. p values < 0.05 were considered statistically significant. All data presented in this study are representatives from three biological independent experiments.

CHAPTER 3. PRL-3 ACTIVATES mTOR SIGNALLING TO PROMOTE CANCER PROGRESSION

3.1. Background

The mechanistic target of rapamycin (mTOR) is a critical regulator of cell growth and homeostasis (Laplante and Sabatini, 2012). It senses and integrates a variety of signals from growth factors, nutrients, and environmental stressors to regulate many biological processes, such as mRNA translation, protein synthesis, metabolism, proliferation, autophagy, cell survival, and cytoskeletal organization (Sarbassov et al., 2005a).

mTOR was first discovered from studies on the action of the macrolide, rapamycin, in the early 1990s (Brown et al., 1994; Chiu et al., 1994; Sabatini et al., 1994; Sabers et al., 1995). It is an evolutionarily conserved atypical serine/threonine protein kinase, particularly in mammals, where it shares a remarkable 95% amino acid sequence identity (Janus et al., 2005). Full-length mTOR has a molecular weight of 289 kDa, and consists of multiple functional motifs (**Figure 3.1**), including two focal adhesion targeting (FAT) domains, a FKPB12-rapamycin binding (FRB) domain, a catalytic kinase (KIN) domain at the C-terminus, and up to 20 tandem repeated motifs at the N-terminus (known as HEAT repeats) (Hoeffer and Klann, 2010; Yip et al., 2010). The FAT domains are essential for mTOR catalytic activity and are highly homologous to the lipid kinase domain of PI3K, thus grouping mTOR as a member of the large PI3K-related kinase (PIKK) family. The FRB domain and HEAT repeats are regions where mTOR binds to other proteins. The KIN domain contains several evolutionarily conserved serine and threonine residues, which can regulate mTOR activity via phosphorylation (Hoeffer and Klann, 2010; Jacinto, 2008). Of particular note is the Ser2448 residue, whose phosphorylation level correlates with mTOR catalytic activity (Chiang and Abraham, 2005; Holz and Blenis, 2005; Reynolds et al., 2002).

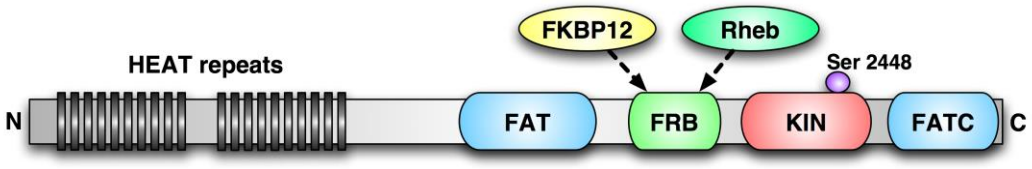

Figure 3.1 mTOR primary structure. Key motifs have been marked.

In cells, mTOR exists as components of large, heteromeric protein complexes, with differing biological functions (Laplante and Sabatini, 2012). At present, two complexes have been identified, namely mTOR complex 1 (mTORC1), and mTOR complex 2 (mTORC2). mTORC1 comprises six known subunits, while mTORC2 comprises seven known subunits (**Figure 3.2**). Both complexes share some common subunits, including mTOR, GβL (also known as mLST8) (Kim et al., 2003), Deptor (Peterson et al., 2009), and the Tti1/Tel2 complex (Kaizuka et al., 2010). mTORC1 also contains its own unique subunits: Raptor (Hara et al., 2002; Kim et al., 2002) and PRAS40 (Sancak et al., 2007; Thedieck et al., 2007; Wang et al., 2007b), while mTORC2-specific components include Rictor (Jacinto et al., 2004; Sarbassov et al., 2004), Protor1/2 (Pearce et al., 2007), and mSin1 (Frias et al., 2006). Of these differences, Raptor and Rictor are classically used to distinguish between mTORC1 and mTORC2, respectively. Interestingly, mTORC1 and mTORC2 exhibit different sensitivities to rapamycin. Unlike mTORC1, mTORC2 does not bind to rapamycin and is much less sensitive to rapamycin treatment (Jacinto et al., 2004; Sarbassov et al., 2004). In these complexes, besides the catalytic core subunit mTOR, other components are also critical to the regulation of mTOR complex activity, functioning as either positive or negative regulators, although their detailed roles still remain largely elusive (Laplante and Sabatini, 2012).

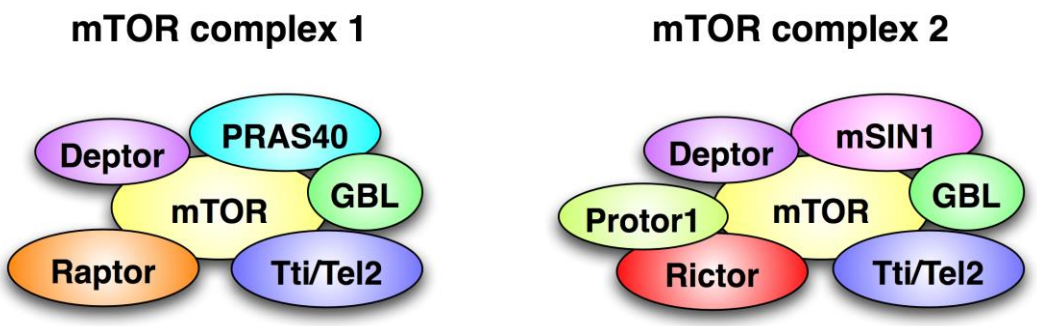

Figure 3. 2 Components of mTORC1 and mTORC2.

Given their unique compositions, mTOR complexes also have their distinct functions. mTORC1 mainly regulates protein synthesis, lipid biogenesis, mitochondrial metabolism, cell growth, and autophagy (Zoncu et al., 2011). It has two well-known, direct, downstream targets: eukaryotic translation initiation factor 4E (eIF4E)-binding protein 1 (4E-BP1), and p70 S6 kinase (p70S6K), both of which function as translational regulators (Ma and Blenis, 2009). The phosphorylation of 4E-BP1 blocks its inhibitory effect on eIF4E, allowing for m7GTP cap-dependent translation to proceed, whereas p70S6K phosphorylation promotes the formation of translation initiation complexes enhancing mRNA translation and thus modulating protein synthesis (Kantidakis et al., 2010). In contrast to mTORC1, much less is known on mTORC2 downstream pathways. It is thought that mTORC2 can regulate anabolism, cell survival, and cytoskeletal organization via phosphorylation of Akt and PKCα (Ikenoue et al., 2008; Oh and Jacinto, 2011; Sarbassov et al., 2005b; Zhang et al., 2012a).

Dysregulation of mTOR signalling occurs in many human diseases (Dazert and Hall, 2011; Laplante and Sabatini, 2012). One example is in cancer, where mTORC1 signalling is frequently hyper-activated (Depowski et al., 2001; Kirkegaard et al., 2005). Recent reports show that up to 80% of human cancers display hyper-activation of mTORC1 signalling due to loss of tumour suppressors or activation of oncogenes

(Cargnello et al., 2015). This constitutive mTORC1 activation is thought to trigger cancer development and progression by enhancing the synthesis of oncogenic proteins that regulate proliferation, energy metabolism, cell survival, cell motility, angiogenesis, and metastasis (Laplante and Sabatini, 2012; Zhou and Huang, 2010).

PRL-3 has previously been reported as a metastasis-associated oncoprotein, whose expression positively correlates with advanced cancer stages (Bessette et al., 2008; Saha et al., 2001). Analysis of cancer patient samples revealed a high frequency of PRL-3 expression in many types of tumours but not in paired normal tissues, highlighting the significance of PRL-3 as a marker of poor prognosis in multiple cancer types (Bessette et al., 2008; Park et al., 2013a; Wang et al., 2010). An understanding of the molecular roles of PRL-3 has thus emerged as a new frontier in cancer research.

Interestingly, like mTORC1, PRL-3 has been shown to promote tumour initiation and progression through various means, including accelerating cell proliferation, preventing cell death, inducing angiogenesis, as well as enhancing cell invasion and metastasis (Al-Aidaroos and Zeng, 2010). Based on this observation, it was hypothesized that PRL-3 might induce cancer progression by potentially regulating mTOR signalling. To test this hypothesis, the following objectives will be addressed:

i) To test whether PRL-3 could activate mTOR signalling; and

ii) To study the biological effects of PRL-3-mediated activation of mTOR signalling.

3.2. Experimental outline

1. Determine the relevance of PRL-3 expression and mTOR activation *in vivo* and *in vitro*.
2. Investigate the effect of PRL-3 overexpression on mTOR signalling under both normal and stressed conditions.
3. Study the biological effect of PRL-3-mediated activation of mTOR signalling under rapamycin treatment.
4. Analyse the colon cancer patient cohorts to elucidate the clinical relevance of the relationship between PRL-3, mTORC1 related genes, and patient survival.

3.3. Results

3.3.1. PRL-3 expression positively correlates with mTOR activity *in vivo*

To investigate the relationship between PRL-3 expression and mTOR activity, 12 sets of tumours and matched normal tissue samples from gastric cancer patients were analysed for protein expression levels of PRL-3 and phosphorylation status of Thr37/46 on 4E-BP1, a direct mTORC1 substrate and an indicator of mTOR oncogenic activity (Brunn et al., 1997). PRL-3 protein was found to be exclusively expressed in all tumour samples, but not in any of the patient-matched normal samples (**Figure 3.3A**). Notably, phosphorylated 4E-BP1 also exhibited a distinct expression pattern between tumours and their matched normal tissues samples. Subsequently, using the software Image J, the densitometric ratio of phosphorylated 4E-BP1/total 4E-BP1 for each sample was quantified and the fold changes between each tumour and paired normal sample were compared. It was found that 9 out of 12 (75%) PRL-3-expressing tumours showed higher ratios of phosphorylated 4E-BP1/total 4E-BP1 than their matched normal tissue samples (*asterisks*, **Figure 3.3B**). These clinical results imply a possible relationship between PRL-3 expression levels and mTOR activity in tumour tissues.

To determine whether changes in PRL-3 expression correlates with mTOR activity *in vivo*, spontaneous mouse mammary tumour virus (MMTV) transgenic models were employed. This model expresses a polyomavirus middle T oncoprotein (PyMT) under the transcriptional control of a MMTV promoter-enhancer, leading to the formation of palpable mammary tumours in female mice as early as 6 weeks old (Guy et al., 1992). In the MMTV-PyMT system, PyMT was highly expressed in mammary tissues at relatively constant levels in heterozygous transgenic adult female mice (**Figure 3.3C**). In contrast, endogenous PRL-3 protein expression increased steadily over the same period,

accumulating at later stages of tumour development (**Figure 3.3C**). Significantly, the increase in PRL-3 expression during mammary tumour development closely correlated with an increase in levels of both phosphorylated 4E-BP1 and phosphorylated Ser2448 of mTOR, but not protein expression levels of either (**Figure 3.3C**). Importantly, Ser2448 of mTOR lies within the C-terminal 'repressor domain' of mTOR, and its phosphorylation is an important marker for activation of the mTOR/4E-BP1 pathway (Chiang and Abraham, 2005; Sekulic et al., 2000).

In conclusion, these *in vivo* observations suggest that I) a correlation between PRL-3 expression levels, mTOR activity, and mTOR activation-associated phosphorylation exists, and II) PRL-3 might regulate mTOR activity by post-translational modification(s) rather than through upregulation of protein expression.

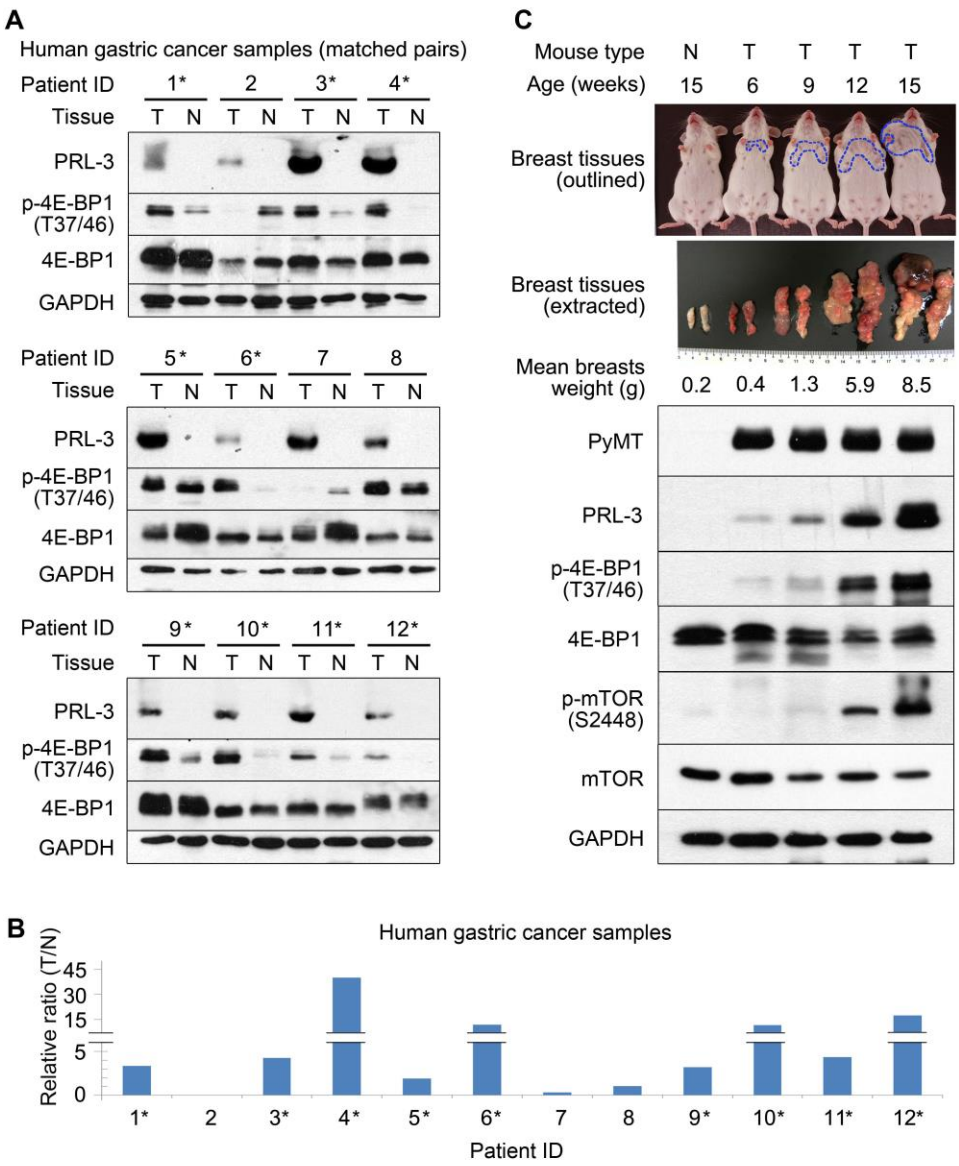

Figure 3. 3 PRL-3 expression positively correlates with mTOR activity *in vivo*.

(A) Twelve pairs of tumour and matched normal tissues from gastric cancer patients were analysed with antibodies against PRL-3, p-4E-BP1 (T37/T46), total 4E-BP1, and GAPDH. **(B)** The ratio of phosphorylated/total 4E-BP1 band densities in tumour tissues were calculated and normalized to the phosphorylated/total 4E-BP1 ratio in matched normal tissues. *Asterisks*, patient tumour samples wherein 4E-BP1 hyperphosphorylation correlates with PRL-3 expression. **(C)** Normal and MMTV-PyMT mammary tissues over the course of spontaneous tumour development (6, 9, 12, and 15 weeks) were analyzed with antibodies against PyMT, PRL-3, p-4E-BP1 (T37/46), 4E-BP1, p-mTOR (S2448), mTOR and GAPDH. Top panel, images of normal mice (N) or transgenic MMTV-PyMT mice (T) between the ages of 6 to 15 weeks. Middle panel, representative images of excised breast tissues from mice. Blue dashed lines, gross size of palpable mammary tumours in MMTV-PyMT mice. Lower panels, correlation between PRL-3 expression and phosphorylation of 4E-BP1 and mTOR.

3.3.2. PRL-3 induces mTOR phospho-activation *in vitro*

Previously, in ovarian cancer, PRL-3 was shown to promote autophagy (Huang et al., 2014), which is a self-degradative process inhibited by mTOR activity (Jung et al., 2010). To clarify the apparent discordance between the activation of both mTOR and autophagy by PRL-3, plasmids encoding EGFP-PRL-3 (PRL-3), EGFP-PRL-3-C104S (C104S; catalytically-inactive mutant), or empty EGFP vector (Vec) were transiently transfected to nine different human cancer cell lines from diverse tissue types. In six out of the nine cell lines tested (67%), consistent 1.4-2.5 fold increase in mTOR phosphorylation was observed upon overexpression of wild-type PRL-3, but not the catalytic-inactive PRL-3 mutant or vector control (**Figure 3.4A**). However, in three out of nine cell lines (33%), no increase in mTOR phosphorylation was observed upon PRL-3 expression (**Figure 3.4B**). Notably, this latter group included A2780 human ovarian cancer cells, wherein PRL-3 was previously reported to activate autophagy (Huang et al., 2014). Interestingly, rapamycin-mediated inhibition of mTOR failed to dampen the increase in autophagy promoted by PRL-3 in A2780 cells (Huang et al., 2014), indicating an mTOR-independent route of autophagy activation by PRL-3 in these cells. Taken together, these results suggest that PRL-3 overexpression results in mTOR phospho-activation in a phosphatase activity-dependent and cell-line specific manner.

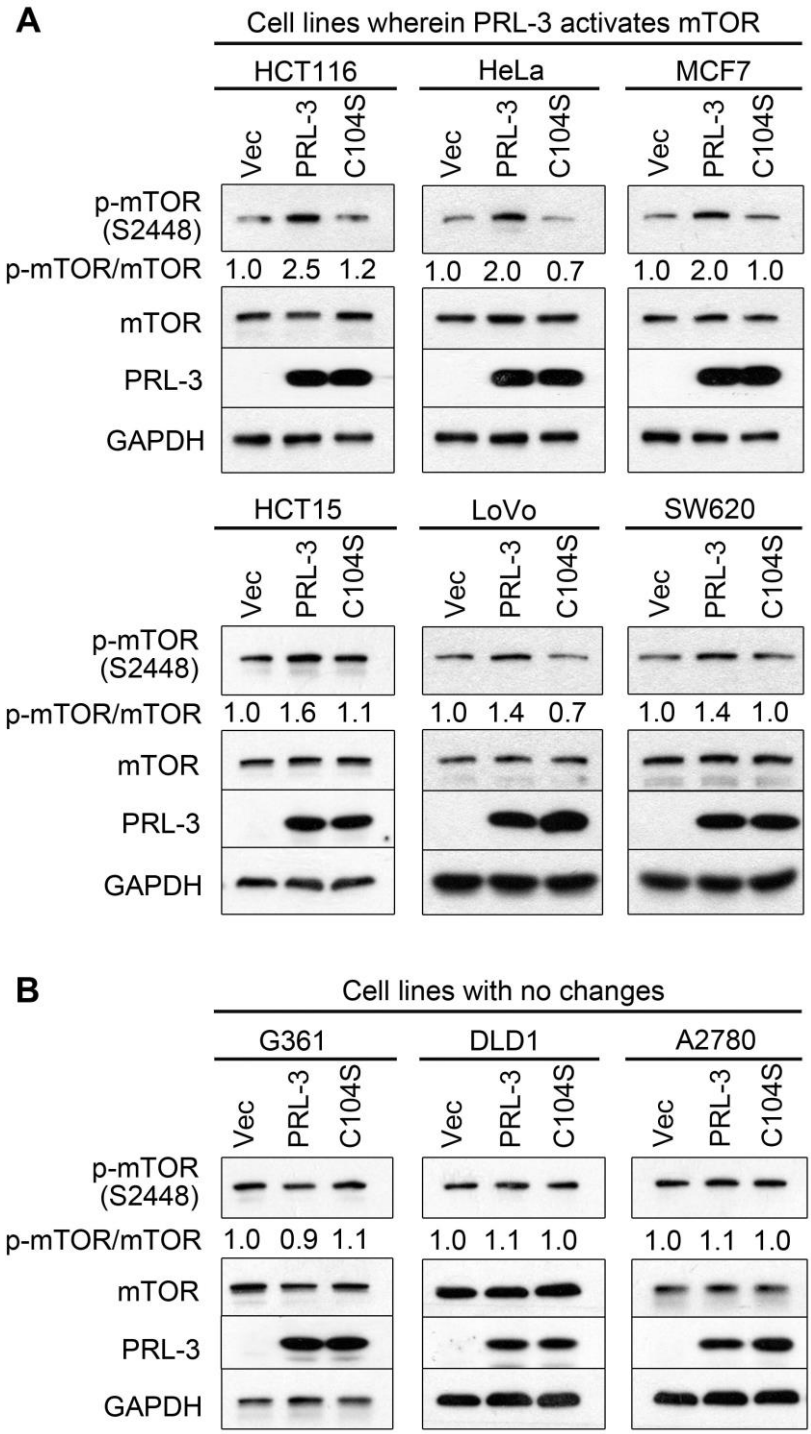

Figure 3. 4 PRL-3 induces mTOR phospho-activation *in vitro*. Overexpression of EGFP vector (Vec), EGFP- PRL-3 (PRL-3) or EGFP-PRL-3-C104S (C104S) in a panel of 9 human cancer cell lines. PRL-3 upregulates mTOR phosphorylation in (A) HCT116, HeLa, MCF7, HCT15, LOVO, and SW620 cells, but not in (B) G361, DLD1 or A2780 cells. GAPDH served as a loading control. For each cell line, the ratio of phosphorylated/total mTOR band densities were calculated and normalized to the phosphorylated/total mTOR ratio in corresponding vector control lanes.

3.3.3. PRL-3 activates mTOR signalling under both normal and stressed conditions

As discussed earlier, the mTOR pathway integrates multiple environmental cues to regulate translation in response to stress. Deprivation of oxygen or nutrients, particularly amino acids, results in reduced mTOR activation and dephosphorylation of downstream effectors of protein translation, including 4E-BP1 and p70S6K (Arsham et al., 2003; Proud, 2002). To investigate whether PRL-3-mediated hyperactivation of mTOR could persist under such stressors, HCT116 cells stably expressing EGFP-PRL-3 (PRL-3), EGFP-PRL-3-C104S (C104S; catalytically-inactive mutant), or empty EGFP vector (Vec), were engineered and cultured under normal, hypoxia (oxygen-deprived), serum free, or amino-acid starved conditions to monitor mTOR activity. Hypoxia, serum deprivation, and amino acid starvation are three well-characterized environmental stressors that inhibit mTOR activity (Bai and Jiang, 2010; Demetriades et al., 2014). Interestingly, despite a reduction in mTOR phosphorylation in cells grown under these stress conditions, HCT116-PRL-3 cells displayed persistent hyperphosphorylation of mTOR relative to HCT116-Vec or HCT116-C104S cells (**Figure 3.5A, lanes 2, 5, 8, 11, 14**). Moreover, a similar trend in the phosphorylation status of mTOR's direct downstream effector-substrates – 4E-BP1 and p70S6K – was also observed. In particularly, the phosphorylation level of 4E-BP1 and p70S6K in HCT116-Vec and HCT116-C104S cells were reduced drastically under hypoxia and amino-acid starved conditions, yet HCT116-PRL-3 cells maintained a high phosphorylation level of these two substrates, indicting persistent activation of mTOR signalling (**Figure 3.5A**).

To discount the possibility of a cell-specific observation, similar experiments were carried out in HeLa cells. Similar results were obtained in this cell line, wherein cells overexpressing PRL-3 persistently promoted mTOR hyperphosphorylation and

downstream signalling relative to cells overexpressing control (Vec) or catalytically-inactive PRL-3 mutant (C104S) (**Figure 3.5B**).

In a complimentary approach, small hairpin RNA (shRNA) constructs were used to stably deplete PRL-3 from HCT116 cells which express endogenous PRL-3 abundantly. In contrast to PRL-3 overexpression, depletion of PRL-3 in HCT116 cells resulted in reduced phosphorylation of mTOR and its downstream effectors 4E-BP1 and p70S6K under normal, hypoxia, serum free, and amino-acid starved conditions (**Figure 3.5C**). Thus, these results suggest that PRL-3 activates mTOR signalling under both normal and stressed cellular conditions.

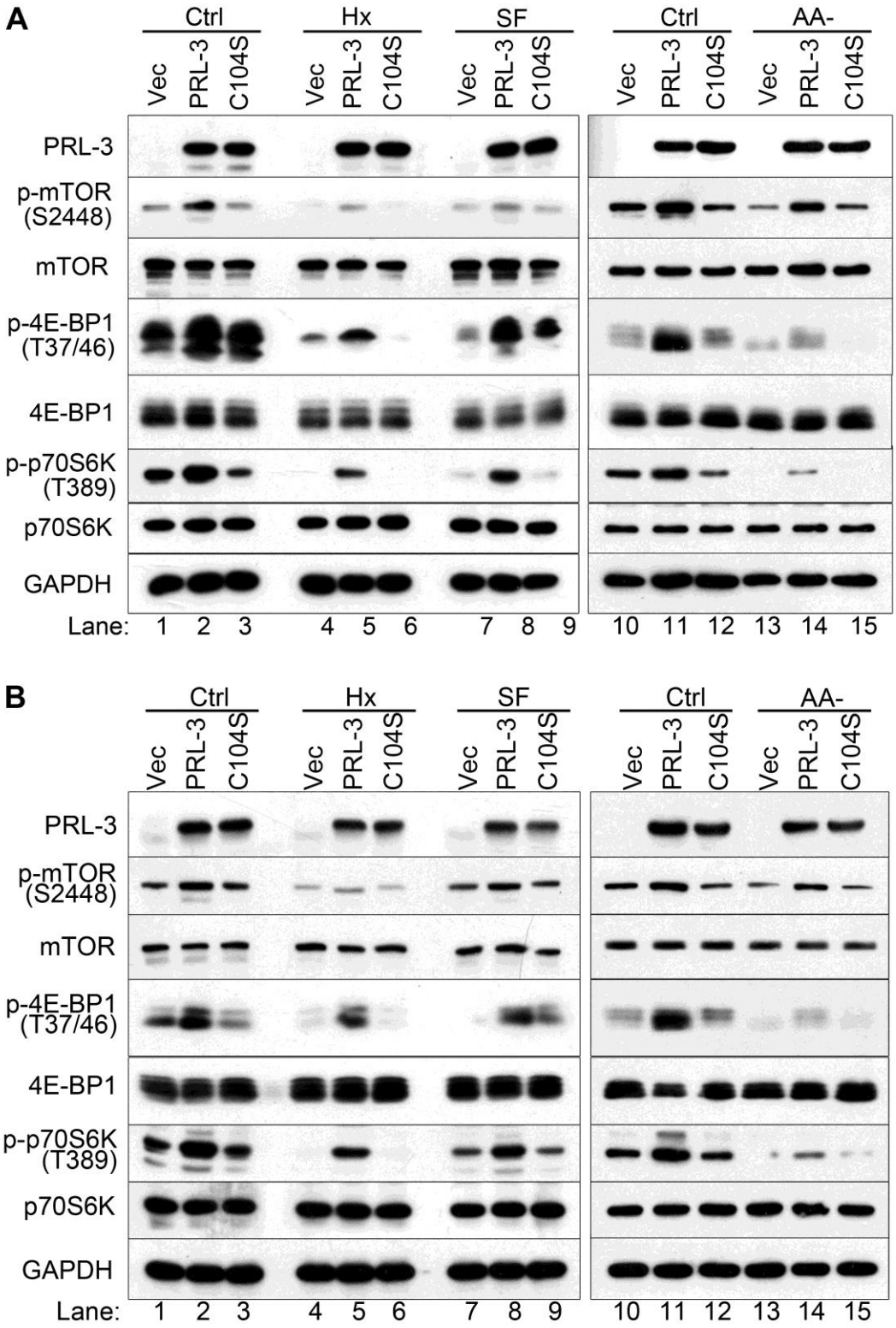
A
Ctrl
Hx
SF
Ctrl
AA-
Vec
PRL-3
C104S
PRL-3
p-mTOR (S2448)
mTOR
p-4E-BP1 (T37/46)
4E-BP1
p-p70S6K (T389)
p70S6K
GAPDH
Lane: 1 2 3 4 5 6 7 8 9 10 11 12 13 14 15
B
Ctrl
Hx
SF
Ctrl
AA-
Vec
PRL-3
C104S
PRL-3
p-mTOR (S2448)
mTOR
p-4E-BP1 (T37/46)
4E-BP1
p-p70S6K (T389)
p70S6K
GAPDH
Lane: 1 2 3 4 5 6 7 8 9 10 11 12 13 14 15

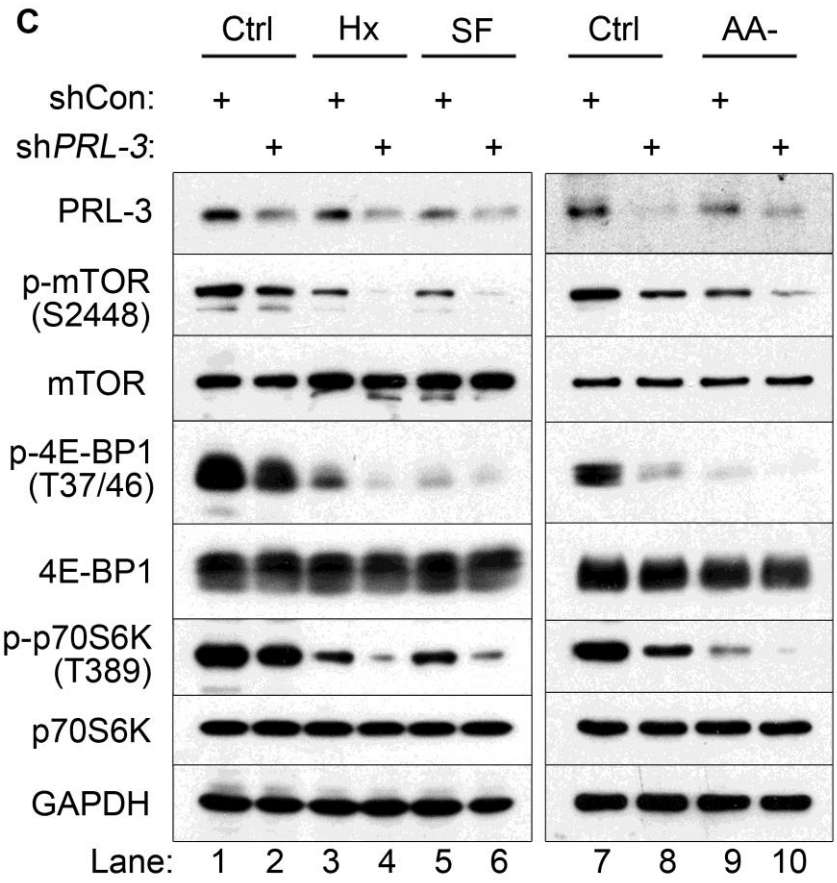

Figure 3. 5 PRL-3 activates mTOR signalling under both normal and stressed conditions. (A) HCT116-Vec, HCT116-PRL-3 and HCT116-C104S cells were cultured for 24 h in full media under normal (Ctrl), hypoxia (Hx), or serum free (SF) conditions, or cultured for 1 h in full media under normal (Ctrl) or amino-acid starved (AA-) conditions. Then cells were lysed and western blot analysis was performed with antibodies against PRL-3, p-mTOR (S2448), mTOR, p70-S6K, p-p70-S6K (T389), 4E-BP1, p-4E-BP1 (T37/T46) and GAPDH. GAPDH used as a loading control. (B) HeLa cells were transfected with EGFP-PRL-3 (PRL-3), EGFP-PRL-3-C104S, or empty EGFP vector (Vec), then cells were cultured and analysed as in (A). (C) HCT116 cells stably expressing small hairpin RNA (shRNA) against PRL-3 (sh*PRL-3*) or control shRNA (shCon) were cultured and analysed as in (A).

3.3.4. PRL-3 sensitizes cell growth to rapamycin treatment.

Oncogenic activation of mTORC1 could enhance cell growth, survival, and proliferation by phosphorylating two main substrates, 4E-BP1and p70-S6K (Laplante and Sabatini, 2012). Since cells overexpressing PRL-3 exhibited increased phosphorylation level of p70-S6K and 4E-BP1, it is necessary to determine the role of PRL-3 on mTOR in mediating cell growth. For this, the MTS assay was utilized to compare the effects of rapamycin treatment on HCT116-Vec or HCT116-PRL-3 cells. In untreated controls, there was an insignificant difference (10%) in cell growth between HCT116-Vec and HCT116-PRL-3 cells. In contrast, in the presence of 100 nM rapamycin, compared to untreated cells, HCT116-PRL-3 cell growth decreased by ~28% while HCT116-Vec cells decreased by ~7%. (**Figure 3.6A, left panel**). Similar results were observed with cells cultured under hypoxia conditions. Upon oxygen deprivation, compared to HCT116-Vec cells, HCT116-PRL-3 cells displayed 7% higher cell growth rate and showed heightened sensitivity to rapamycin treatment; at the present of 100 nM rapamycin, the HCT116-PRL-3 cell growth decreased by ~20% while HCT116-Vec cells decreased by 5% **(Figure 3.6A, right panel)**. In addition, analysis of two parental colon cancer cell lines, DLD-1 (PRL-3 negative) and HCT116 (PRL-3 positive) (**Figure 3.6B**) showed that HCT116 cells were more sensitive to rapamycin treatment compared to DLD-1 cells. Compared to matched untreated controls, a significant reduction (~22%) in cell growth was observed in HCT116 cells after 48 hours incubation with 100 nM rapamycin compared with only 8% for DLD-1 cells. Similar results were also observed for cells under hypoxia (**Figure 3.6C**). Collectively, these data revealed that cells with higher PRL-3 expression are more sensitive to rapamycin treatment, implying that PRL-3 may sensitize cell growth to rapamycin treatment and mTOR signalling pathway might be involved in PRL-3-mediated cell growth.

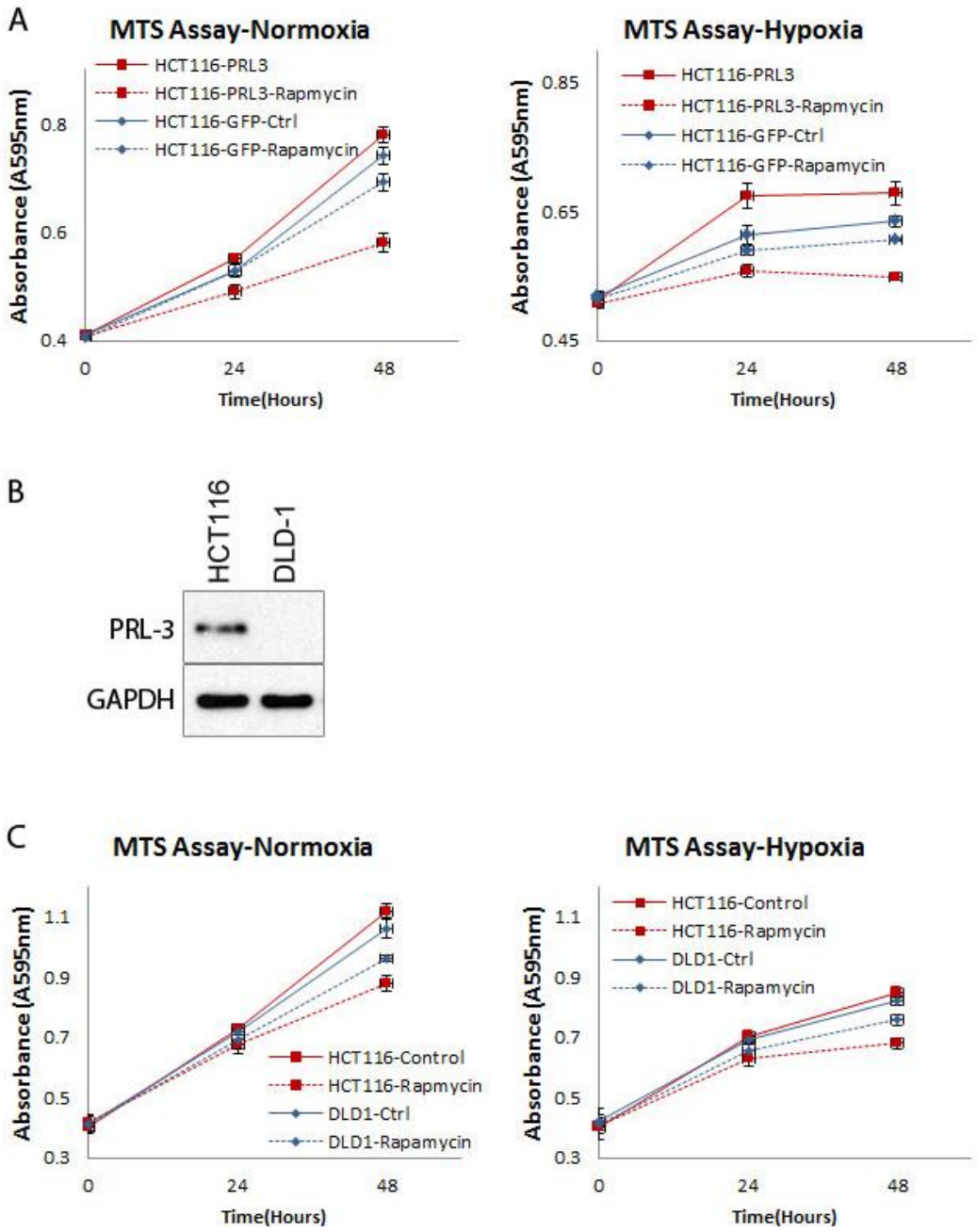

Figure 3. 6 PRL-3 sensitizes cell growth to rapamycin treatment. (A) HCT116-Vec, HCT116-PRL-3 and HCT116-C104S cells were cultured in full media in the presence of DMSO (Ctrl) or 100 nM rapamycin (rapamycin) for 48 hours under normoxia (left panel) or hypoxia (right panel) condition. Relative proliferation rates were assessed by MTS assay. (B) DLD-1 cells and HCT116 cells lysed and western blot analysis was performed with antibodies against PRL-3 and GAPDH. (C) DLD-1 cells (PRL-3 negative) and HCT116 cells (PRL-3 positive) were cultured in full media in the presence of DMSO (Ctrl) or 100 nM rapamycin (rapamycin) for 48 hours under normoxia (left panel) or hypoxia (right panel) condition. Relative proliferation rates were measured using the MTS assay method. Three independent experiments were repeated and all data were shown as mean ± SE.

3.3.5. PRL-3 promotes cancer cell motility and invasiveness in a rapamycin-sensitive manner

PRL-3 has been described to promote cancer metastasis by increasing both motility and invasiveness of cancer cells (Al-Aidaroos and Zeng, 2010). To understand the mechanistic basis of this phenomenon, a wound healing assay on HCT116-Vec and HCT116-PRL-3 cells was conducted in the presence of DMSO or rapamycin. Supporting a pro-motile role for PRL-3, HCT116-PRL-3 cells displayed complete wound closure within 48 hours compared to HCT116-Vec cells which still had a large gap (**Fig. 3.7A, panels i-ii**). Remarkably, the motility of both cell lines were completely suppressed by rapamycin treatment (**Fig. 3.7A, panels iii-iv**). , suggesting a role for mTOR signalling in PRL-3-driven motility.

Besides increased motility, the ability of tumour cells to degrade the ECM is an essential property for tumour invasion into surrounding tissues. Previously, overexpression of PRL-3 was reported to promote invasiveness of colon cancer cells (Peng et al., 2009) and correlate significantly with clinical hepatocellular carcinoma invasiveness (Zhao et al., 2008). In agreement with these previous findings, overexpression of PRL-3 significantly increased the invasiveness of HCT116 cells through a basement matrix relative to control cells (**Figure. 3.7B; p = 5.988E-05**). Notably, rapamycin treatment suppressed invasiveness of PRL-3-overexpressing cells to similar levels as the control cells (**Figure. 3.7B**). Collectively, these results suggest that mTOR is an important mediator of both PRL-3-driven motility and invasion.

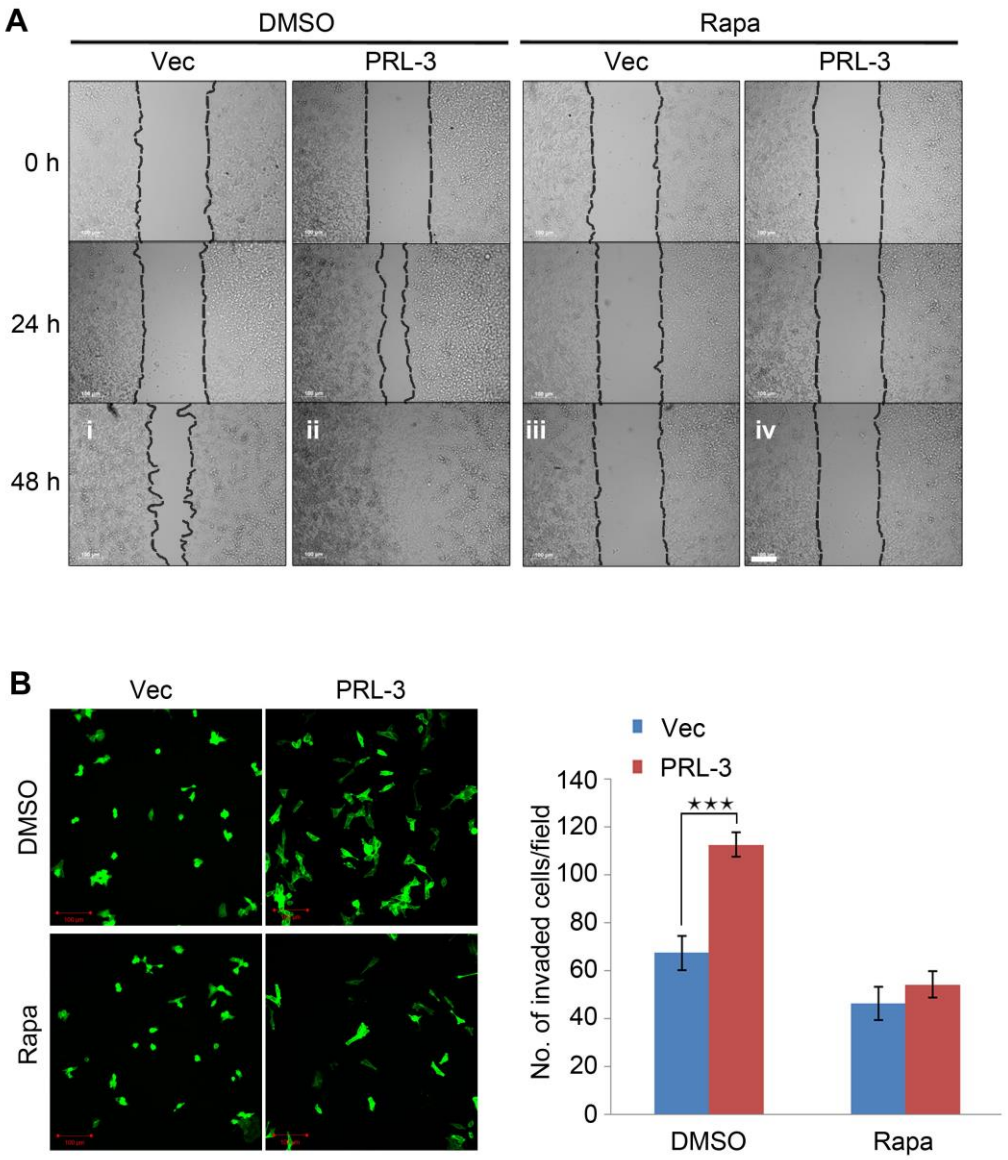

Figure 3. 7 PRL-3 promotes cancer cell motility and invasiveness in a rapamycin-sensitive manner. (A) Monolayers of HCT116 cells stably overexpressing EGFP vector only (Vec) or EGFP-tagged wild-type PRL-3 (PRL-3) were 'wounded' and monitored over 48 h in the presence or absence of 100 nM rapamycin (Rapa). Phase-contrast images were captured at the indicated intervals. Dashed lines, boundary of cell monolayers on either side of the wound. Scale bar, 200 μm. (B) A transwell assay was used to determine the invasion potentials of HCT116-EGFP (Vec) or HCT116-EGFP-PRL-3 (PRL-3) cells. The images of invaded HCT116 cells stably overexpressing EGFP vector only (Vec) or EGFP-tagged wild-type PRL-3 (PRL-3) through a basement matrix were captured by microscopy after culturing in the presence or absence of 100 nM rapamycin. Cell numbers from three randomly-selected fields were counted and graphed. Results are depicted as mean ± S.D; ***p = 5.988E-05. Experiments were repeated twice with similar results. Scale bar, 100 μm.

3.3.6. PRL-3 upregulates production of MMP-2 and MMP-9

MMP-2 and MMP-9 are enzymes that can degrade ECM and activate a number of growth factors, thus playing important roles in tumour invasion and metastasis (Gialeli et al., 2011; Pratheeshkumar et al., 2012). Production of MMP-2 and MMP-9 has been reported to be up-regulated by increased mTOR activity and suppressed on rapamycin treatment (Pratheeshkumar et al., 2012; Zhang et al., 2004). Since PRL-3 activated mTOR signalling and enhanced cell invasiveness, the effect of PRL-3 on MMPs production was examined. Interestingly, overexpression of PRL-3 increased the production of MMP-2 and MMP-9 at both mRNA and protein levels (**Figure 3.8A**). Subsequently, the relation between PRL-3-mediated mTORC1 activation and MMPs secretion was investigated. Compared to HCT116-Vec cells, HCT116-PRL-3 cells had higher levels of secreted MMP-2 and MMP-9 protein in conditioned media (**Figure 3.8B)**. Notably, rapamycin treatment abolished PRL-3-induced secretion of MMP-2 and MMP-9, concomitant with suppression of phosphorylation of 4E-BP1 and p70-S6K (**Figure 3.8B**), suggesting that PRL-3 might upregulate MMP-2 production via increased mTORC1 activity.

To further study the relationship of PRL-3 and mTORC1 activation, a publically available clinical dataset from colon cancer patients (GSE40967, n = 566) was analysed. PRL-3 expression was found to positively correlate with the mRNA expression of several matrix metalloproteinase proteins, including MMP-2 and MMP-9, in addition to mTOR regulators, LAMTOR 1 and 2 (lysosomal adaptor and mitogen-activated protein kinase (MAPK) and mTOR activator/regulator 1 and 2) (**Table 3.1**). Indeed, in HCT116 cells, overexpression of PRL-3 induced MMP-2 and MMP-9 expression at transcriptional level (**Figure 3.8A**), corroborating these clinical observations.

Interestingly, the cohort analysis of colon cancer patients revealed that MMP-2 expression had a high prognostic value for patient survival when PRL-3 was highly expressed ($p < 0.05$; **Figure 3.8C, right panel**), but not when PRL-3 was expressed at lower levels ($p = 0.851$; **Figure 3.8C, left panel**). This suggested that MMP-2 may be useful as a prognostic marker when there is PRL-3-driven mTOR hyperactivity.

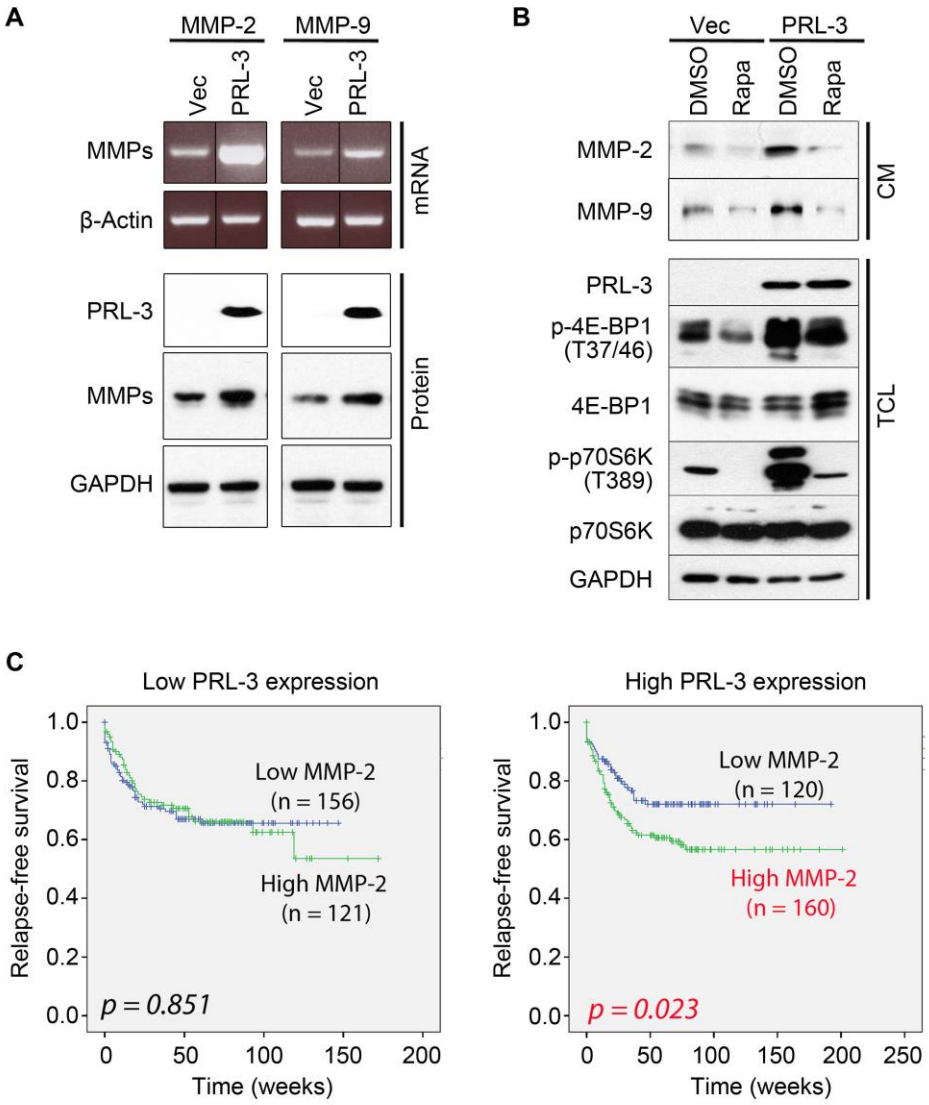

Figure 3. 8 PRL-3 upregulates MMP2/9 production. (A) mRNA and protein levels of MMP-2 and MMP-9 in HCT116-Vec and HCT116-PRL-3 cells. (B) The conditioned media (CM) from HCT116-Vec or HCT116-PRL-3 cells after culturing in the presence or absence of 100 nM rapamycin for 24 h was harvested, concentrated, and analysed by immunoblotting with indicated antibodies. *CM*, conditioned media. *TCL*, total cell lysates from matched cell cultures. (C) Kaplan-Meier analysis of colorectal cancer patient cohort GSE40967 (*n* = 557) stratified by low or high PRL-3 expression.

TABLE 3. 1 Spearman's correlation between PRL-3 gene expression and mTORC1 related genes in colon cancer patient dataset (GSE 40967, n = 566)

	PRL-3	MMP-2	MMP-9	LAMTOR1	LAMTOR2
PRL-3 Correlation Coefficient	1.000	0.160	0.112	0.266	0.106
p-value		0.000**	0.008**	0.000**	0.012*

Statistical significance, $^{**}p < 0.01$, $^{*}p < 0.05$

3.4. Discussion

In this study, a positive correlation between PRL-3 expression and mTOR activity was characterized in human cancer samples and the spontaneous breast tumor MMTV-PyMT mouse model. This result is consistent with previous reports that PRL-3 expression was highly upregulated (Wang et al., 2010) and mTOR activity was abnormally activated in many types of human cancers (Advani, 2010). In the MMTV-PyMT system, increasing expression of PRL-3 correlated with increased mTOR activity during tumour development, indicating a potential regulatory relationship.

In addition, PRL-3 overexpression induced an aberrant activation of mTOR in cancer cells, as reflected by the hyperphosphorylation of the direct substrates of mTORC1, 4E-BP1 and p70S6K. Interestingly, this phenomenon was still observed under conditions of oxygen, serum, or amino acid deprivation, wherein PRL-3 sustained mTORC1 activation despite these growth-suppressing limitations. Furthermore, PRL-3 overexpression enhanced cell motility and invasiveness, and promoted the expression and secretion of oncogenic collagenases MMP-2 and MMP-9. Importantly, these PRL-3-driven effects could be effectively suppressed by rapamycin treatment. These results collectively suggest that mTOR is an important effector of PRL-3-mediated tumour progression.

It has been previously reported that PRL-3 could promote proliferation of cytokine-dependent cells under limited cellular resources (Park et al., 2013b). In agreement with this result, PRL-3 overexpressing cells displayed a higher proliferative ability relative to their corresponding control cells under both normal and hypoxia conditions. Intriguingly, compared to control cells, cells with higher PRL-3 expression (either endogenous or exogenous) showed heightened sensitivity to rapamycin treatment. A possible explanation to this interesting observation is "oncogene addiction", wherein inhibition of a dominant oncogene or hyperactive signalling pathway results in detrimental effects in tumor cells (Weinstein and Joe, 2008). Many oncogenes have been reported to confer addiction (Sharma and Settleman, 2007). For example, multiple myeloma cells and glioblastoma cell lines lacking PTEN (a suppressor of the mTOR signalling pathway) appear more sensitive to mTOR inhibitors, an effect thought to depend on the increased mTOR activity in PTEN-/- cells during tumour development (Neshat et al., 2001). Similarly, PRL-3 may induce hypersensitivity to mTOR inhibition due to hyperactive mTOR signalling addiction. Indeed, rapamycin treatment abolished the PRL-3-medicated cell proliferation, motility and invasion, suggesting a key role for mTOR as PRL-3's oncogenic effector.

Interestingly, MMP-2 expression correlated with shorter patient survival when PRL-3 was highly expressed. Further analysis of a clinical dataset showed a positive correlation between PRL-3 expression levels and that of the downstream targets of mTORC1, MMP-2 and MMP-9. In cultured cells, PRL-3 overexpression resulted in an mTORC1-dependent increase in the production of oncogenic MMP-2 and MMP-9, two key collagenases involved in invasion and metastasis, and markers of poor prognosis in multiple cancers (Kurschat et al., 2002; van Kempen and Coussens, 2002). Although a previous report indicates the involvement of integrin beta-1-ERK signalling in PRL-3-mediated upregulation of MMP-2 (Peng et al., 2009), here we found that

PRL-3-induced MMP-2 and MMP-9 secretion was sensitive to rapamycin-mediated mTORC1 inhibition. It is possible that cross-activation between the Ras-MAPK and PI3K-mTORC1 pathways might account for the co-regulation of MMP-2 and MMP-2 expression, leading to increased tumour invasiveness. Indeed, activation of the RAS-ERK pathway has been shown to increase mTORC1 activity through increased ERK and RSK signalling to the TSC complex (Mendoza et al., 2011).

It was proposed that by endowing tumour cells with the ability to disseminate from unfavourable microenvironments (such as limited nutrient availability and/or limited oxygen) in search of more favourable conditions, PRL-3 may provide a strategic survival advantage to tumour cells via increased mTOR-dependent cell motility, invasiveness and production of MMP-2 and MMP-9.

Collectively, these data reveal a novel pathway for PRL-3-mediated cancer progression via mTORC1 activation.

CHAPTER 4: PRL-3 REQUIRES AKT-TSC2-RHEB AND RAG GTPASE TO ACTIVATE mTOR SIGNALLING

4.1. Background

The activity of mTORC1 can be altered based on availability of growth factors, nutrients, energy and stress signals (Caron et al., 2010). By integrating signals from upstream signalling pathways, such as PI3K/Akt, Ras/Erk and LKB1/AMPK pathways, as well as Rag GTPases, mTOR thus functions as a master regulator of environmental cues within cells (Laplante and Sabatini, 2012) (**Figure 4.1**).

PI3K/Akt and Ras/ERK are two mitogen-related signalling pathways, which are mediated by receptor tyrosine kinases (RTKs) and are important for cell growth and homeostasis (Hemmings and Restuccia, 2015; Sundaram, 2006). In the presence of growth factors, RTKs such as epidermal growth factor receptor, insulin receptor, and insulin-like growth factor receptor become activated. These RTKs then recruit the lipid kinase PI3K to the cellular membrane, resulting in the activation of PI3K and subsequent phosphorylation of its substrate phosphatidylinositol-(4,5)-bisphosphate ($PI(4,5)P_2$) to phosphatidylinositol-3,4,5-trisphosphate ($PI(3,4,5)P_3$) (Cantley, 2002). Accumulated $PI(3,4,5)P_3$ attracts Akt to the cell membrane, where it is directly phosphorylated by phosphoinositide dependent protein kinase 1 (PDK1) and PDK2 (known as mTORC2), leading to its activation (Sarbassov et al., 2006; Vanhaesebroeck and Alessi, 2000). Alternatively, RTKs can also induce ERK activation through the Ras-Raf-MEK-ERK kinase cascade (Ma et al., 2005). These two effector kinases, Akt and ERK, finally induce mTORC1 activation via the TSC (tuberous sclerosis complex)-Rheb (Ras homolog enriched in brain) axis (Mendoza et al., 2011; Steelman et al., 2011).

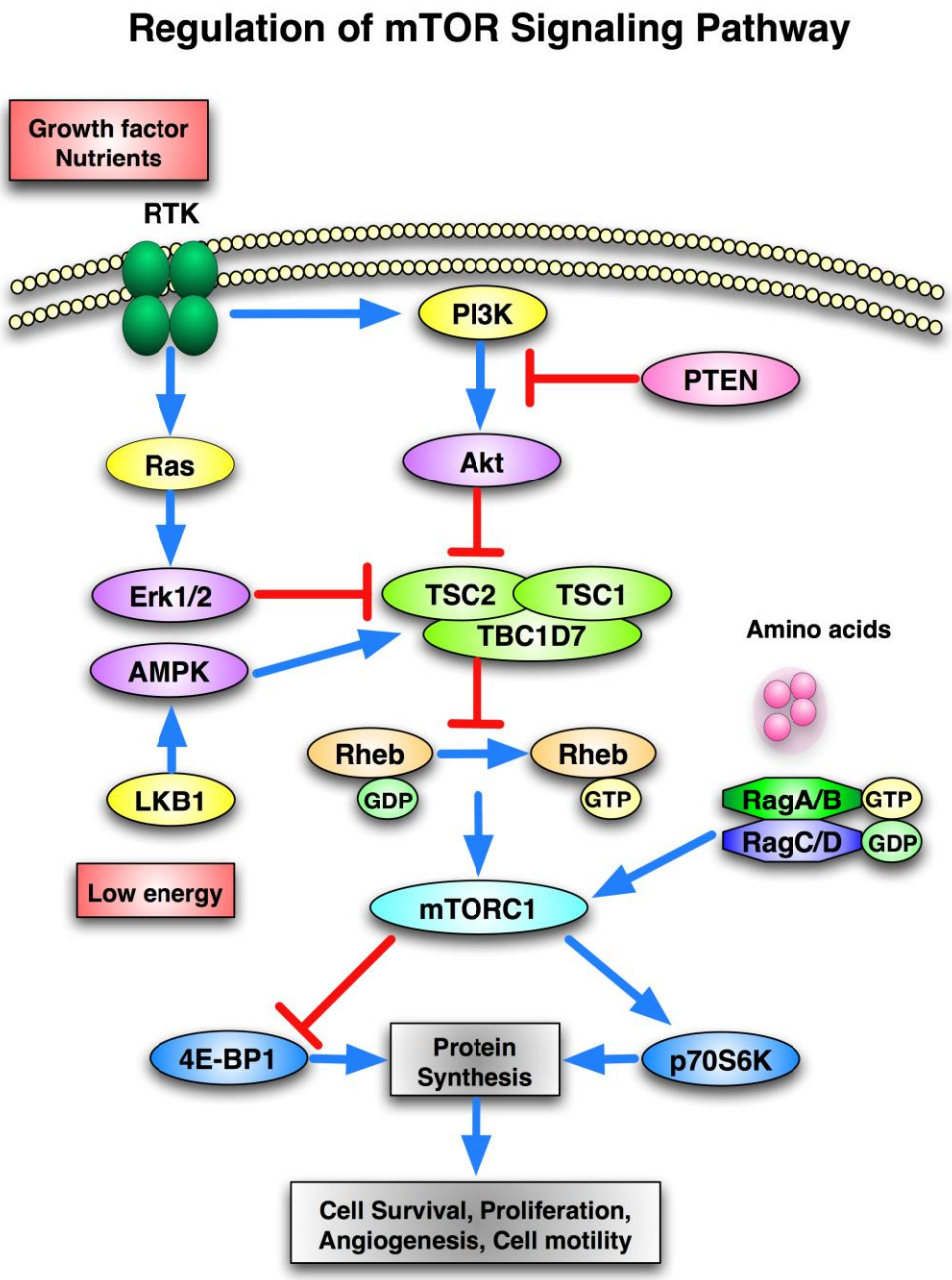

Figure 4. 1 Regulation of mTOR signalling pathway.

In contrast, mTORC1 activity is suppressed by AMPK (Shaw, 2009). AMPK is a metabolism regulator that monitors cellular energy status, as reflected by the ratio of intracelluar AMP to ATP. In response to high AMP:ATP, such as during energy stresses such as glucose deprivation or ischemia, AMPK is activated by phosphorylation (Towler

and Hardie, 2007). Activated AMPK inhibits mTORC1 activity by directly phosphorylating two of its downstream targets, raptor and TSC (Gwinn et al., 2008; Inoki et al., 2003b).

The activity of TSC, a heterotrimeric complex consisting of TSC1, TSC2 and TBC1D7, is regulated by many upstream signals through a series of phosphorylation events (Dibble et al., 2012). For example, AMPK activates TSC, while Akt and Erk inhibit its activity by phosphorylating the catalytic subunit TSC2 at distinct sites (Huang and Manning, 2008). TSC functions as a GTPase-activating protein (GAP) toward the small GTPase Rheb, negatively regulating mTORC1 activity by converting active GTP-bound Rheb into its inactive GDP-bound state at the lysosome (Menon et al., 2014; Tee et al., 2003). When Rheb is in its GTP-bound state, it directly interacts with mTORC1 and strongly stimulates its kinase activity. However, on activation, TSC will induce GDP-bound Rheb accumulation, leading to mTORC1 inhibition (Inoki et al., 2003a; Tee et al., 2003).

Furthermore, to be physically activated by GTP-bound Rheb, mTORC1 must translocate to cellular endomembranes where Rheb is localized (Betz and Hall, 2013). This process requires participation of the Rag GTPases, which are a group of Ras-related small GTPases (Kim et al., 2008; Sancak et al., 2008). In mammals, Rag GTPases are comprised of four members: RagA, RagB, RagC, and RagD. They form obligate heterodimers composed of either RagA or RagB bound to RagC or RagD. The two members of the heterodimer have antithetical nucleotide loading states, wherefore when RagA/B is loaded with GTP, RagC/D is loaded with GDP and vice versa. $RagA/B^{GTP}$ and $RagC/D^{GDP}$ are active forms, which are essential for the activation of mTORC1 (Sancak et al., 2008). Mechanistically, Ragulator, a Rag guanine nucleotide exchange factor, responds to the presence of amino acids by promoting the loading of RagA/B with GTP, thereby enabling Rag heterodimers to interact with mTOR and raptor and recruit

mTORC1 to lysosomes. This relocalization of mTORC1 leads to its encounter with GTP-bound Rheb, and activation (Bar-Peled et al., 2012; Sancak et al., 2010).

Collectively, full mTORC1 activation is a two-pronged process, requiring upstream signals (such as PI3K/Akt, Ras/ERK or LKB1/AMPK) to activate the TSC-Rheb axis, and mTOR translocation to Rheb-resident endomembranes, particularly lysosomes (Betz and Hall, 2013).

In chapter 3, PRL-3 was characterized to promote mTORC1 activation and consequent cell growth, motility and invasiveness under both normal and stressed conditions. However, the molecular mechanism underlying how PRL-3 activated mTORC1 was unknown. In this chapter, the mechanism of PRL-3-mediated activation of mTORC1 is explored.

4.2. Experimental outline

1. Investigate the effect of PRL-3 on TSC2-Rheb signalling.
2. Define which upstream signalling pathway(s) activates PRL-3-driven TSC2-Rheb-mTORC1 activation.
3. Study the effect of PRL-3 on mTOR translocation.
4. Ascertain if Rag GTPase participates in PRL-3-mediated accumulation of lysosomal mTOR
5. Investigate the effect of Rag GTPase on PRL-3

4.3. Results

4.3.1 PRL-3 modulates TSC2-Rheb signalling

One of the best-known upstream regulators of mTORC1 is the TSC-Rheb axis. TSC, a negative regulator of mTORC1, directly regulates GTPase activity of Rheb to modulate mTORC1 activity (Inoki et al., 2002). To understand how PRL-3 activates mTORC1, the effect of PRL-3 on TSC-Rheb axis was first assessed. In HCT116 cells, overexpression of EGFP-PRL-3 (PRL-3), but not the EGFP-PRL-3-C104S (catalytically-inactive mutant, C104S) or EGFP-vector control (Vec), induced phosphorylation of TSC2 on Ser939, a key functional site whose phosphorylation inhibits TSC2 activity (Aicher et al., 2001). This phenomenon was observed under normal, hypoxia, serum free and amino-acid starved conditions (**Figure 4.2A**). Consistent results were observed in HeLa cells overexpressing PRL-3 (**Figure 4.2B**). Conversely, depletion of endogenous PRL-3 with shRNA in HCT116 cells led to reduced TSC2 phosphorylation on Ser939 (**Figure 4.2C**). These results indicated that PRL-3 might suppress TSC2 activity.

To validate whether inhibition of TSC2 by PRL-3 affected downstream Rheb activation, a Rheb activation assay was employed to study the levels of active GTP-bound Rheb (Rheb-GTP) in PRL-3-overexpressing cells. Relative to HCT116-Vec or HCT116-C104S cells, Rheb-GTP levels were higher in HCT116-PRL-3 cells under basal, hypoxic, serum-free and amino-acid starved conditions (**Fig. 4.2D, lanes 2, 5, 8, 11, 14**). Similar results were also found in HeLa cells (**Figure 4.2E, lanes 2, 5, 8, 11, 14**). These results were in agreement with TSC2 inhibition by PRL-3, and suggested that PRL-3 modulates TSC2-Rheb signalling.

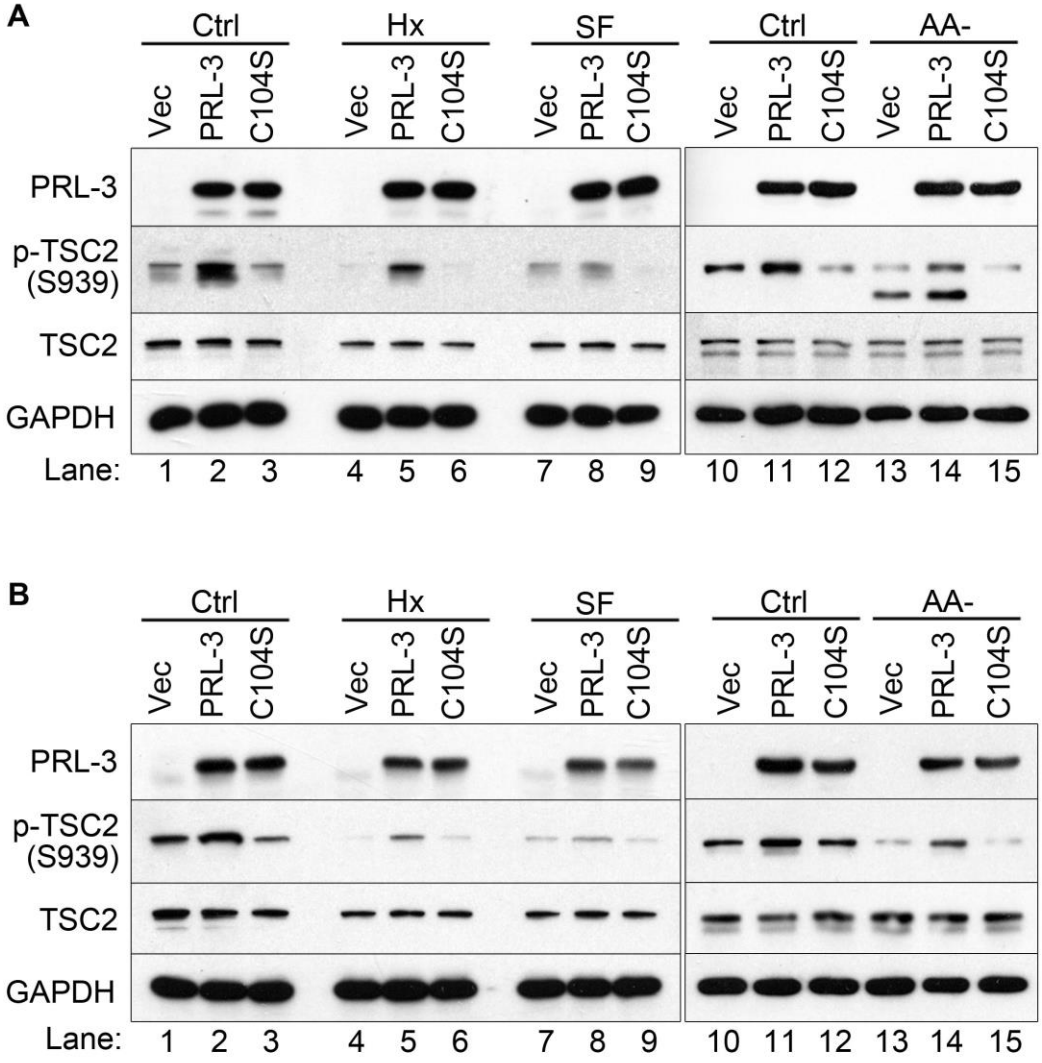
A
Ctrl
Hx
SF
Ctrl
AA-
Vec
PRL-3
C104S
PRL-3
p-TSC2 (S939)
TSC2
GAPDH
Lane: 1 2 3 4 5 6 7 8 9 10 11 12 13 14 15
B
Ctrl
Hx
SF
Ctrl
AA-
Vec
PRL-3
C104S
PRL-3
p-TSC2 (S939)
TSC2
GAPDH
Lane: 1 2 3 4 5 6 7 8 9 10 11 12 13 14 15
C
Ctrl
Hx
SF
Ctrl
AA-
shCon: + + + + +
shPRL-3: + + + + +
PRL-3
p-TSC2 (S939)
TSC2
GAPDH
Lane: 1 2 3 4 5 6 7 8 9 10

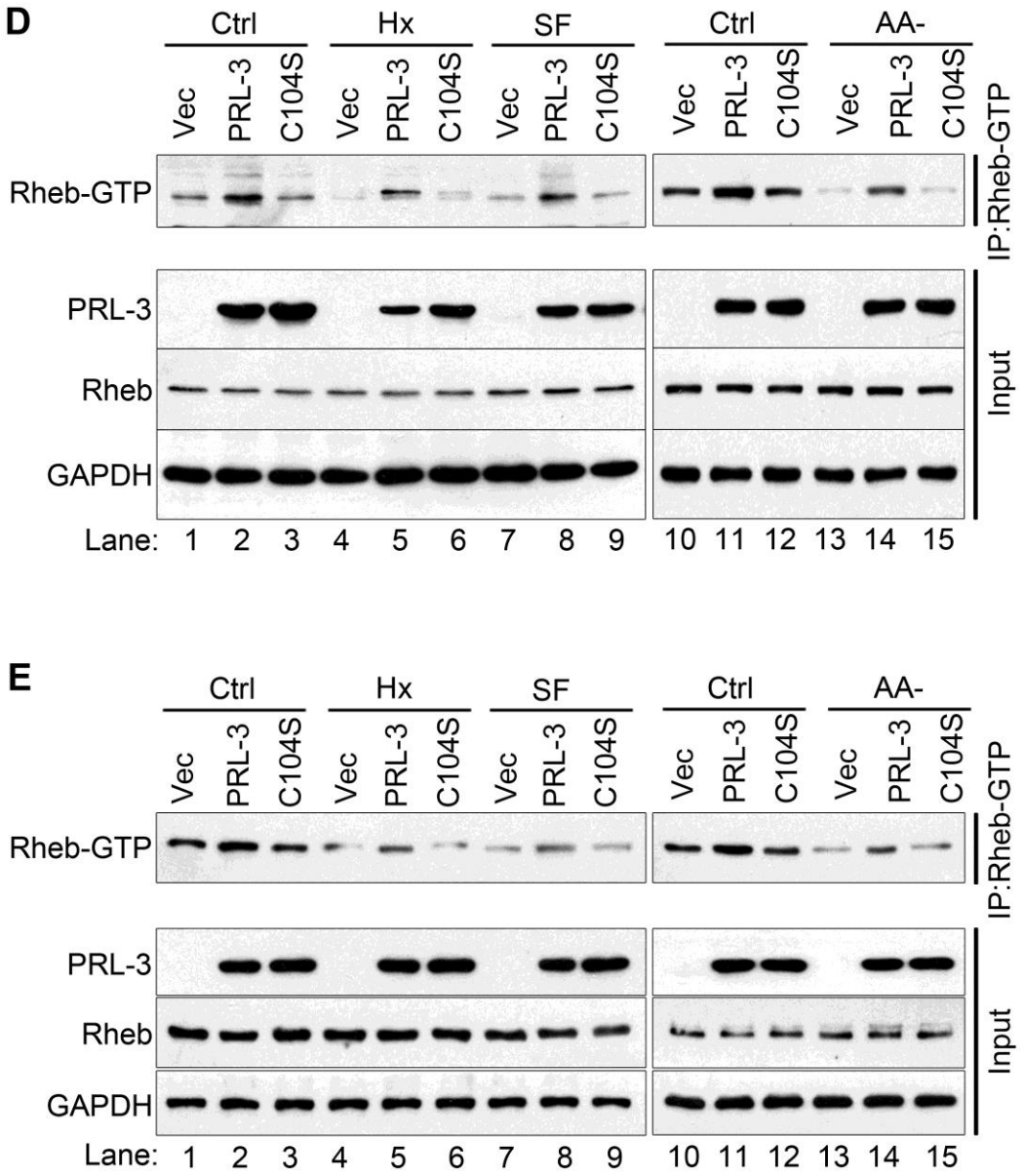

Figure 4. 2 PRL-3 modulates TSC2-Rheb signalling. (A) HCT116-Vec, HCT116-PRL-3 and HCT116-C104S cells were cultured for 24 hours under normal (Ctrl), hypoxia (Hx), or serum free (SF) conditions, or cultured for 1 h under normal (Ctrl) or amino-acid starved (AA-) conditions, prior to lysis and western blot analysis with the antibodies against PRL-3, p-TSC2(S939), TSC2 and GAPDH. GAPDH used as a loading control. (B) Hela cells were transfected with empty EGFP vector (Vec), EGFP-PRL-3 (PRL-3) or EGFP-C104S (C104S) plasmids, then cells were cultured and analyse as in (A). Western blot analysis was performed with indicated antibodies. (C) HCT116 cells expressing small hairpin RNA (shRNA) against PRL-3 (sh*PRL-3*) or control shRNA (shCon) were cultured and analysed as in (A). (D) Cell lysates from (A) were immunoprecipitated with a configuration-specific anti-Rheb-GTP antibody and analysed by immunoblotting with the indicated antibodies. (E) Cell lysates from (B) were analysed as in (D).

4.3.2 PRL-3-mediated mTORC1 activation requires the activity of Akt but not Erk1/2 or AMPK

The process of TSC-Rheb axis transmitting signals that converge on mTORC1 is controlled by many upstream signalling pathways, including the PI3K/Akt pathway, Ras/ERK pathway and LKB1/AMPK pathway (Huang and Manning, 2008). To elucidate which pathway(s) PRL-3 uses to activate the TSC2-Rheb-mTORC1 cascade, the activities of three pathways were examined by evaluating the activation-associated phosphorylation levels of their key kinases upon PRL-3 overexpression. Interestingly, compared with HCT116-Vec or HCT116-C104S cells, HCT116-PRL-3 cells displayed higher phosphorylation levels of Akt on Ser473, a critical activation site on this kinase (Bayascas and Alessi, 2005). This phenomenon was observed under normal, hypoxia, serum-free and amino-acid starved conditions (**Figure 4.3A**). However, the phosphorylation levels of two other kinases, Erk1/2 and AMPKα, showed no response to PRL-3 overexpression, despite a decrease in Erk1/2 phosphorylation and a slight increase in AMPKα phosphorylation in cells grown under stressed conditions (**Figure 4.3A**). Similar results were also observed in HeLa cells (**Figure 4.3B**). Moreover, suppression of endogenous PRL-3 in HCT116 cells reduced Akt phosphorylation under both normal and stressed conditions (**Figure 4.3C**). Notably, this PRL-3-mediated phosphorylation of Akt correlated well with a corresponding increase or decrease in phosphorylation of TSC2, mTOR and its downstream substrates, 4E-BP1 and p70S6K, suggesting that PRL-3 might regulate TSC2-Rheb-mTORC1 axis through the PI3K/Akt pathway.

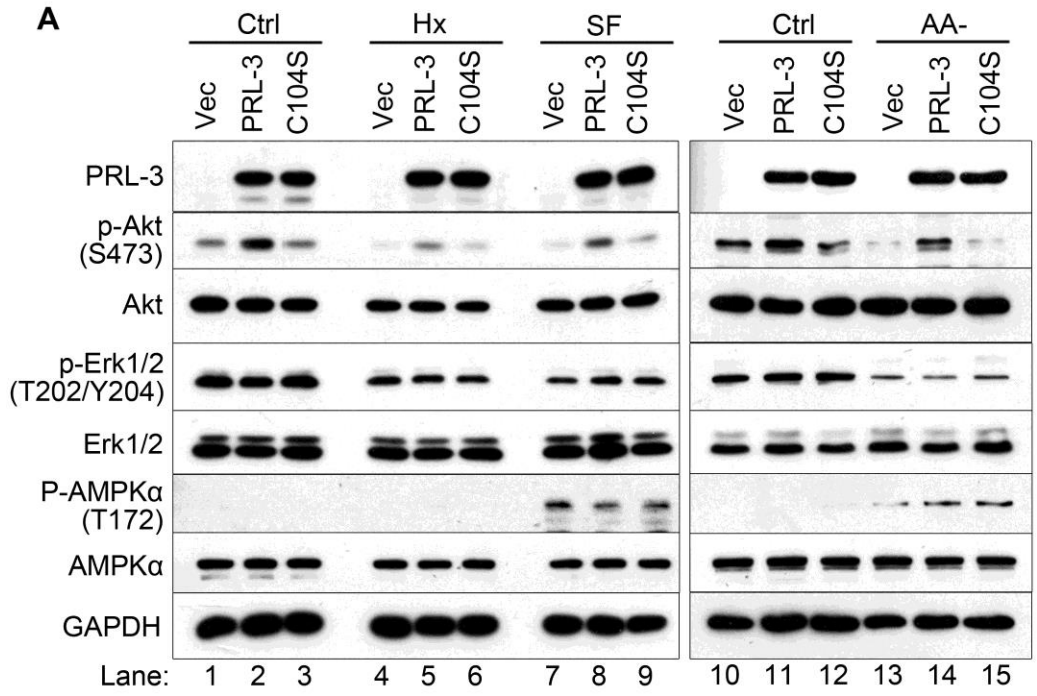
A
Ctrl
Hx
SF
Ctrl
AA-
Vec
PRL-3
C104S
PRL-3
p-Akt (S473)
Akt
p-Erk1/2 (T202/Y204)
Erk1/2
P-AMPKα (T172)
AMPKα
GAPDH
Lane: 1 2 3 4 5 6 7 8 9 10 11 12 13 14 15

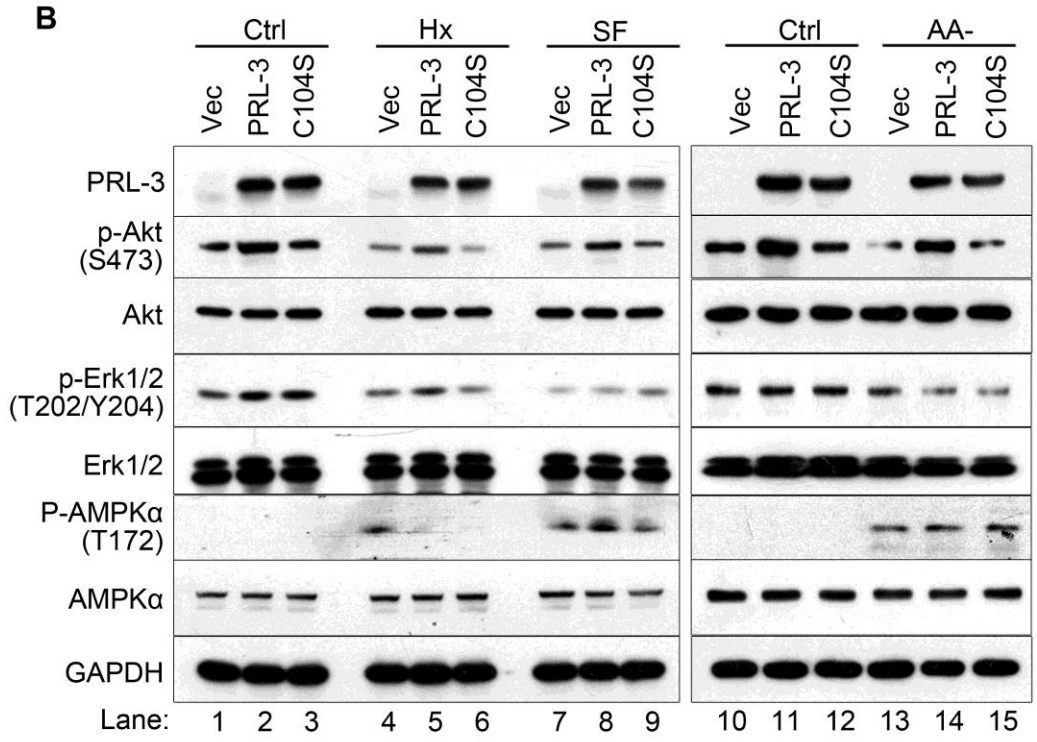
B
Ctrl
Hx
SF
Ctrl
AA-
Vec
PRL-3
C104S
PRL-3
p-Akt (S473)
Akt
p-Erk1/2 (T202/Y204)
Erk1/2
P-AMPKα (T172)
AMPKα
GAPDH
Lane: 1 2 3 4 5 6 7 8 9 10 11 12 13 14 15

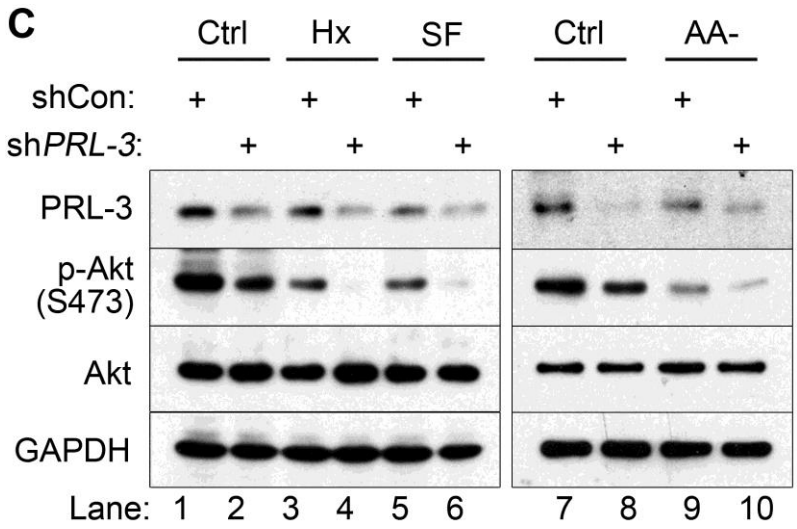

Figure 4. 3 PRL-3 stimulates Akt activation. (A) HCT116-Vec, HCT116-PRL-3 or HCT116-C104S cells were cultured for 24 hours under normal (Ctrl), hypoxia (Hx), or serum free (SF) conditions, or cultured for 1 h under normoxia (Ctrl) or amino-acid starved (AA-) conditions. Cells were lysed and analysed by Western blotting with antibodies against the indicated proteins. GAPDH served as a loading control. (B) HeLa-Vec, HeLa-PRL-3 or HeLa-C104S cells were analyzed as in (A). (C) HCT116 cells expressing small hairpin RNA (shRNA) against PRL-3 (sh*PRL-3*) or control shRNA (shCon) were cultured and performed as in (A).

Under all the conditions tested, the activity of AMPKα, unlike mTOR, was extremely low under normal and hypoxia conditions (**Figure 4.3A-B**). In contrast to this, high activities of Akt and Erk1/2 were detected under both normal and stressed conditions (**Figure 4.3A-B**). To confirm a role of Erk1/2 in PRL-3-mediated mTOR hyperactivation, U0126, a MEK specific inhibitor, was used to block Ras/ERK signalling. Inhibition of Erk1/2 activity did not dampen phosphorylation of TSC2, mTOR, 4E-BP1 and p70S6K, as well as Akt in both HCT116 and HeLa cells overexpressing PRL-3 (**Figure 4.4AB**).

To validate the role of Akt in PRL-3-modulated TSC2-Rheb-mTORC1 activation, two approaches were employed to block Akt signalling: i) small interfering RNA (siRNA)-mediated depletion of AKT transcripts, and ii) small-molecule antagonist-mediated inhibition of Akt. siRNA-mediated *AKT* depletion reduced PRL-3-driven phosphorylation of TSC2, mTOR, and its downstream effectors, 4E-BP1 and p70S6K (**Figure 4.4C, panel 1**). Likewise, treatment of cells with the Akt inhibitor VIII (AktiVIII), a highly selective and potent small-molecule inhibitor of Akt, also reduced PRL-3-induced hyperphosphorylation of TSC2, mTOR, 4E-BP1, and p70S6K (**Figure 4.4C, panel 2**). However, HCT116-PRL-3 cells still had higher 4E-BP1 and p70S6K phosphorylation relative to HCT116-Vec cells under these treatments, suggesting that Akt inhibition did not completely abolish the ability of PRL-3 to enhance p70S6K and 4E-BP1 phosphorylation. Similar results were also observed in HeLa cells (**Figure 4.4C, panel 3-4**).

Collectively, while these results point to a role for Akt signalling in PRL-3-mediated mTORC1 hyperphosphorylation, the elevated activity of 4E-BP1 and p70S6K despite Akt inhibition hints at the existence of a secondary, Akt-independent PRL-3-driven mTORC1 activation mechanism.

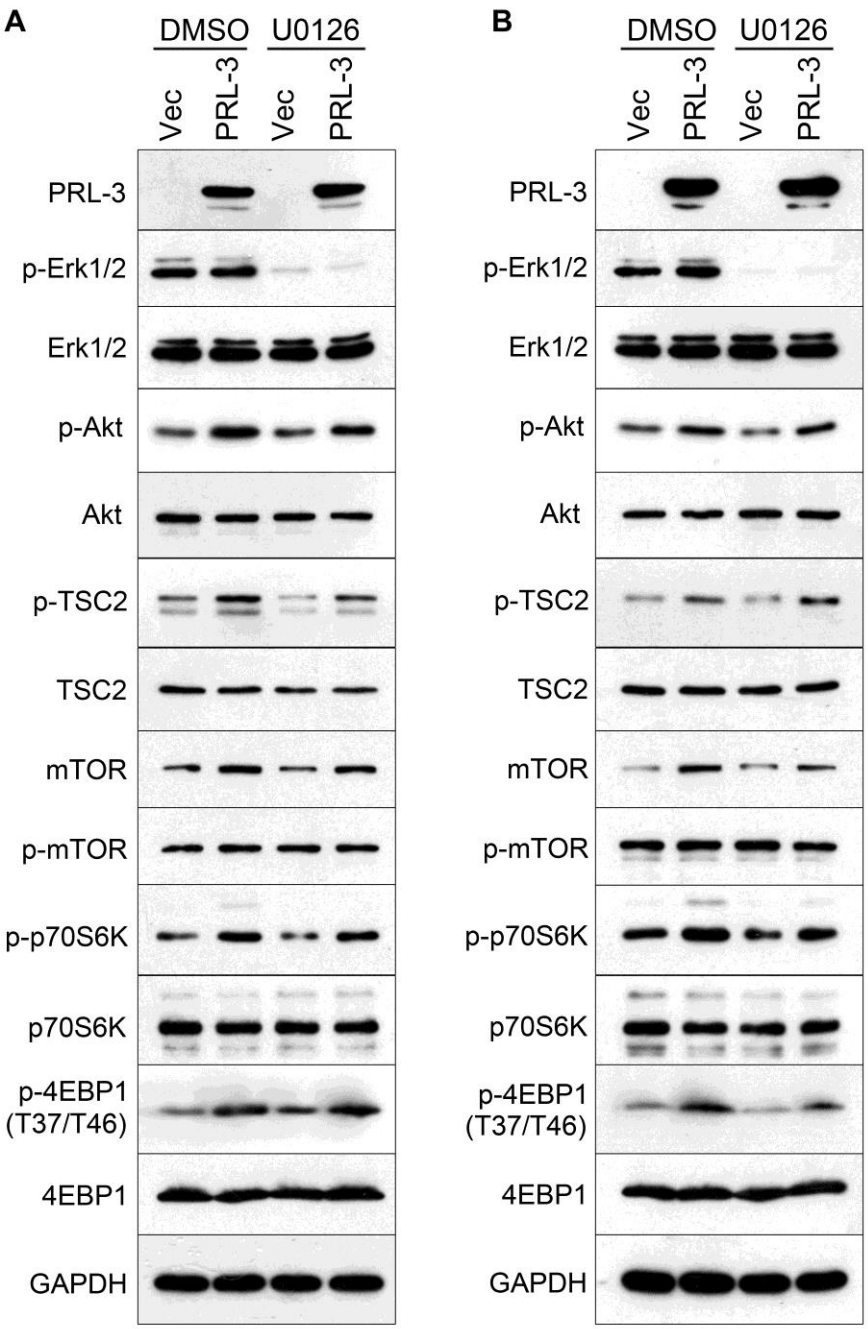
A
DMSO
U0126
Vec
PRL-3
Vec
PRL-3
PRL-3
p-Erk1/2
Erk1/2
p-Akt
Akt
p-TSC2
TSC2
mTOR
p-mTOR
p-p70S6K
p70S6K
p-4EBP1 (T37/T46)
4EBP1
GAPDH
B
DMSO
U0126
Vec
PRL-3
Vec
PRL-3
PRL-3
p-Erk1/2
Erk1/2
p-Akt
Akt
p-TSC2
TSC2
mTOR
p-mTOR
p-p70S6K
p70S6K
p-4EBP1 (T37/T46)
4EBP1
GAPDH

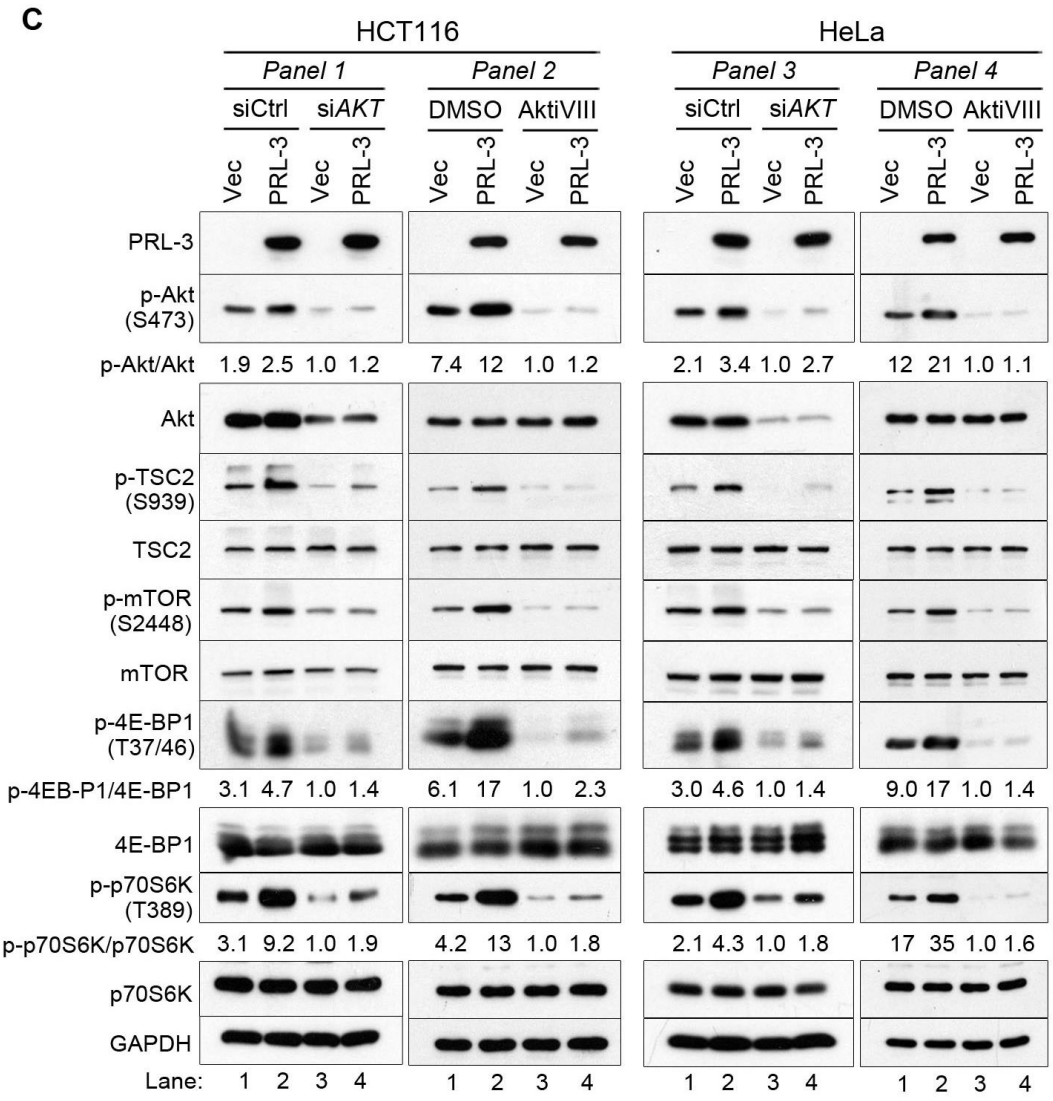

Figure 4. 4 Akt activity is required for PRL-3-mediated hyperactivation of mTOR signalling. (A) Erk1/2 activity in HCT116-Vec or HCT116-PRL-3 cells was inhibited using U0126. Then the activity of TSC2-Rheb-mTOR pathway was analysed. (B) Erk1/2 activity in Hela-Vec or Hela-PRL-3 cells was inhibited using U0126, then performed as in (A). (C) *Panel 1*. Akt in HCT116-Vec or HCT116-PRL-3 cells were transiently depleted using scrambled small interfering RNA (siCtrl) or AKT-targeting siRNA (si*AKT*) and cultured for 48 hours before analysis of Akt-TSC2-mTOR pathway activity. *Panel 2*. Akt in HCT116 Vec or PRL-3 cells was inhibited using Akt inhibitor VIII (AktiVIII) before analysis of Akt-TSC2-mTOR pathway activity. *Panel 3*. Akt in Hela-Vec or Hela-PRL-3 were transiently depleted using scrambled small interfering RNA (siRNA; siCon) or AKT-targeting siRNA (si*AKT*) and cultured for 48 hours before analysis of Akt-TSC2-mTOR pathway activity. *Panel 4*. Akt in Hela-Vec or Hela-PRL-3 was inhibited using Akt inhibitor VIII (AktiVIII) before analysis of Akt-TSC2-mTOR pathway activity. The ratio of phosphorylated/total band densities for Akt, 4E-BP1, and p70S6K were calculated and normalized to their cognate phosphorylated/total protein ratio in lane 3.

4.3.3 PRL-3 promotes the relocalization and accumulation of lysosomal mTOR

Despite a reduction in overall mTOR phosphorylation levels in cells grown under hypoxia, serum deprivation, or amino acid starvation, the PRL-3-driven increase in phosphorylation of mTOR substrates 4E-BP1 and p70S6K under each of these stressors consistently appeared greater compared to the increase in mTOR S2448 phosphorylation itself. This suggests that the heightened resistance conferred by PRL-3 against mTOR inactivation under limited oxygen or nutrient supply might be due to some additional regulatory mechanism(s) on mTOR. In addition to canonical PI3K/Akt signalling, which regulates mTORC1 activity via TSC2-Rheb axis, mTORC1 is also tightly regulated by changes in its localization within the cell (Betz and Hall, 2013). To check the subcellular localization of mTOR, immunofluorescence analysis was conducted in HCT116-Vec and HCT116-PRL-3 cells. Unlike vector control cells, which had a somewhat more diffuse mTOR intracellular staining pattern (**Figure 4.5, panels i-iii**), PRL-3 overexpression in HCT116 cells promoted mTOR accumulation predominantly in perinuclear regions regardless of basal, hypoxic, or serum-fee conditions (**Figure 4.5, panels iv-vi**). Importantly, the perinuclear mTOR staining pattern was consistently well co-localized with the lysosomal membrane marker, LAMP2, under all conditions as well, indicating persistent lysosomal enrichment of mTOR in PRL-3-overexpressing cells despite oxygen or serum deprivation (**Figure 4.5**).

Furthermore, the same experiment was repeated upon amino acid withdrawal, a stressor which typically results in rapid delocalization of mTORC1 away from lysosomes, effectively inactivating this kinase (Demetriades et al., 2014). In HCT116-Vec cells, amino acid starvation for 1 h resulted in a loss of mTOR/LAMP2 colocalization (**Figure 4.6A, panel ii**). In contrast, mTOR/LAMP2 colocalization, albeit reduced, could still be observed in amino acid-starved HCT116-PRL-3 cells (**Figure 4.6A, panel iv**). The

ability of PRL-3 to maintain lysosomal mTOR accumulation suggested that PRL-3 overexpression might 'mimic' amino acid stimulation, supporting our earlier observation of sustained mTOR activity induced by PRL-3 under basal and stressed conditions. To confirm these results, the mTOR/LAMP2 colocalization was analysed in HCT116 cells stably depleted of PRL-3. Depletion of endogenous PRL-3 resulted in a decrease in mTOR/LAMP2 colocalization not only under amino-acid starved conditions, but also under basal, amino-acid-replete conditions (**Figure. 4.6B, panel iii, iv**), suggesting an important role for endogenous PRL-3 in regulating the recruitment/retention of lysosomal mTOR.

To further address if enhanced PI3K/Akt signalling might account for the increased lysosomal localisation of mTOR, we treated HCT116 cells with an Akt inhibitor and analysed mTOR/LAMP2 colocalization. No changes in mTOR/LAMP2 colocalization were observed under these conditions (**Figure 4.7**), suggesting that the increased lysosomal accumulation of mTOR occurred via a mechanism independent of Akt activity.

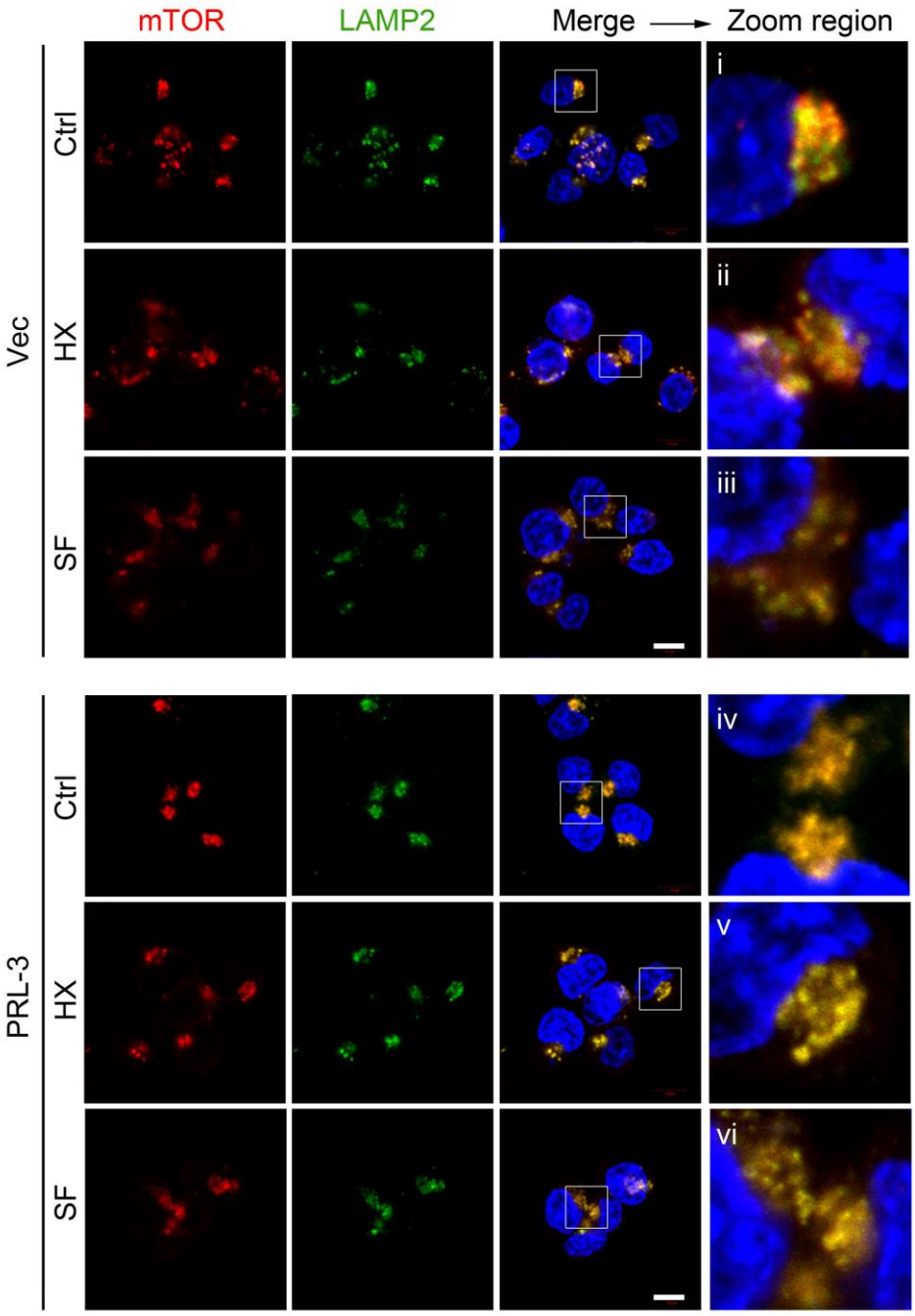

Figure 4. 5 PRL-3 promotes the accumulation of lysosomal mTOR. (A) Immunofluorescence analysis of mTOR and LAMP2 in HCT116-Vec or HCT116-PRL-3 cultured for 24 hours under normal (Ctrl), hypoxia (Hx) or serum Free (SF) conditions. Antibodies against human LAMP2 and mTOR were used. Red, mTOR signal; green, LAMP2 signal; merge, merged mTOR, LAMP2, and DNA (DAPI) signals. Scale bar, 10 μm. A zoomed area within each merged panel enables better visualize mTOR/LAMP2 colocalization.

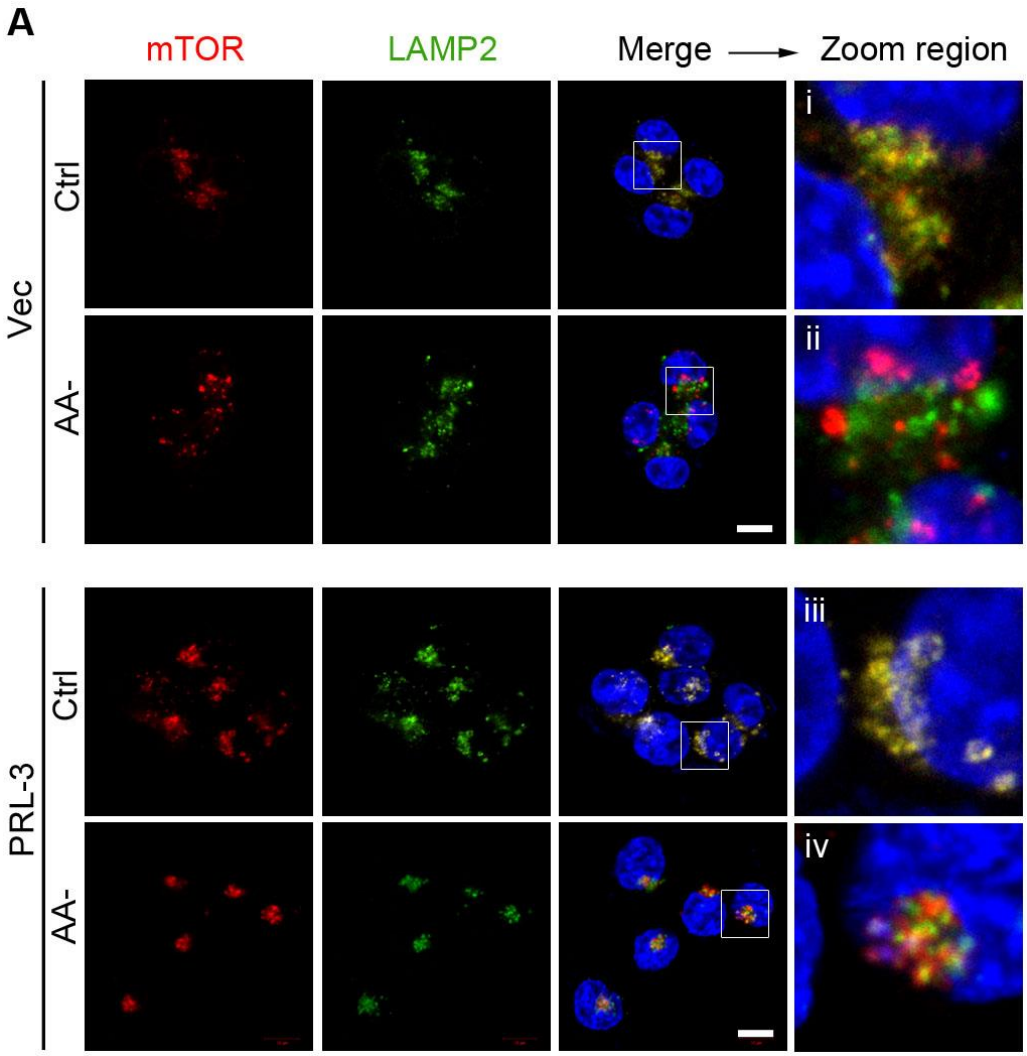
A
mTOR
LAMP2
Merge
Zoom region
Vec
Ctrl
AA-
PRL-3
Ctrl
AA-
i
ii
iii
iv

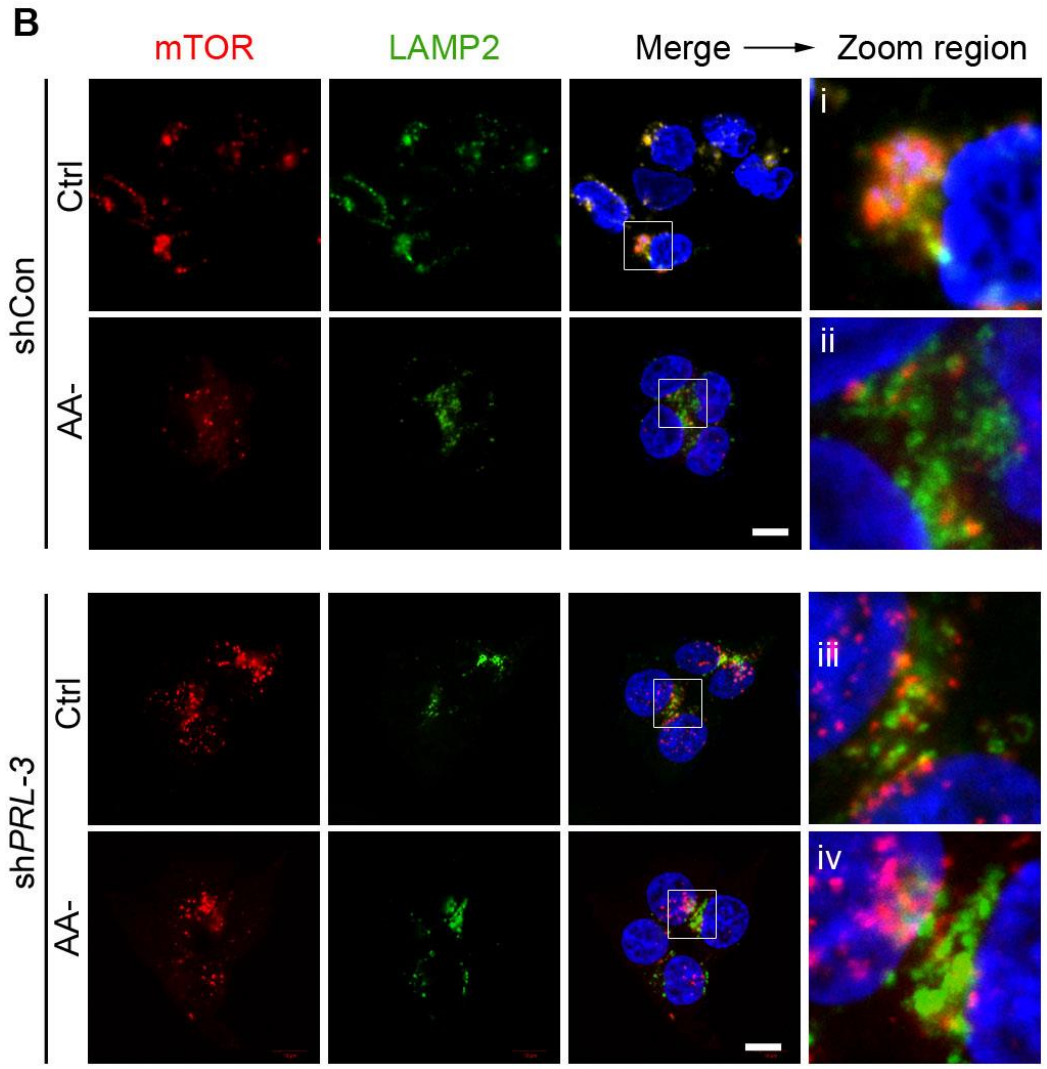

Figure 4. 6 PRL-3 modulates the relocalization of lysosomal mTOR under amino-acid starved condition. (A) Immunofluorescence analysis of mTOR and LAMP2 in HCT116-Vec and HCT116-PRL-3 cultured for 1 hours in full media (Ctrl) or amino-acid starvation media (AA-). Antibodies against human LAMP2 and mTOR were used. Red, mTOR signal; green, LAMP2 signal; merge, merged mTOR, LAMP2, and DNA (DAPI) signals. Scale bar, 10 μm. A zoomed area within each merged panel enables better visualize mTOR/LAMP2 colocalization. *Scale bar*, 10 μm. (B) HCT116 cells stably expressing small hairpin RNA (shRNA) against PRL-3 (shPRL-3) or control shRNA (shCon) were cultured and analysed as in (A). Scale bar, 10 μm.

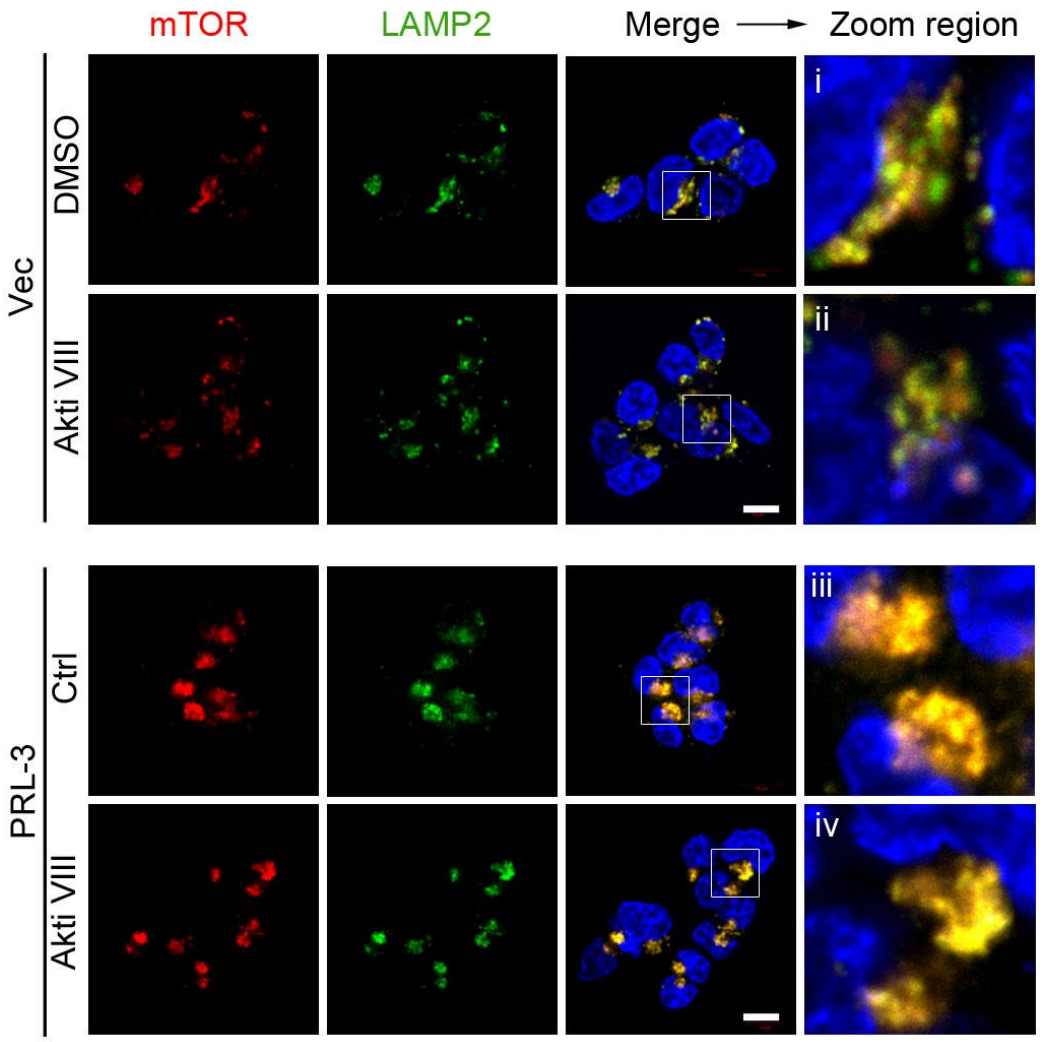

Figure 4. 7 PRL-3-modulated relocalization of lysosomal mTOR is Akt-independent. HCT116-Vec and HCT116-PRL-3 cells were treated with DMSO or Akt Inhibitor VIII (AktiVIII) for 30 min and analyzed by dual dual immunfluoresence using antibodies against mTOR and LAMP2. Red, mTOR signal; green, LAMP2 Scale bar, 10 μm.

4.3.4 PRL-3 promotes mTOR hyperactivation through RagGTPase-mediated lysosomal relocalization

The Rag small GTPases are critical regulators for mTOR lysosomal relocalization and activation. Upon amino acid stimulation, Rag GTPases associate with mTORC1 as heterodimers, recruiting it to late endosomal and lysosomal compartments for subsequent Rheb-mediated activation (Sancak et al., 2008).

To explore the role of Rag GTPases in PRL-3-induced lysosomal accumulation of mTOR, Rag GTPase heterodimeric complexes (RagB-RagC) were co-expressed in either HCT116-Vec or HCT116-PRL-3 cells, and binding affinities of Rag GTPases to mTOR, raptor, and rictor were examined. Compared with control cells, PRL-3 overexpression increased the binding affinity of Rag GTPase heterodimers to both mTOR and raptor, a component of mTORC1, under basal conditions (**Figure 4.8A, lane 2**). Notably, no binding between Rag GTPases and rictor, a component of mTORC2, was observed in either cell line (**Figure 4.8A**). Importantly, PRL-3-overexpressing cells maintained strong binding of Rag GTPase heterodimers to mTORC1 (mTOR and raptor) persistently under hypoxic and serum-free conditions (**Figure 4.8A, lanes 4, 6**). Expectedly, the PRL-3-mediated Rag-mTORC1 interaction was slightly reduced under amino-acid starved condition. Consistently, HCT116 cells depleted of PRL-3 displayed reduced Rag-mTOR-Raptor interaction under all basal and stressed conditions (**Figure 4.8B, lanes 2, 4, 6 and 8**). These results are in agreement with our observations showing that persistent lysosomal accumulation and elevated mTOR signalling were induced by PRL-3 under both basal and stressed conditions. Therefore, a correlation seems to exist between the Rag-mTORC1 interaction and mTOR lysosomal relocalization and activation.

To test whether elevated Rag GTPase activity affected PRL-3-mediated mTORC1 activation, dominant-negative GST-tagged RagBT54L-RagDQ121L heterodimers (Rag^{DN}) or empty vector (Ctrl) were co-expressed in either HCT116-Vec or HCT116-PRL-3 cells and phosphorylation levels of various components of the Akt-mTOR signalling pathway were examined. Interestingly, overexpression of Rag^{DN} did not rescue mTOR phosphorylation levels (**Figure 4.8C, lane 4**), despite potently blocking PRL-3-mediated accumulation of mTOR at LAMP2-enriched puncta **(Fig. 4.8D, panel vi)**. However, a reduction in phosphorylation levels of p70S6K and 4E-BP1 was observed, suggesting partial suppression of mTOR kinase activity and downstream signalling by Rag^{DN} (**Figure 4.8AC, lane 4**). Notably, no changes in PRL-3-induced phosphorylation of Akt were observed upon Rag^{DN} expression (**Figure 4.8C, lane 4**), in agreement with the earlier data suggesting that Akt lay upstream of mTORC1.

Taken together, these data show that independently of activation of mTOR via the PI3K-Akt-TSC2-Rheb pathway, PRL-3 also promotes mTORC1 lysosomal translocation and activation in a Rag GTPase-dependent manner.

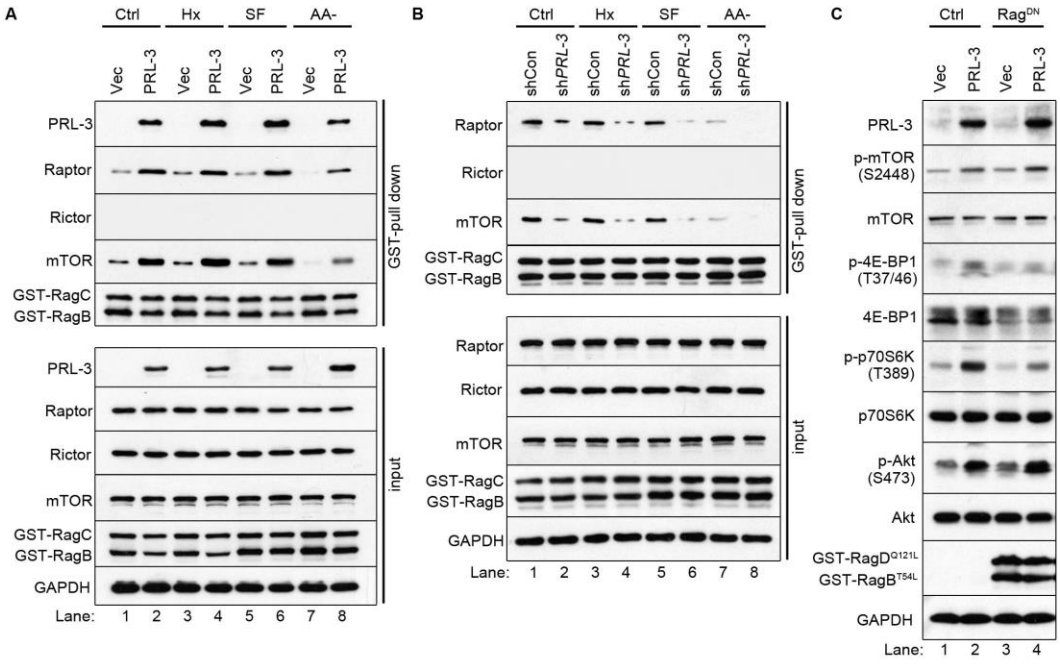
A
Ctrl
Hx
SF
AA-
Vec
PRL-3
PRL-3
Raptor
Rictor
mTOR
GST-RagC
GST-RagB
GST-pull down
GAPDH
input
Lane: 1 2 3 4 5 6 7 8
B
shCon
shPRL-3
C
Rag^DN
p-mTOR (S2448)
4E-BP1
p-4E-BP1 (T37/46)
p-p70S6K (T389)
p70S6K
p-Akt (S473)
Akt
GST-RagD^Q121L
GST-RagB^T54L
Lane: 1 2 3 4

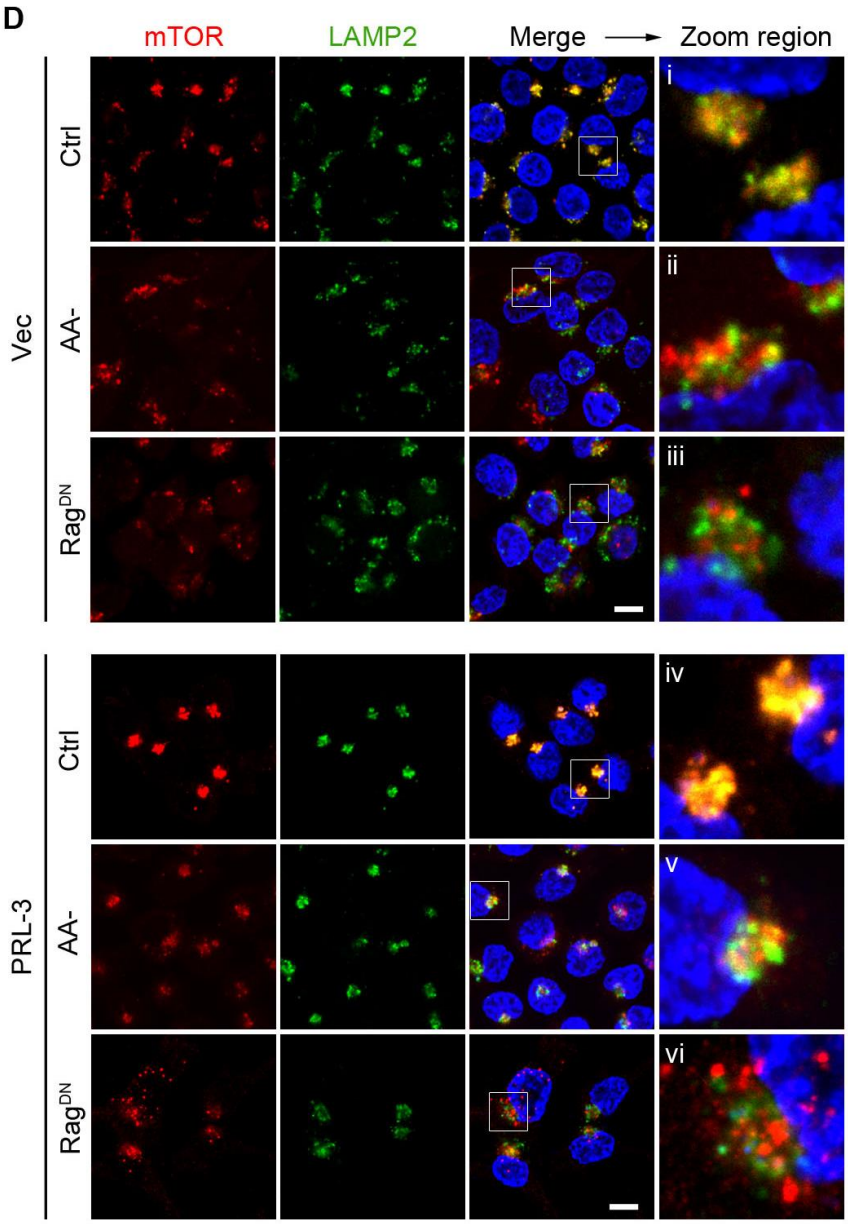

Figure 4. 8 PRL-3 promotes the accumulation and activation of lysosomal mTOR via increased Rag GTPase binding. (A) HCT116-Vec or HCT116-PRL-3 cells were co-transfected with GST-RagB/C and cultured for 24 hours under normal (Ctrl), hypoxic (Hx), serum free (SF) or amino-acid starved conditions before GST pull-down and analysis by immunoblotting. *Top panel*, GST-enriched fraction; *bottom panel*, total protein input. (B) HCT116 cells stably expressing small hairpin RNA (shRNA) against PRL-3 (sh*PRL-3*) or control shRNA (shCon) were performed and analysed as in (A). (C) HCT116-Vec or HCT116-PRL-3 cells were transfected with empty vector (Ctrl) or dominant negative $RagB^{T54L}$-$RagD^{Q121L}$ (Rag^{DN}) for 24 hours, western blot was analyzed with the indicated antibodies. (D) HCT116-Vec or HCT116-PRL-3 cells were transfected with empty vector (Ctrl) or dominant negative $RagB^{T54L}$-$RagD^{Q121L}$ (Rag^{DN}) for 24 h, or starved of amino acid for 1 h, before dual immunfluoresence analysis using antibodies against mTOR and LAMP2. *Red*, mTOR signal; *green*, LAMP2. Scale bar, 10 μm.

4.4. Discussion

In this chapter, PRL-3 was characterized to function as a unique mTOR regulator in that it both: 1) activates TSC2-Rheb via Akt signalling pathway; and, in parallel, 2) promotes recruitment of mTORC1 to Rheb-resident lysosomes via interaction with Rag GTPase proteins, leading to sustained, efficient mTORC1 activation under basal and stressed conditions. This novel mechanism might explain how PRL-3 promotes cancer progression through the mTOR signalling pathway.

As a molecular switchboard regulating mTORC1 activation, the activity of TSC2 was previously reported to be controlled by many upstream regulators via direct phosphorylation at different residues (Huang and Manning, 2008), including Akt-mediated phosphorylation of Ser939 and Thr1462 (Roux et al., 2004), Erk1/2-mediated phosphorylation of Ser540 and Ser644 (Ma et al., 2005) and AMPK-mediated phosphorylation of Thr1227 and Ser1345(Corradetti et al., 2004). Overexpression of PRL-3 induced Rheb GTPase activity and TSC2 phosphorylation on Ser939 under both normal and stressed conditions, raising the possibility that Akt may be involved in this regulation. Indeed, activation-associated phosphorylation of Akt was found to increase upon PRL-3 overexpression, even under hypoxia, serum-free and amino-acid starved conditions. These results are supported by previous studies, showing that PRL-3 activates Akt signalling via various pathways, including downregulation of phosphatase and tensin homologue (PTEN) (Wang et al., 2007a) and hyperactivation of receptor tyrosine kinases (Al-Aidaroos et al., 2013). However, different from the earlier report that inhibition of PRL-3 reduces Erk1/2 phosphorylation in A549 cells (Ming et al., 2009), PRL-3 overexpression showed no effect on Erk1/2 phosphorylation in both HCT116 and HeLa cells, which might be explained by cell-specific function of PRL-3. Moreover, inhibition of Akt, but not Erk1/2, suppressed PRL-3-mediated

TSC2-Rheb-mTORC1 activity. Surprisingly, this suppression is not complete. Minor increases in phosphorylation levels of 4E-BP1 and p70S6K, but not mTOR, still could be observed in PRL-3-overexpressed cells despite Akt inhibition, indicating that besides the enhancement of Akt-TSC2-Rheb cascade, another Akt-independent PRL-3-driven mTORC1 activation mechanism exists.

Furthermore, PRL-3 was shown to induce mTOR accumulation at lysosomes where it can be fully activated, leading to mTORC1 activation. In agreement with previous reports that lysosomal positioning of mTOR is regulated by Rag GTPases in response to amino acids (Jewell et al., 2013), Rag GTPases are implicated in PRL-3-mediated lysosomal mTOR accumulation, as the mTOR/LAMP2 colocalization could be effectively abolished upon overexpression of dominant-negative Rag^{DN} GTPase in HCT116-PRL-3 cells. Interestingly, PRL-3 increased the binding affinity of Rag GTPase to its target proteins, mTOR and Raptor, under both basal and stressed conditions, suggesting an elevated GTPase activity. Such PRL-3-driven Rag-GTP accumulation, which was previously reported to enhance mTOR recruitment to lysosomes (Jewell et al., 2013), occurred in an Akt-independent manner, thereby constituting a novel mechanism of mTORC1 regulation distinct from PI3K/Akt activation by PRL-3. This yet-uncharacterized, Akt-independent pathway for PRL-3 to activate Rag GTPases might occur via the regulation of Rag activity via the Ragulator complex which, by promoting Rag-GTP formation, has been shown to be necessary for targeting mTORC1 to lysosomes (Bar-Peled et al., 2012; Sancak et al., 2010).

Intriguingly, the Rag-mTOR binding is unlikely to solely account for the mTOR-LAMP2 colocalization observed. Particularly, in amino acid-starved HCT116-PRL-3 cells, the slight reduction in the Rag-mTOR interaction (**Figure 4.8A, lane 8**) did not correlate exactly with the loss of colocalization between mTOR and LAMP2 (**Figure 4.6A, panel**

iv). Similarly, in amino acid-replete conditions, the difference in Rag-mTOR interaction between HCT116-Vec and HCT116-PRL-3 cells (**Figure 4.8A, lanes 1-2**) did not perfectly recapitulate the difference in mTOR/LAMP2 colocalization (**Figure 4.6A, panels i and iii**). A possible explanation is that the Rag GTPase-mTOR interaction seen in pull-down experiments might also persist on non-LAMP2 positive endomembranes, and this might warrant further investigation.

CHAPTER 5: PRL-3 PROTECTS AGAINST COCL2-INDUCED APOPTOSIS IN A P38 MAPK-DEPENDENT MANNER

5.1 Background

In response to environmental stress, cells integrate external stress signals to determine death or survival. Among the various stress-responsive signalling pathways, the mitogen-activated protein kinase (MAPK) family proteins are widely used by eukaryotic cells to transduce extracellular signals into intracellular responses, and are extremely crucial for the maintenance of cellular homeostasis (Cowan and Storey, 2003).

MAPKs are a group of serine/threonine protein kinases involved in many fundamental cellular processes, including cell growth, differentiation, inflammation, and apoptosis (Cargnello and Roux, 2011) (**Figure 5.1**). Conventional MAPKs consist of four major subfamily members: ERKs, JNKs, ERK5 and p38 MAPKs (Zarubin and Han, 2005). They are highly conserved and share an activation loop designated as "Thr-X-Tyr". Dual Thr and Tyr phosphorylation in this activation loop fully activates MAPKs activity (Cargnello and Roux, 2011). Activation of MAPKs is achieved by a three-tier protein kinase cascade, where MAPKs are phosphorylated by dual specificity serine-threonine MAPK kinases (MAPKKs), while these MAPKKs are phosphorylated and activated by upstream MAPKK kinases (MAPKKKs) (Roux and Blenis, 2004). Notably, among these conventional MAPKs, the ERKs are preferentially activated by mitogens, while JNKs and p38 MAPKs are mainly activated by environmental stresses such as inflammatory stimulation, heat shock, UV irradiation, and oxidative stress (Cobb et al., 1994; Johnson and Lapadat, 2002).

In mammals, the p38 MAPKs are represented by four isoforms: p38α, p38β, p38δ, and p38γ, which share approximately 60% homology in their amino acid sequences (Zarubin and Han, 2005). These four isoforms are encoded by different genes, exhibiting distinct expression patterns and affinities for upstream activators and downstream effectors (Ono

and Han, 2000). Unlike the ubiquitous p38α, the other three isoforms are expressed in a tissue-specific manner (Cuadrado and Nebreda, 2010). Notably, p38α knock-out mice are embryonically lethal, while deficiency of other p38 isoforms does not affect normal development in mice (Beardmore et al., 2005; Sabio et al., 2005; Tamura et al., 2000). p38 MAPKs are known to be activated by two major MAPKKs, MKK3 and MKK6. MKK6 is a common activator of all four p38 isoforms, whereas MKK3 is unable to activate p38β (Enslen et al., 2000). Besides MKK3 and MKK6, MKK4, an upstream kinase of JNKs, can also activate p38α and p38β in specific cell types (Brancho et al., 2003). Once activated, p38 MAPKs can orchestrate cellular responses by directly phosphorylating and regulating various substrates, which range from protein kinases to transcription factors (Sui et al., 2014).

The function of p38α MAPK (hereafter referred to as p38 MAPK) in cancer is controversial. Although some reports have described a potential oncogenic function for p38 MAPK, the majority of studies suggest p38 MAPK serves as a tumour suppressor by playing a critical role in the regulation of apoptosis (Peter and Dhanasekaran, 2003; Sui et al., 2014). Apoptosis is a form of programmed cell death that can maintain body health by eliminating damaged or defective cells. Defective or inefficient apoptosis is one of the major reasons leading to cancer development. When too little apoptosis occurs, malignant cells will survive and expand, leading to tumour progression and metastasis (Lowe and Lin, 2000). Although a few studies have reported that p38 MAPK suppressed apoptosis in some cell lines, a growing body of evidence showed that activation of p38 MAPK induces apoptosis in various types of cells, supporting a pro-apoptotic role of p38 MAPK (Jinlian et al., 2007; Sui et al., 2014).

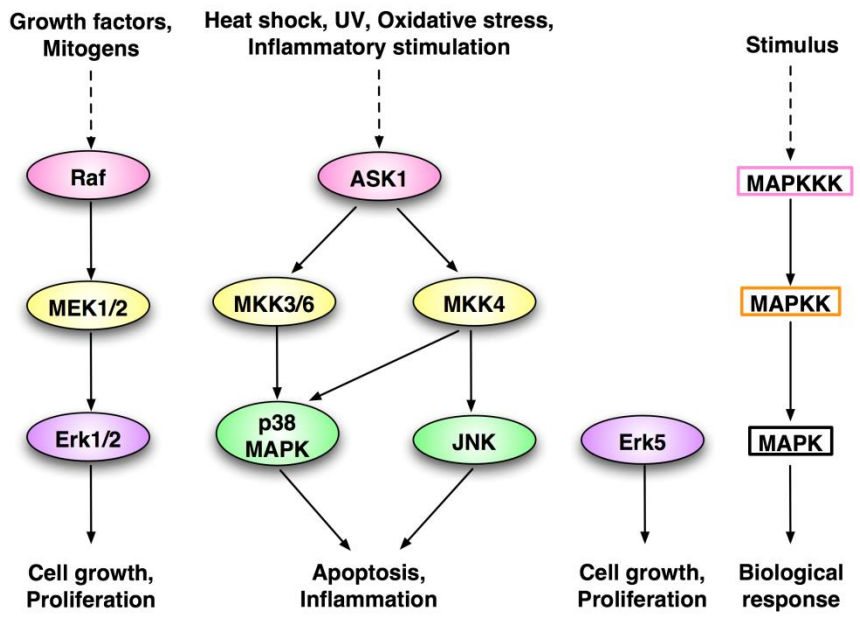

Figure 5. 1 Regulation of MAPKs signalling.

PRL-3 plays an important role in the regulation of cancer cell survival. Several reports have shown that PRL-3 causes drug resistance in cancer cells by suppressing apoptotic cell death (Min et al., 2010; Qu et al., 2014). However, the underlying mechanism(s) of PRL-3-mediated suppression of apoptosis remains largely unknown. Therefore, an understanding of the mechanism(s) involved would be a pivotal step to overcome PRL-3-induced drug resistance and improve cancer therapeutic efficacy. Despite the importance and involvement of p38 MAPK and PRL-3 in apoptosis regulation and cancer development, only two published papers have mentioned this interaction, and they described contradicting observations. One paper found that PRL-3 depletion led to p38 MAPK activation in MEFs (Basak et al., 2008), while another paper reported that PRL-3 overexpression induced p38 MAPK activation in A431 cancer cells (Al-Aidaroos et al., 2013). Hence, the interaction between p38 MAPK and PRL-3 requires further investigation. In this study, the anti-apoptotic role of PRL-3 is validated, accompanied by the molecular investigation for this phenomenon.

5.2. Experimental outline

1. Investigate the protective effect of PRL-3 in $CoCl_2$-induced apoptosis.
2. Define which signalling pathway(s) are involved in PRL-3-mediated anti-apoptosis.
3. Determine whether PRL-3-mediated inhibition of p38 MAPK phospho-activation is ROS-independent.
4. Investigate if PRL-3 could directly dephosphorylate p38 MAPK.

5.3. Results

5.3.1. PRL-3 suppresses $CoCl_2$-induced apoptosis

To investigate the role of PRL-3 in cell death, DLD-1 cells stably expressing EGFP-PRL-3 (PRL-3), EGFP-PRL-3-C104S (C104S; catalytically-inactive mutant), or empty EGFP vector (Vec), were generated and then treated with cobalt chloride ($CoCl_2$), a hypoxia-mimetic agent which has been previously reported to induce reactive oxygen species (ROS) generation and cell death (Kotake-Nara and Saida, 2007; Liu et al., 2008a). Dose response and time course analysis revealed higher sensitivity of DLD-1-Vec and DLD-1-C104S cells to $CoCl_2$ toxicity, with cells appearing smaller and rounded up. In contrast, DLD-1-PRL-3 cells maintained similar morphology despite similar $CoCl_2$ treatment dose or duration (**Figure 5.2A-B**).

As cell shrinkage is a typical morphological feature of cell apoptosis (Saraste and Pulkki, 2000), these data implied that PRL-3 may block $CoCl_2$-induced apoptosis in a phosphatase activity-dependent manner. However, $CoCl_2$ has been shown to induce both apoptotic and necrotic cell death (Jung et al., 2008; Rovetta et al., 2013). To confirm the pathway involved, cells were treated with $CoCl_2$ in the presence or absence of an apoptosis inhibitor, z-VAD-fmk, or a necrosis inhibitor, necrosulfonamide (NSA) (Nicholson et al., 1995; Zhou et al., 2012b). Interestingly, compared with control and $CoCl_2$ treatment groups, z-VAD-fmk, but not NSA, effectively abolished $CoCl_2$-induced cell shrinkage of DLD-1-Vec and DLD-1-C104S cells (**Figure 5.3A**). Notably, these treatments did not alter the cell morphology of DLD-1-PRL-3 cells (**Figure 5.3A**). Cell viability measurements revealed that the viability of DLD-1-Vec and DLD-1-C104S cells decreased to ~38% and ~34% respectively, while the viability of DLD-1-PRL-3 cells only decreased to ~70% (**Figure 5.3B**). Intriguingly, z-VAD-fmk treatment significantly

rescued $CoCl_2$-induced loss of cell viability for DLD-1-Vec and DLD-1-C104S cells to ~59% and ~61% respectively ($p < 0.01$; **Figure 5.3B**). Similar results were observed in MCF-7 cells (**Figure 5.3C-D**).

Poly(ADP-ribose) polymerase (PARP) cleavage, a hallmark of caspase activation and apoptosis (Saraste and Pulkki, 2000), was next assessed to determine the involvement of caspase activation in $CoCl_2$-induced cell death. Western blot analysis by using a cleaved-PARP-specific antibody revealed that $CoCl_2$ induced the PARP cleavage in DLD-1-Vec and DLD-1-C104S cells (**Figure 5.4A**). This $CoCl_2$-induced PARP cleavage was dose- and time-dependent, which became significant after 5 μM $CoCl_2$ treatment for 24 hours. Interestingly, compared to DLD-1-Vec or DLD-1-C104S cells, PARP cleavage was dramatically reduced in DLD-1-PRL-3 cells upon $CoCl_2$ treatment (**Figure 5.4A**). Similar results were obtained in MCF-7 cells (**Figure 5.4B**). Collectively, these data suggests PRL-3 could protect against $CoCl_2$-induced apoptosis.

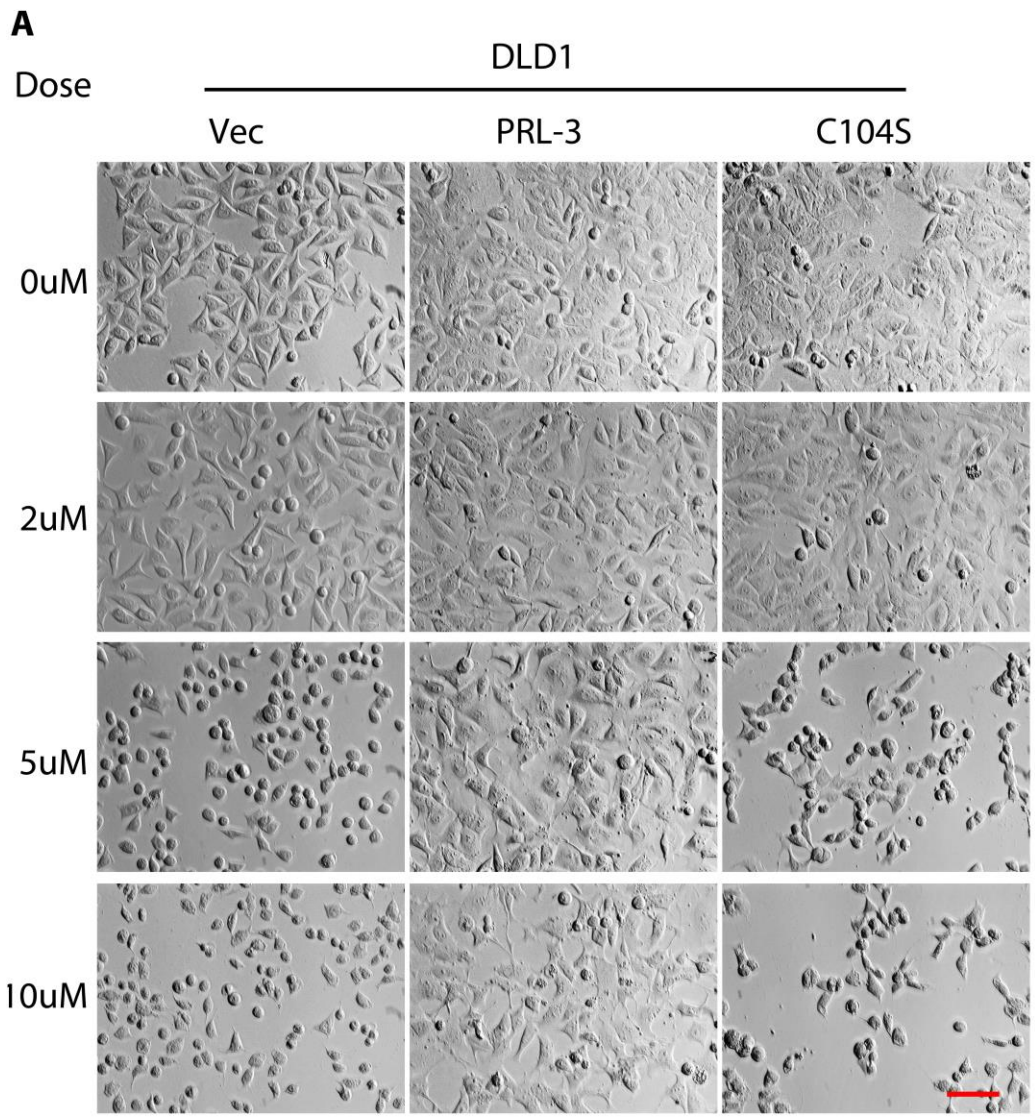
A
Dose
DLD1
Vec
PRL-3
C104S
0uM
2uM
5uM
10uM

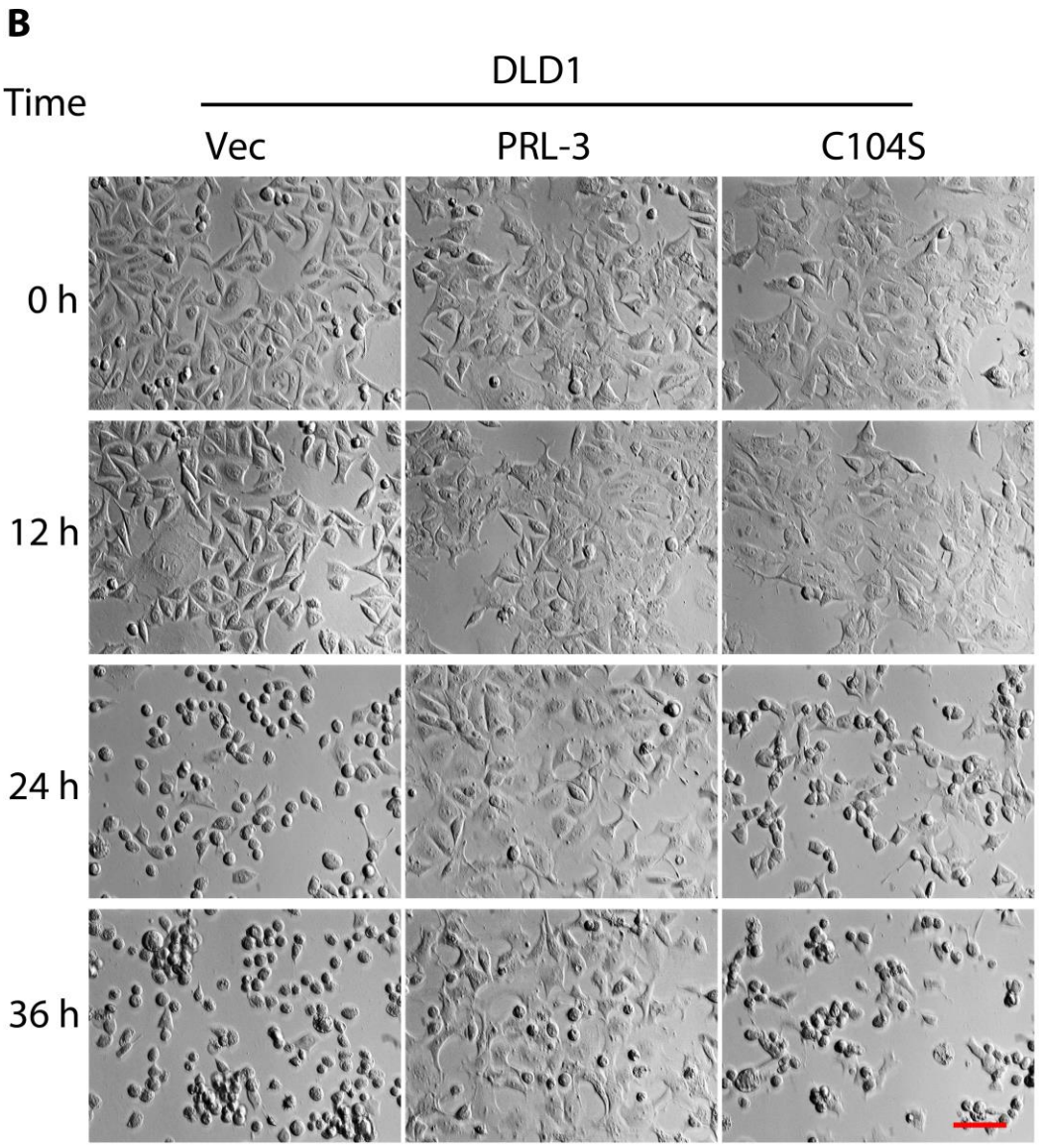

Figure 5. 2 PRL-3 suppresses $CoCl_2$-induced cell death. (A) DLD-1-Vec, DLD-1-PRL-3 and DLD-1-C104S cells were treated with $CoCl_2$ at the concentrations of 0, 2, 5 or 10 μM for 24 h. Cell morphology was captured using microscopy. (B) DLD-1-Vec, DLD-1-PRL-3 and DLD-1-C104S cells were incubated with 5 μM $CoCl_2$ for 0, 12, 24 or 36 h time intervals. Scale bar, 100 μm.

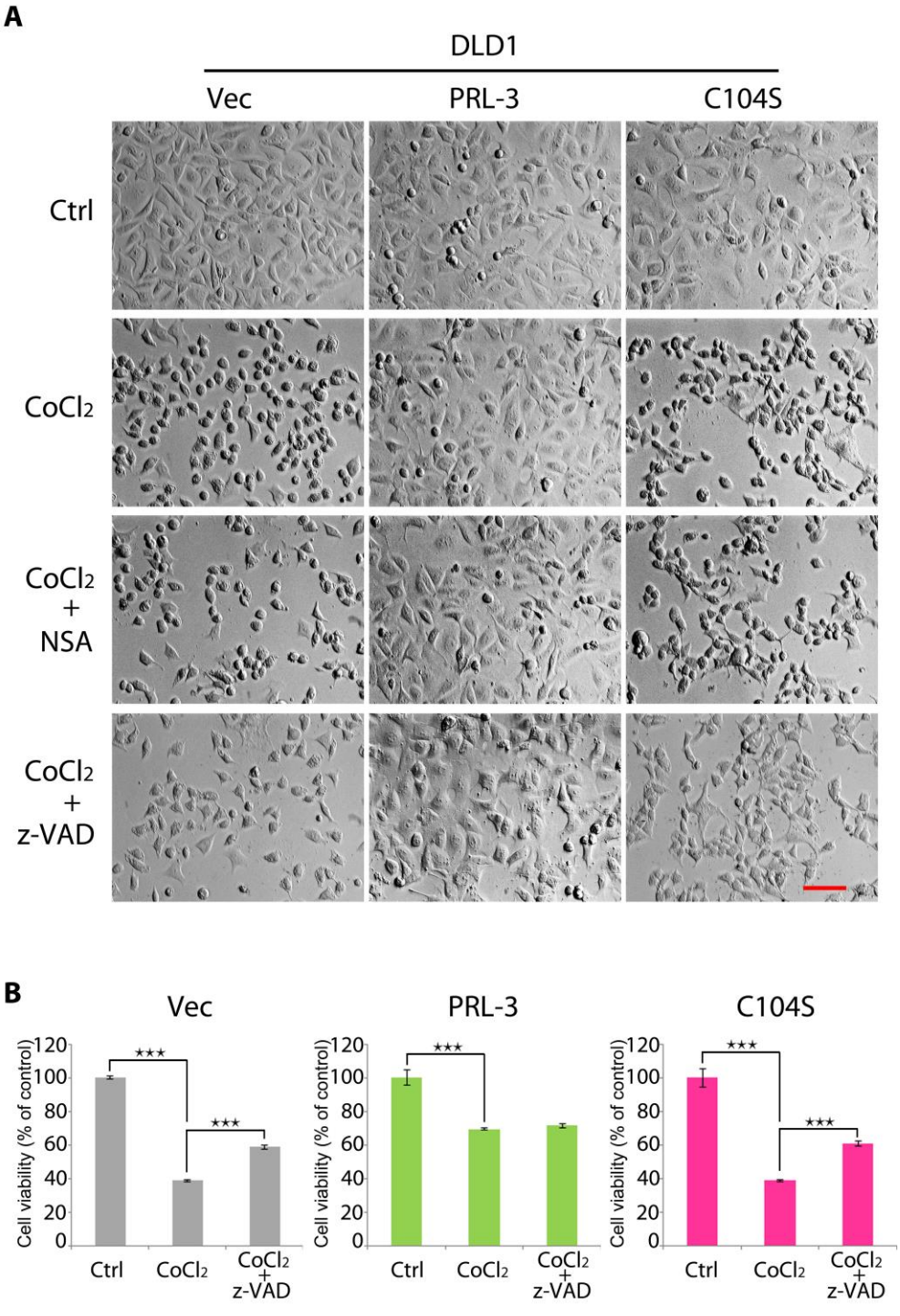
A
DLD1
Vec
PRL-3
C104S
Ctrl
CoCl2
CoCl2 + NSA
CoCl2 + z-VAD
B
Vec
PRL-3
C104S
Cell viability (% of control)
120
100
80
60
40
20
0
***
***
Ctrl
CoCl2
CoCl2 + z-VAD

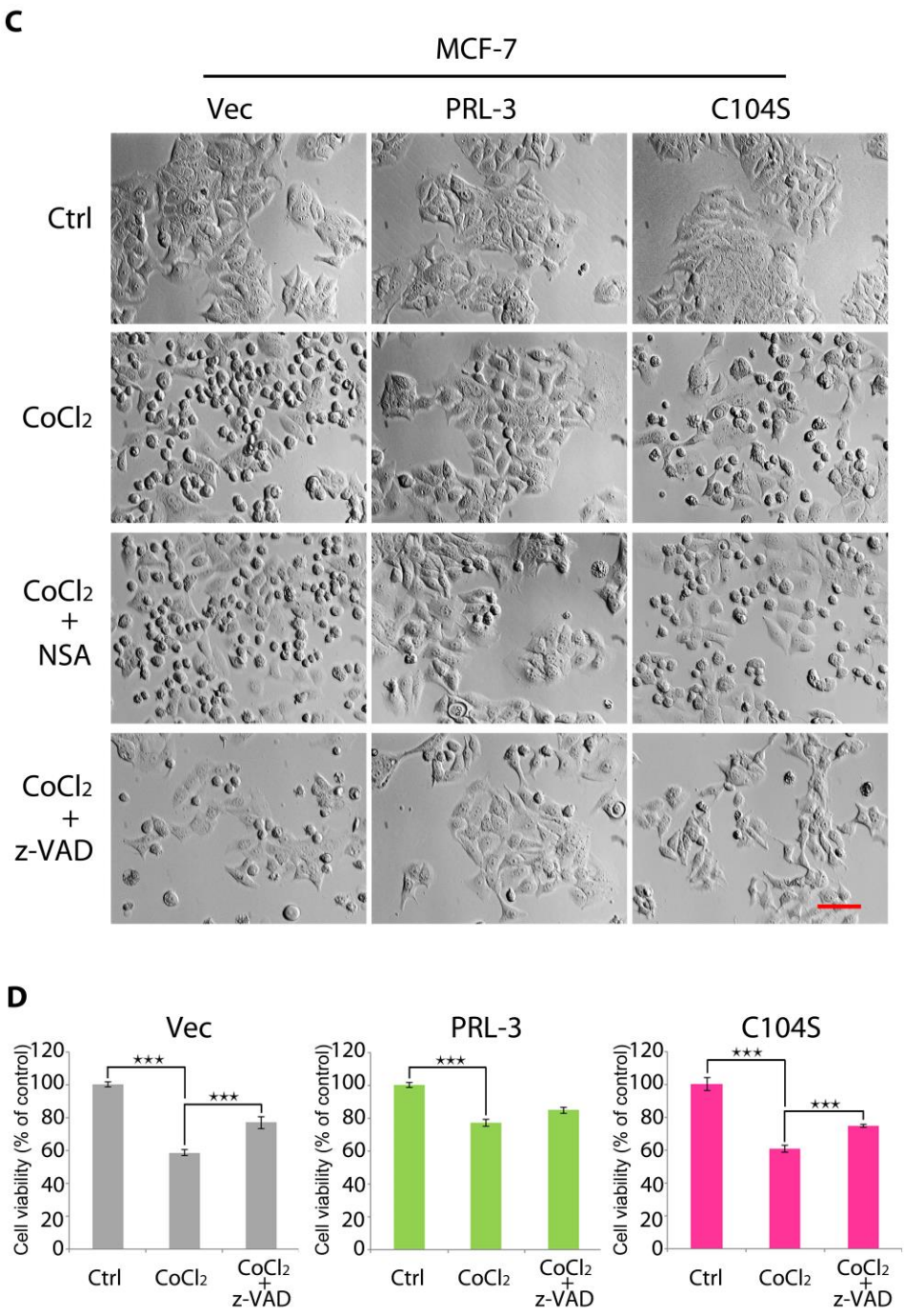

Figure 5. 3 z-VAD suppresses $CoCl_2$-induced cell death. (A) DLD-1-Vec, DLD-1-PRL-3 and DLD-1-C104S cells were treated with 5 μM $CoCl_2$ in the presence or absence of z-VAD-fmk (50 μM), or Necrosulfonamide (NSA) (10 μM) for 24 h. (B) DLD-1-Vec, DLD-1-PRL-3 and DLD-1-C104S cells were treated as in (A). Cell viability was then assayed using the MTS assay. Data are from three replicate experiments (mean ± SEM). (E) MCF-7 cells stably overexpressing EGFP vector only (Vec), EGFP-tagged wild-type PRL-3 (PRL-3) or EGFP-tagged catalytic-inactive PRL-3 C104S (C104S) were treated as in (A). (F) MCF-7-Vec, MCF-7-PRL-3 and MCF-7-C104S cells were treated as in (A). Then cell viability was assayed using MTS assay. Data are from three replicate experiments (mean ± SEM). Scale bar, 100 μm.

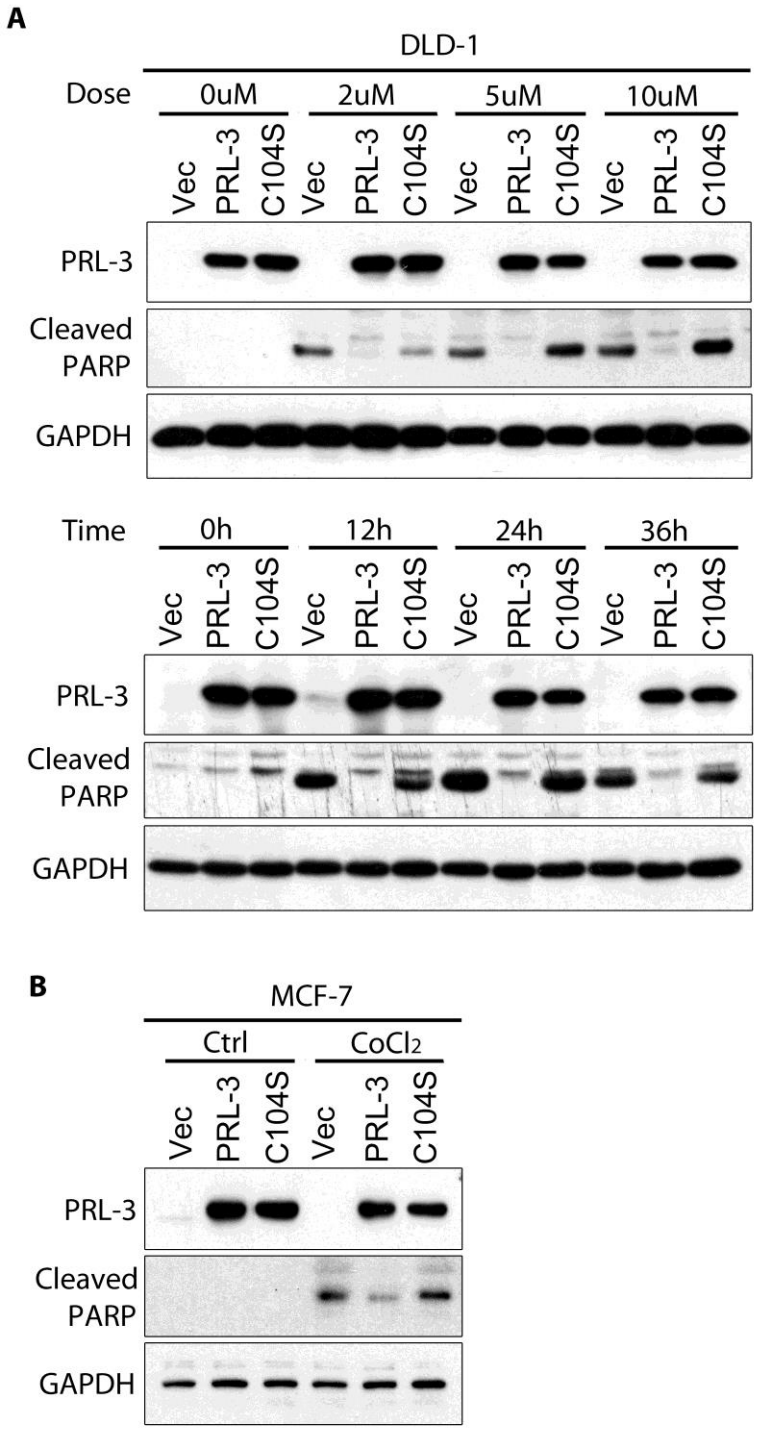

Figure 5. 4 PRL-3 reduces PARP cleavage. (A) DLD-1-Vec, DLD-1-PRL-3 and DLD-1-C104S cells were treated with $CoCl_2$ at the concentrations of 0, 2, 5 or 10 μM for 24 h. Cells were lysed and western blot analysis was performed with antibodies against PRL-3, cleaved-PARP (Asp214) and GAPDH. GAPDH used as a loading control. (B) MCF-7-Vec, MCF-7-PRL-3 and MCF-7-C104S cells were treated with 5 μM $CoCl_2$ for 24 h. Cells were subsequently lysed and analysed as in (A).

5.3.2. p38 MAPK participates in PRL-3-mediated cell survival

Determination of cell fate is coordinated by pro-survival and pro-apoptotic signals (Fulda et al., 2010). It is known that cancer cells can sustain survival and inhibit apoptosis via activation of diverse pro-survival signalling pathways (Brumatti et al., 2010; Buchheit et al., 2014). Some pro-survival pathways, such as Ras/Erk, PI3K/Akt, Src/STAT and JAK/STAT pathways, were previously reported to be activated in PRL-3-overexpressed cancer cells (Liang et al., 2007; Ming et al., 2009; Walls et al., 2013; Wang et al., 2007a). To examine whether these oncogenic pathways are involved in PRL-3-mediated cell survival, specific inhibitors were utilized to block them. Interestingly, upon inhibition of Ras/Erk (with U0126), PI3K/Akt (with LY294002), Src/STAT(with PP2), or Jak/STAT (with AG490), DLD-1-PRL-3 cells still displayed high resistance to $CoCl_2$-mediated cell death, suggesting that these signalling pathways might be not implicated in PRL-3-mediated cell survival (**Figure 5.5A**). PRL-3 was previously shown to promote autophagy under starvation in A2780 cells (Huang et al., 2014), which might increase stress tolerance and protect the cell from apoptosis (He and Levine, 2010). To determine if autophagy participates in PRL-3-mediated anti-apoptosis, Bafilomycin A1 (BafA1) was employed to inhibit autophagy. However, upon BafA1 treatment, PRL-3 still displayed an anti-apoptotic behavior in response to $CoCl_2$-induced cell death (**Figure 5.5A**).

JNK and p38 MAPK signalling pathways are two well-known pro-apoptosis pathways which are activated in response to chemotherapeutic agents, resulting in cell death (Sui et al., 2014). To determine the mechanism by which PRL-3 inhibits $CoCl_2$-induced apoptosis, cells were pretreated with the p38 MAPK inhibitor SB30580 or JNK inhibitor SP60125, prior to $CoCl_2$ exposure. Surprisingly, blockade of p38 MAPK, but not JNK, conferred apoptosis-resistance in both DLD-1-Vec and DLD-1-C104S cells upon $CoCl_2$

exposure (**Figure 5.5B**). This observation was further supported by cell viability assays. As shown in **Figure 5.5C,** SB30580 treatment significantly rescued the $CoCl_2$-induced loss of cell viability from 34% to 62% in DLD-1-Vec cells, and from 35% to 56% in DLD-1-C104S cells.

Furthermore, the activities of MAPK signalling pathways were evaluated upon $CoCl_2$ treatment by western blotting analysis. Dose response analysis showed that $CoCl_2$ induced phospho-activation of Erk1/2, JNK and p38 MAPKs (**Figure 5.6A**). However, compared with DLD-1-Vec and DLD-1-C104S cells, DLD-1-PRL-3 cells showed significantly less phosphorylation of p38 MAPK, suggesting PRL-3 may block the activation of p38 MAPK signalling pathway. Likewise, time course analysis revealed that phosphorylated p38 MAPK was highly expressed in $CoCl_2$-treated DLD-1-Vec and DLD-1-C104S cells, yet completely suppressed in DLD-1-PRL-3 cells (**Figure 5.6B**). Notably, this PRL-3-mediated inhibition of p38 MAPK phosphorylation was well correlated with a decrease in PARP cleavage. Thus, these data suggest PRL-3 may protect $CoCl_2$-induced apoptosis by inhibition of p38 activation.

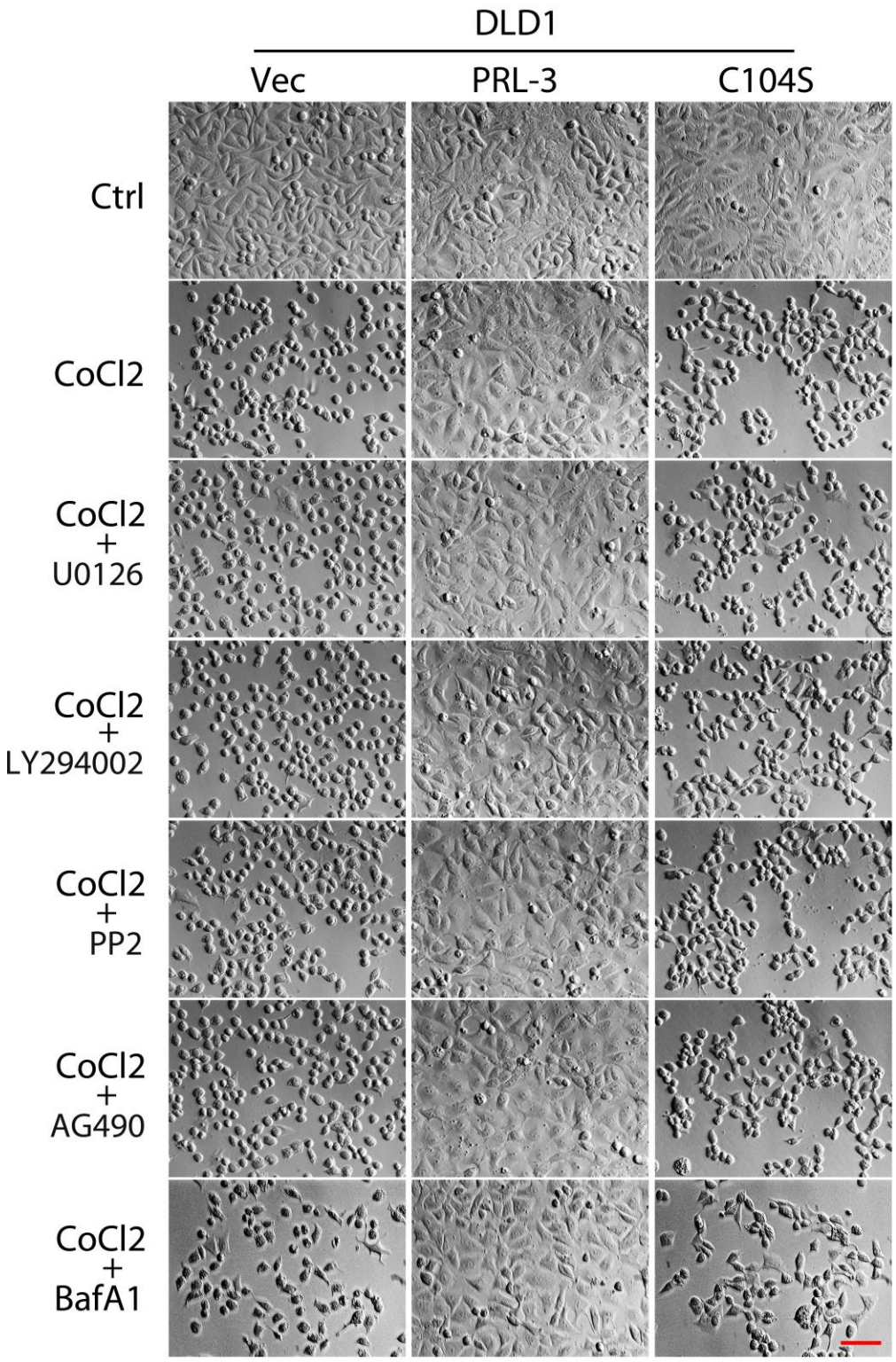
DLD1
Vec
PRL-3
C104S
Ctrl
CoCl2
CoCl2 + U0126
CoCl2 + LY294002
CoCl2 + PP2
CoCl2 + AG490
CoCl2 + BafA1

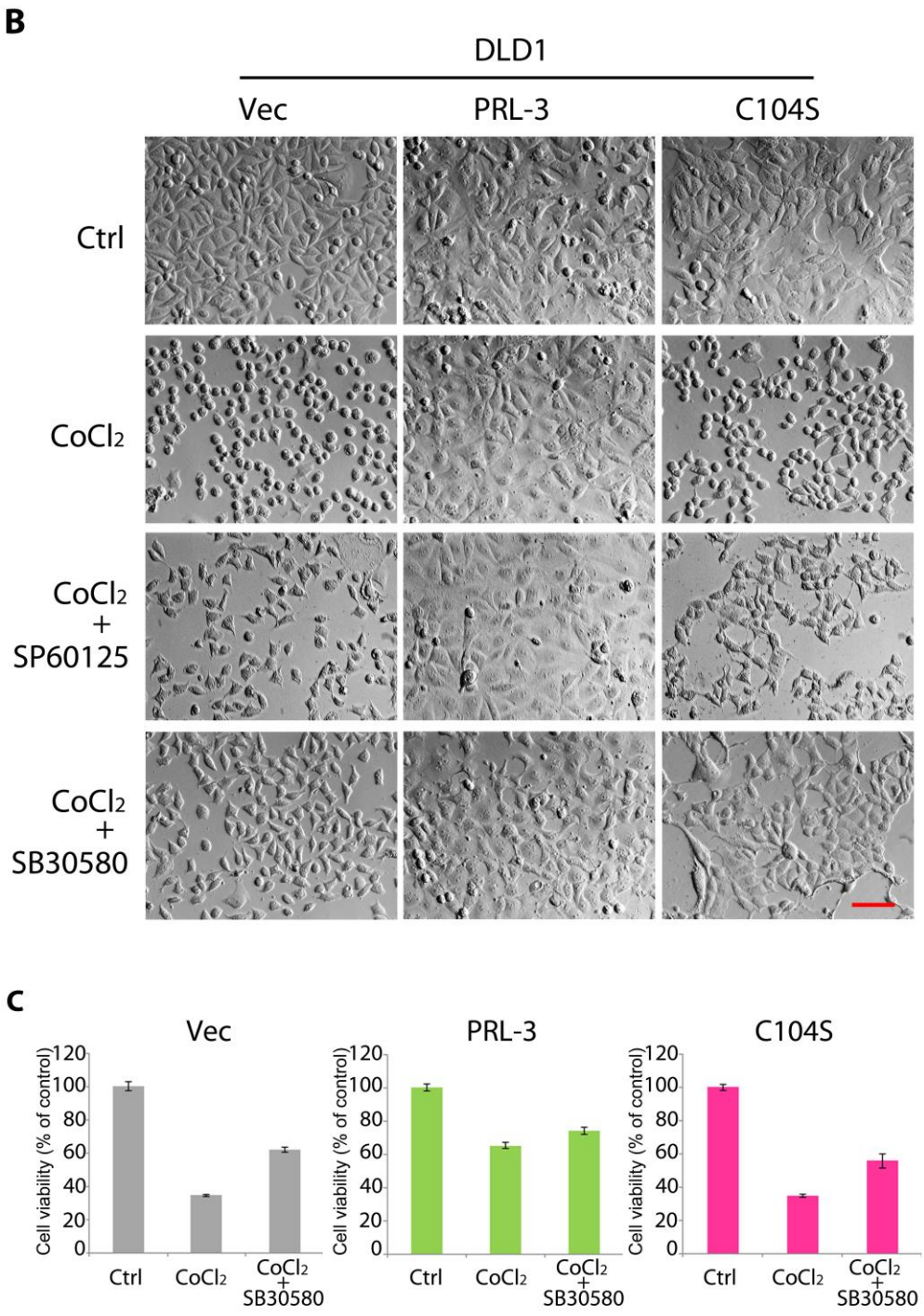

Figure 5. 5 p38 MAPK inhibitor protects against $CoCl_2$-induced apoptosis. (A) DLD-1-Vec, DLD-1-PRL-3 and DLD-1-C104S cells were pretreated with U0126 (10 μM), LY294002 (10 μM), PP2 (10 μM), AG490 (10 μM) or BafA1 (10 μM) for 1 h, and then 5 μM $CoCl_2$ was added for 24 h incubation. Cell morphology was captured using microscopy. (B) DLD-1-Vec, DLD-1-PRL-3 and DLD-1-C104S cells were pretreated with SP60125 (10 μM) or SB30580 (10 μM) for 1 h, and then 5 μM $CoCl_2$ was added for 24 h incubation, and then cell morphology was captured using microscopy. (C) After treatment as described in panel B, cell viability was assayed using MTS assay. Data were from three replicate experiments (mean ± SEM). Scale bar, 100 μm.

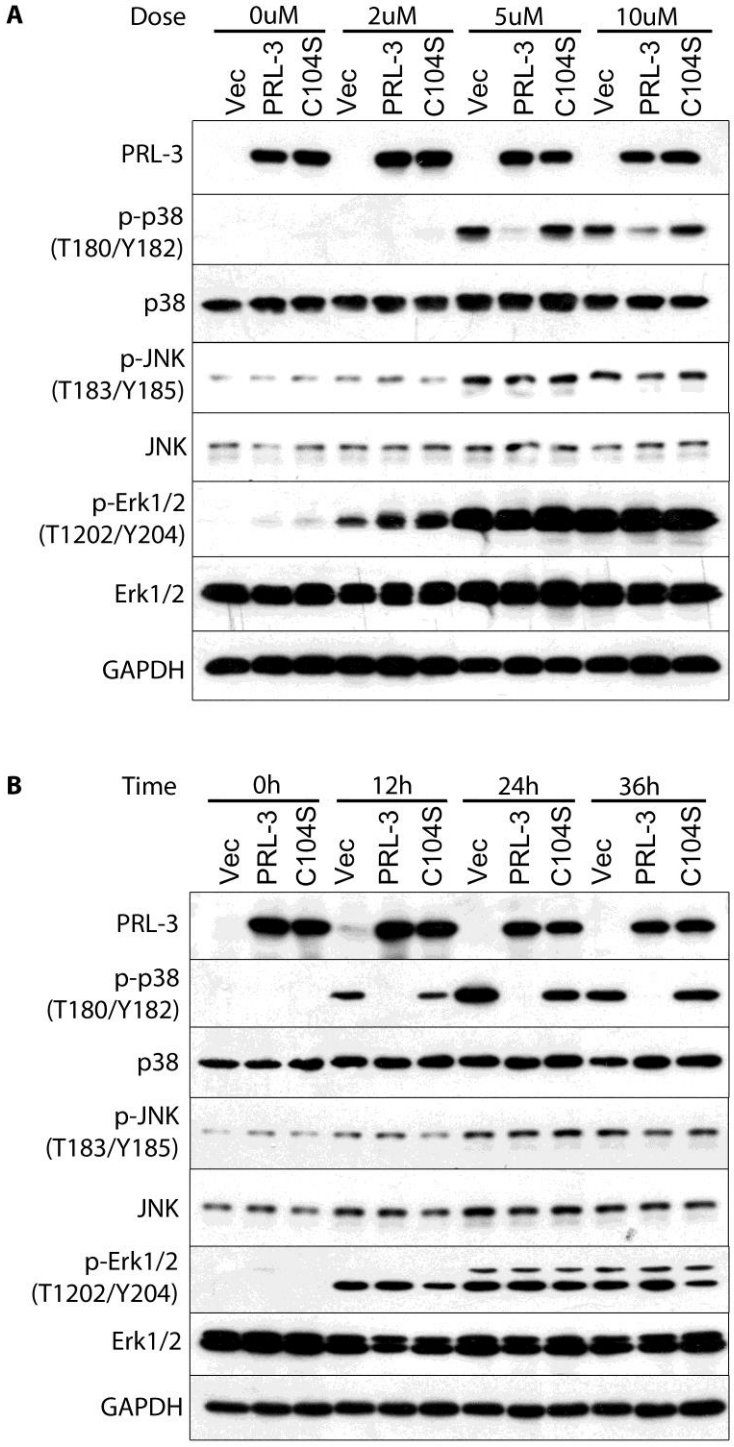

Figure 5. 6 p38 MAPK participates in PRL-3-mediated cell survival. (A) DLD-1-Vec, DLD-1-PRL-3 and DLD-1-C104S cells were treated with $CoCl_2$ at the concentrations of 0, 2, 5 or 10 μM for 24 h. Then cells were lysed and western blot analysis was performed with the indicated antibodies. GAPDH used as a loading control. (B) DLD-1-Vec, DLD-1-PRL-3 and DLD-1-C104S cells were incubated with 5 μM $CoCl_2$ for 0, 12, 24 or 36 h time intervals. Then cells were lysed and analysed as in (A).

5.3.3. PRL-3-mediated inhibition of p38 MAPK activation is ROS-independent

$CoCl_2$ is a ROS inducer (Kotake-Nara and Saida, 2007). Excess ROS could promote oxidation of cellular macromolecules and impair protein function, leading to apoptosis (Simon et al., 2000). Many reports have demonstrated that ROS induces cell death in response to drug treatment via the activation of p38 MAPK (Choi et al., 2015; Dong et al., 2015; Lin et al., 2014).

To evaluate the effect of PRL-3 on ROS generation, the level of ROS in cells was measured by the CM-H_2DCFDA (5-(and-6)-chloromethyl-2',7' -dichlorodihydrofluorescein diacetate) fluorescence assay. As shown in **Figure 5.7A**, compared with untreated cells, $CoCl_2$-treated cells showed higher levels of CM-H_2DCFDA fluorescence, indicating increased ROS generation. However, no significant difference in CM-H_2DCFDA fluorescence intensity was observed between DLD-1-Vec, DLD-1-PRL-3, and DLD-1-C104S cells (**Figure 5.7B**). More precisely, upon $CoCl_2$ treatment, the intracellular level of ROS increased by 1.66 fold in DLD-1-Vec cells, 1.63 fold in DLD-1-PRL-3 cells, and 1.71 fold in DLD-1-C104S cells (**Figure 5.7C**). These data suggest PRL-3 does not affect ROS generation in DLD-1 cells.

Next, the activities of ROS-sensitive ASK1, and its downstream effectors MKK4 and MKK3/6, which in turn regulate p38 MAPK (Han et al., 2010), were quantified by western blotting analysis. Dose response analysis demonstrated that $CoCl_2$ induced the phosphorylation of ASK1 and MKK4, but not MKK3/6. However, PRL-3 overexpression did not alter their phosphorylation levels (**Figure 5.7D**). Similar results were observed over a time course analysis (**Figure 5.7E**). These data suggest that while $CoCl_2$ can induce apoptosis through the activation of the ROS via the ASK1-MKK4-p38 MAPK signalling, PRL-3 did not seem to suppress p38 MAPK via this pathway.

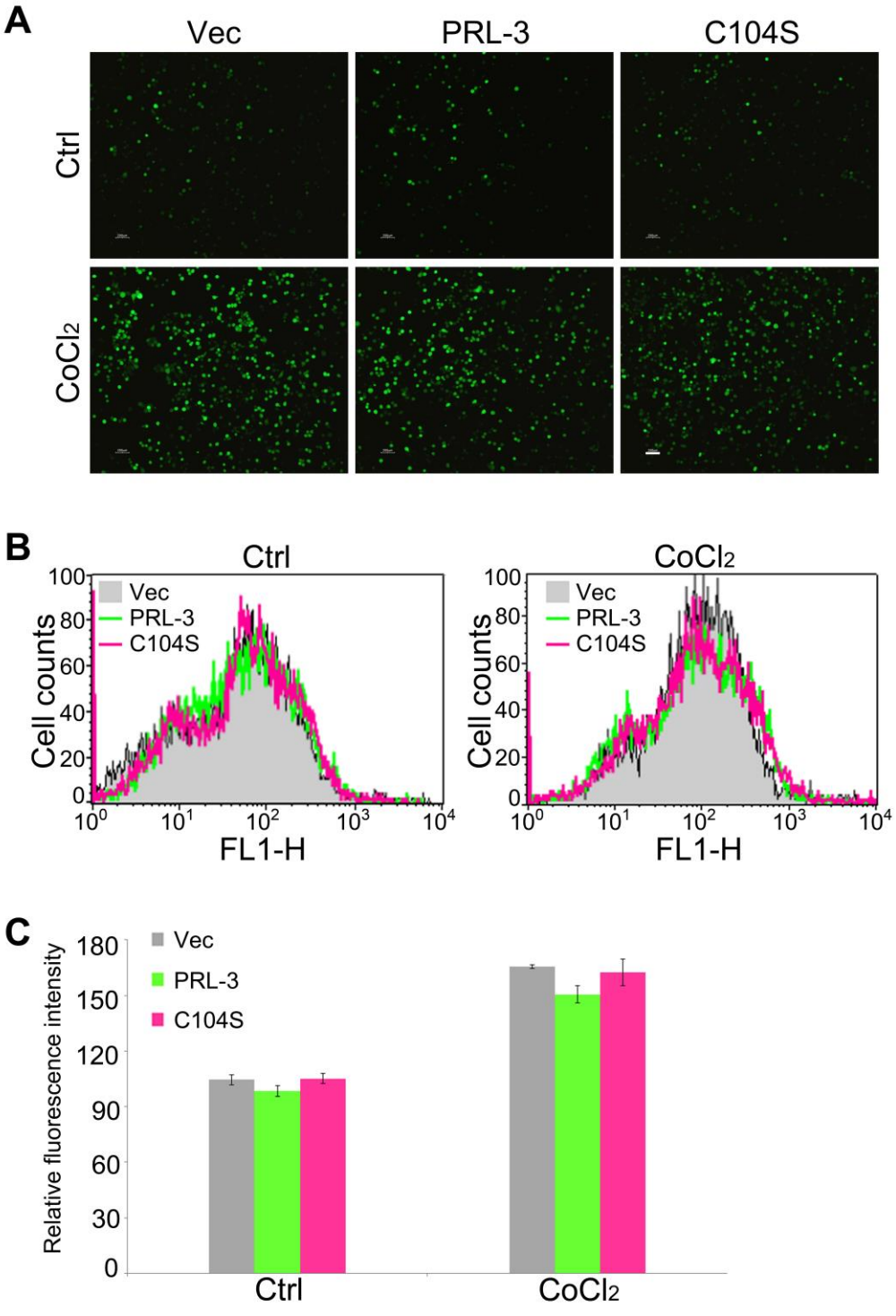
A
Vec
PRL-3
C104S
Ctrl
CoCl2
B
Ctrl
CoCl2
Vec
PRL-3
C104S
Cell counts
FL1-H
C
Relative fluorescence intensity
Ctrl
CoCl2

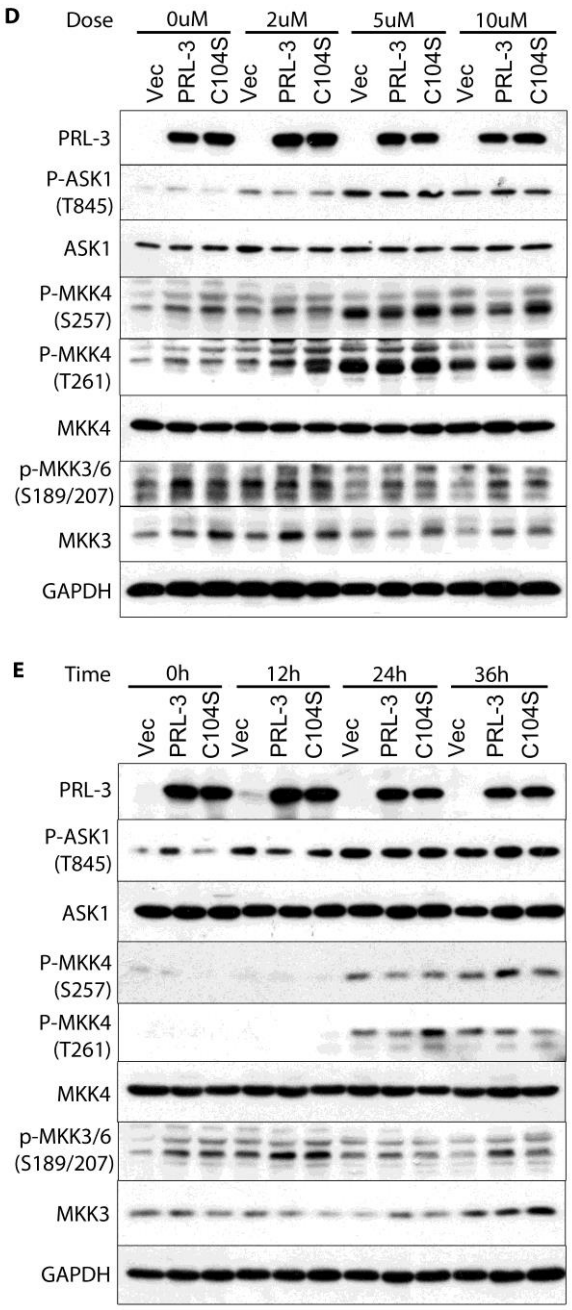

Figure 5. 7 PRL-3-mediated inhibition of p38 MAPK activation is ROS-independent. (A) DLD-1 cells overexpressing pCMV-vector (Vec), pCMV-PRL-3 (Vec) (PRL-3) or pCMV-PRL-3-C104S (C104S) were treated with 5 μM $CoCl_2$ for 24 h. Intracellular ROS were detected by staining with CM-H2DCFDA that turns into a fluorescent compound upon oxidation. Fluorescence images were captured using confocal microscope. (B) Cells were treated as in (A), CM-H2DCFDA fluorescence intensity was analysed by FACS. (C) Cells were analysed as in (B), data were from three replicate experiments (mean ± SEM). (D) DLD-1-Vec, DLD-1-PRL-3 and DLD-1-C104S cells were treated with $CoCl_2$ at the concentrations of 0, 2, 5 or 10 μM for 24 h. Then cells were lysed and western blot analysis was performed with the indicated antibodies. GAPDH served as a loading control. (E) DLD-1-Vec, DLD-1-PRL-3 and DLD-1-C104S cells were incubated with 5 μM $CoCl_2$ for 0, 12, 24 or 36 h. Cells were subsequently lysed and analysed as in (E). Scale bar, 200 μm.

5.3.4 PRL-3 binds p38 MAPK and promotes its dephosphorylation *in vitro*

To further explore how PRL-3 might downregulate the phosphorylation of p38 MAPK, the interaction of PRL-3 with p38 MAPK was analysed using co-immunoprecipitation. Notably, in DLD-1 cells, PRL-3 could directly bind to p38 MAPK, but not its upstream regulators ASK1 (**Figure 5.8A**). Moreover, reverse co-immunoprecipitation validated the interaction between PRL-3 and p38 MAPK in DLD-1 cells (**Figure 5.8B**).

Since PRL-3 is a phosphatase, the interaction between PRL-3 and p38 MAPK suggested that PRL-3 might dephosphorylate p38 MAPK directly. To test this idea, recombinant PRL-3 was incubated with p38 MAPK immunopurified from DLD-1 cells and assayed *in-vitro* using a malachite green phosphate-release assay. In this assay, an increase in malachite green corresponds to an increase in released phosphate, such as upon protein dephosphorylation. Interestingly, GST-PRL-3, but not GST, resulted in p38 MAPK dephosphorylation (**Figure 5.8C**). Collectively, these data suggest PRL-3 may protect $CoCl_2$-induced apoptosis by dephosphorylating p38 MAPK.

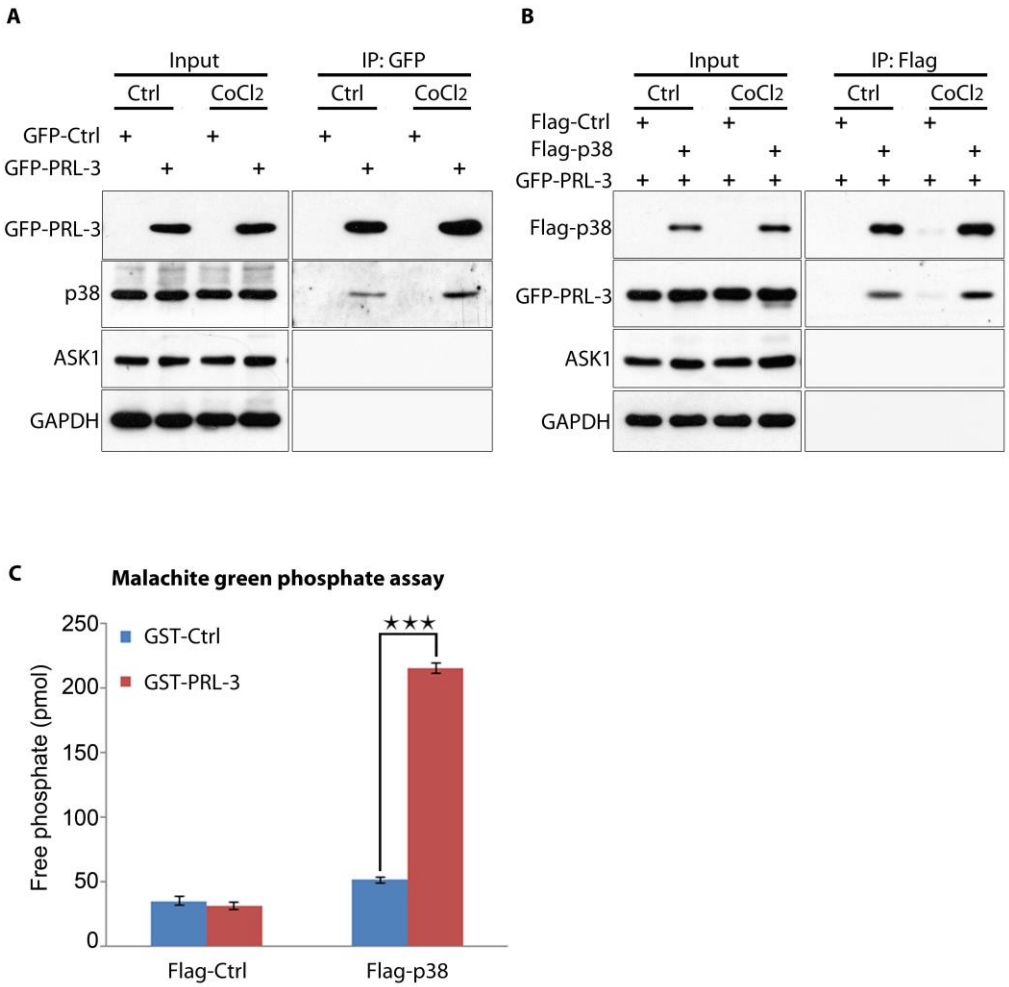

Figure 5. 8 PRL-3 binds p38 MAPK and promotes its dephosphorylation *in vitro*. (A) DLD-1 cells transfected with pEGFP-C1 vector alone (GFP-Ctrl) or pEGFP-PRL-3 (GFP-PRL-3) were incubated with or without 5 μM $CoCl_2$ for 24 h. Anti-EGFP immunoprecipitates from DLD-1-EGFP-Ctrl or DLD-1-EGFP-PRL-3 were probed with antibodies against PRL-3, p38, ASK1 and GAPDH. (B) DLD-1 cells were co-transfected with pEGFP-PRL-3 and pCDNA3-Flag-p38 or pCDNA3 vector only. Cells were then incubated with or without 5 μM $CoCl_2$ for 24 h. Anti-Flag immunoprecipitates from cells were analyzed by western blotting, and probed with antibodies against p38, PRL-3, ASK1 and GAPDH as indicated. (C) Recombinant GST or GST-PRL-3 was incubated with Flag-tagged immunoprecipitates purified from DLD-1 cells expressing Flag vector alone (Flag-ctrl) or Flag-tagged p38 (Flag-p38). Malachite green phosphatase assay was conducted as described in the Materials & Methods.

5.4. Discussion

In this chapter, PRL-3 was shown to suppress $CoCl_2$-induced apoptosis by preventing cellular shrinkage, promoting cell viability, and reducing PARP cleavage. These results are consistent with previous reports that PRL-3 could prevent cell death and sustain cell survival under stress conditions (Huang et al., 2014; Lian et al., 2012; Park et al., 2013a; Qu et al., 2014).

To define how PRL-3 protected against $CoCl_2$-induced apoptosis, multiple pro-survival signalling pathways, including Ras/Erk, PI3K/Akt, Src/STAT, JAK/STAT and autophagy, which were previously reported to be activated by PRL-3 (Huang et al., 2014; Lian et al., 2012; Park et al., 2013a; Qu et al., 2014), were blocked by specific inhibitors prior to $CoCl_2$ treatment. However, unlike previous reports suggesting the involvement of these oncogenic pathways in cell survival (Buchheit et al., 2014), none of these pathways affected PRL-3-mediated cell survival upon inhibition.

Since $CoCl_2$ was reported to activate two pro-apoptosis pathways, JNK and p38 MAPK (Lan et al., 2011; Zou et al., 2002), the effects of PRL-3 on these two signalling pathways were examined. Interestingly, PRL-3 was found to significantly inhibit p38 MAPK activity in $CoCl_2$-treated cells, but had no effect on JNK activity. Moreover, the p38 inhibitor SB30580 effectively rescued $CoCl_2$-induced cell shrinkage and loss of cell viability, which are two effects of PRL-3 overexpression, suggesting that p38 MAPK may participate in PRL-3-mediated anti-apoptotic effect. These findings showed a negative role of PRL-3 on p38 MAPK activation, which is generally consistent with previous report showing that p38 MAPK is activated upon knockdown of PRL-3 (Basak et al., 2008). However, there is also a contrasting study showing that PRL-3-induced phosphorylation of p38 MAPK (Al-Aidaroos et al., 2013). This inconsistency could be

due to the different conditions or different cell lines used. Unlike this study, the previous study detected the basal levels of p-p38 MAPK in A431 cells under nutrition abundant condition, but not the hyperactivated p38 status in DLD-1 cells upon stress stimuli. Therefore, a more systematic study, which includes different conditions and different cell lines, is required for a more comprehensive understanding in the future.

p38 MAPK is a tumor suppressor which induces apoptosis in response to multiple stress conditions such as inflammatory stimulation, hyperosmosis, heat shock, UV irradiation, and oxidative stress (Cuenda and Rousseau, 2007). High ROS stimulates the ASK1-MKK cascade, resulting in activation of p38 MAPK (Hsieh and Papaconstantinou, 2006). As $CoCl_2$ is a ROS inducer, the effect of PRL-3 on intracellular ROS generation was assessed. Although ROS increased upon $CoCl_2$ treatment, PRL-3 overexpression did not change the rate of ROS production. Consistently, the phosphorylation levels of ASK1and MKK4 increased upon $CoCl_2$ treatment, but maintained similar levels upon PRL-3 overexpression, suggesting PRL-3-mediated inhibition of p38 AMPK is ROS-independent. Since PRL-3 promoted a loss of p38 MAPK phosphorylation without a reduction in the activity of the latter's upstream kinases, the potential for PRL-3 to directly bind and dephosphorylate p38 MAPK was investigated. Indeed, an interaction between PRL-3 and p38 MAPK was observed in DLD-1 cells. Furthermore, PRL-3 could dephosphorylate p38 MAPK using an *in vitro* reaction with immunopurified p38. These results indicate that p38 MAPK might be a direct substrate of PRL-3.

As yet, many DUSPs have been reported to bind and dephosphorylate MAPKs (Theodosiou and Ashworth, 2002). However, none of them have shown the unique specificity towards p38 MAPK; for example, DUSP8, DUSP10, and UUSP16 can dephosphorylate JNK in addition to p38 MAPK (Muda et al., 1996; Tanoue et al., 2001; Theodosiou et al., 1999). In contrast, PRL-3 appears highly specific for the inactivation

of p38 MAPK, and does not inhibit JNK activation under cellular stress. Although more experiments are needed to further validate these findings, this study suggests that p38 MAPK might be a novel substrate of PRL-3 and PRL-3 may specifically dephosphorylate p38 MAPK under cellular stress to prevent apoptosis.

CHAPTER 6: CONCLUSION

In this thesis, the functions and related mechanisms of PRL-3 in cancer development modulation were systematically investigated. Firstly, the key role of hyperactivated mTOR signalling in PRL-3-driven oncogenesis was described. Secondly, the synergy between Akt-TSC2-Rheb signalling and Rag GTPases in driving PRL-3-mediated mTOR hyperactivation was characterised. Finally, in a separate vein, a novel role of p38 MAPK in apoptosis resistance by PRL-3 was unravelled. A hypothetical model summarizing the findings herein is proposed in **Figure 6.1**.

In the first part of the study, the relationship between PRL-3 expression and mTOR activity was investigated. Based on the positive correlation between PRL-3 expression and mTOR activity *in vivo* and *in vitro*, a causative link between elevated PRL-3 expression and mTOR activation was subsequently found under both normal and stressed conditions. Importantly, PRL-3 sensitized cellular responses to rapamycin treatment, particularly cell growth, motility, and invasiveness. From a clinical perspective, these findings reveal an Achilles' heel for PRL-3-overexpressing cancers, highlighting the possibility to target mTOR signalling in curtailing PRL-3-driven cancers.

In the second part of the study, the mechanism underlying PRL-3-driven mTORC1 activation was explored. Remarkably, PRL-3 induced mTORC1 activation via 2 parallel pathways: 1) activation of Akt-TSC2-Rheb signalling and 2) enhancement of Rag GTPase-mediated mTORC1 lysosomal recruitment. As yet, this is the first report of an mTORC1 regulator that affects both regulatory streams in parallel, effectively bringing activated Rheb (via Akt-TSC2) into proximity with mTORC1 at lysosomes (via Rag GTPase activity). This reveals the synergistic pathways PRL-3 function in oncogenesis, and cast some light into its reported pleiotropic effects.

Finally, in the third part of the study, the role of PRL-3 in $CoCl_2$-induced apoptosis was investigated. PRL-3 endowed cells with the ability to survive challenge with high doses of $CoCl_2$, even over prolonged periods, which was enough to kill cells without PRL-3 overexpression. This was linked to a suppression of pro-apoptotic p38 MAPK activity, as inferred by the decrease in p38 MAPK phosphorylation in PRL-3-overexpressing cells, as well as the ability for a p38 MAPK inhibitor to suppress this pro-survival phenotype. Intriguingly, PRL-3 was found to bind p38 MAPK in cells, and could dephosphorylate p38 MAPK when reconstituted in an *in vitro* system, suggesting that p38 MAPK might be a *bona fide* PRL-3 substrate. Notably, a limitation of this study was the use of $CoCl_2$ to induce apoptosis - future work will require validation of the pro-survival response upon challenge with other physiologically-relevant apoptosis inducers.

With pronounced overexpression in multiple human cancers and direct implication in tumour development, PRL-3 is regarded as a prognostic marker and a promising target for cancer therapy (Al-Aidaroos and Zeng, 2010). Although several PRL-3 inhibitors have been identified, none of them have reached clinical trials to date. Given the fact that mTOR is targeted pharmacologically in several pathologies, with several mTOR inhibitors already approved for cancer therapy (temsirolimus, everolimus), the finding of the critical role of mTOR in PRL-3-driven cancer progression more directly suggests a potential clinical value for mTOR inhibitors against PRL-3-overexpressing tumors, a hypothesis testable in future studies. Together with the advent of PRL-3-specific agents (Guo et al., 2011), further studies investigating the combinatorial value of drugs targeting both PRL-3 and mTOR might be warranted for improved anti-cancer effects.

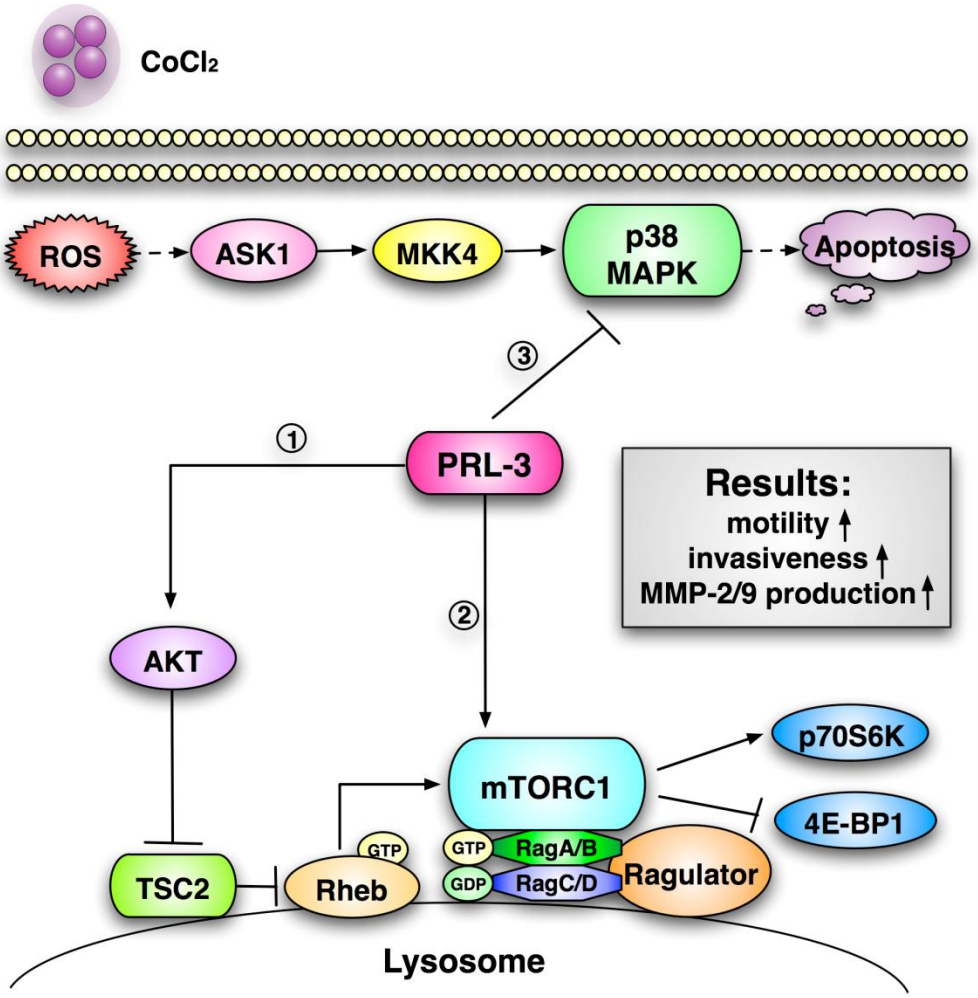

Figure 6. 1 Proposed model of the regulatory role of PRL-3 in mTOR signalling and p38 MAPK signalling. PRL-3 promotes mTORC1 activation by (1) activating Akt-TSC2-Rheb cascades and (2) enhancing Rag GTPases-mediated mTORC1 recruitment to lysosomes for activation, leading to an increase in cell motility, invasiveness, and MMP-2/9 production. (3) PRL-3 suppresses p38 MAPK activity to block apoptosis. Solid lines indicate direct regulation, while dotted line indicated indirect regulation.

Reference

Advani, S.H. (2010). Targeting mTOR pathway: A new concept in cancer therapy. Indian J Med Paediatr Oncol *31*, 132-136.

Ahn, J.H., Kim, S.J., Park, W.S., Cho, S.Y., Ha, J.D., Kim, S.S., Kang, S.K., Jeong, D.G., Jung, S.K., Lee, S.H., *et al.* (2006). Synthesis and biological evaluation of rhodanine derivatives as PRL-3 inhibitors. Bioorg Med Chem Lett *16*, 2996-2999.

Aicher, L.D., Campbell, J.S., and Yeung, R.S. (2001). Tuberin phosphorylation regulates its interaction with hamartin. Two proteins involved in tuberous sclerosis. J Biol Chem *276*, 21017-21021.

Al-Aidaroos, A.Q., Yuen, H.F., Guo, K., Zhang, S.D., Chung, T.H., Chng, W.J., and Zeng, Q. (2013). Metastasis-associated PRL-3 induces EGFR activation and addiction in cancer cells. J Clin Invest *123*, 3459-3471.

Al-Aidaroos, A.Q., and Zeng, Q. (2010). PRL-3 phosphatase and cancer metastasis. J Cell Biochem *111*, 1087-1098.

Alonso, A., Sasin, J., Bottini, N., Friedberg, I., Friedberg, I., Osterman, A., Godzik, A., Hunter, T., Dixon, J., and Mustelin, T. (2004). Protein tyrosine phosphatases in the human genome. Cell *117*, 699-711.

Arsham, A.M., Howell, J.J., and Simon, M.C. (2003). A novel hypoxia-inducible factor-independent hypoxic response regulating mammalian target of rapamycin and its targets. J Biol Chem *278*, 29655-29660.

Bai, X., and Jiang, Y. (2010). Key factors in mTOR regulation. Cell Mol Life Sci *67*, 239-253.

Baker, M. (2005). Upping the ante on antibodies. Nat Biotechnol *23*, 1065-1072.

Bar-Peled, L., Schweitzer, L.D., Zoncu, R., and Sabatini, D.M. (2012). Ragulator is a GEF for the rag GTPases that signal amino acid levels to mTORC1. Cell *150*, 1196-1208.

Bardelli, A., Saha, S., Sager, J.A., Romans, K.E., Xin, B., Markowitz, S.D., Lengauer, C., Velculescu, V.E., Kinzler, K.W., and Vogelstein, B. (2003). PRL-3 expression in metastatic cancers. Clin Cancer Res *9*, 5607-5615.

Basak, S., Jacobs, S.B., Krieg, A.J., Pathak, N., Zeng, Q., Kaldis, P., Giaccia, A.J., and Attardi, L.D. (2008). The metastasis-associated gene Prl-3 is a p53 target involved in cell-cycle regulation. Mol Cell *30*, 303-314.

Bayascas, J.R., and Alessi, D.R. (2005). Regulation of Akt/PKB Ser473 phosphorylation. Mol Cell *18*, 143-145.

Beardmore, V.A., Hinton, H.J., Eftychi, C., Apostolaki, M., Armaka, M., Darragh, J., McIlrath, J., Carr, J.M., Armit, L.J., Clacher, C., *et al.* (2005). Generation and

characterization of p38beta (MAPK11) gene-targeted mice. Mol Cell Biol *25*, 10454-10464.

Bessette, D.C., Qiu, D., and Pallen, C.J. (2008). PRL PTPs: mediators and markers of cancer progression. Cancer Metastasis Rev *27*, 231-252.

Betz, C., and Hall, M.N. (2013). Where is mTOR and what is it doing there? J Cell Biol *203*, 563-574.

Bilici, A., Ustaalioglu, B.B., Yavuzer, D., Seker, M., Mayadagli, A., and Gumus, M. (2012). Prognostic significance of high phosphatase of regenerating liver-3 expression in patients with gastric cancer who underwent curative gastrectomy. Digestive diseases and sciences *57*, 1568-1575.

Brancho, D., Tanaka, N., Jaeschke, A., Ventura, J.J., Kelkar, N., Tanaka, Y., Kyuuma, M., Takeshita, T., Flavell, R.A., and Davis, R.J. (2003). Mechanism of p38 MAP kinase activation in vivo. Genes Dev *17*, 1969-1978.

Brown, E.J., Albers, M.W., Shin, T.B., Ichikawa, K., Keith, C.T., Lane, W.S., and Schreiber, S.L. (1994). A mammalian protein targeted by G1-arresting rapamycin-receptor complex. Nature *369*, 756-758.

Brumatti, G., Salmanidis, M., and Ekert, P.G. (2010). Crossing paths: interactions between the cell death machinery and growth factor survival signals. Cell Mol Life Sci *67*, 1619-1630.

Brunn, G.J., Hudson, C.C., Sekulic, A., Williams, J.M., Hosoi, H., Houghton, P.J., Lawrence, J.C., Jr., and Abraham, R.T. (1997). Phosphorylation of the translational repressor PHAS-I by the mammalian target of rapamycin. Science *277*, 99-101.

Buchheit, C.L., Weigel, K.J., and Schafer, Z.T. (2014). Cancer cell survival during detachment from the ECM: multiple barriers to tumour progression. Nat Rev Cancer *14*, 632-641.

Buffart, T.E., Coffa, J., Hermsen, M.A., Carvalho, B., van der Sijp, J.R., Ylstra, B., Pals, G., Schouten, J.P., and Meijer, G.A. (2005). DNA copy number changes at 8q11-24 in metastasized colorectal cancer. Cell Oncol *27*, 57-65.

Burnett, G., and Kennedy, E.P. (1954). The enzymatic phosphorylation of proteins. J Biol Chem *211*, 969-980.

Campbell, I.D. (2008). Studies of focal adhesion assembly. Biochem Soc Trans *36*, 263-266.

Cantley, L.C. (2002). The phosphoinositide 3-kinase pathway. Science *296*, 1655-1657.

Cargnello, M., and Roux, P.P. (2011). Activation and function of the MAPKs and their substrates, the MAPK-activated protein kinases. Microbiol Mol Biol Rev *75*, 50-83.

Cargnello, M., Tcherkezian, J., and Roux, P.P. (2015). The expanding role of mTOR in cancer cell growth and proliferation. Mutagenesis *30*, 169-176.

Caron, E., Ghosh, S., Matsuoka, Y., Ashton-Beaucage, D., Therrien, M., Lemieux, S., Perreault, C., Roux, P.P., and Kitano, H. (2010). A comprehensive map of the mTOR signaling network. Mol Syst Biol *6*, 453.

Casey, R., and Li, W.W. (1997). Factors controlling ocular angiogenesis. Am J Ophthalmol *124*, 521-529.

Cates, C.A., Michael, R.L., Stayrook, K.R., Harvey, K.A., Burke, Y.D., Randall, S.K., Crowell, P.L., and Crowell, D.N. (1996). Prenylation of oncogenic human PTP(CAAX) protein tyrosine phosphatases. Cancer Lett *110*, 49-55.

Chiang, G.G., and Abraham, R.T. (2005). Phosphorylation of mammalian target of rapamycin (mTOR) at Ser-2448 is mediated by p70S6 kinase. J Biol Chem *280*, 25485-25490.

Chiu, M.I., Katz, H., and Berlin, V. (1994). RAPT1, a mammalian homolog of yeast Tor, interacts with the FKBP12/rapamycin complex. Proc Natl Acad Sci U S A *91*, 12574-12578.

Choi, H.S., Hwang, C.K., Song, K.Y., Law, P.Y., Wei, L.N., and Loh, H.H. (2009). Poly(C)-binding proteins as transcriptional regulators of gene expression. Biochem Biophys Res Commun *380*, 431-436.

Choi, J.Y., Cho, H.J., Hwang, S.G., Kim, W.J., Kim, J.I., Um, H.D., and Park, J.K. (2015). Podophyllotoxin acetate enhances gamma-ionizing radiation-induced apoptotic cell death by stimulating the ROS/p38/caspase pathway. Biomed Pharmacother *70*, 111-118.

Choi, M.S., Min, S.H., Jung, H., Lee, J.D., Lee, T.H., Lee, H.K., and Yoo, O.J. (2011). The essential role of FKBP38 in regulating phosphatase of regenerating liver 3 (PRL-3) protein stability. Biochem Biophys Res Commun *406*, 305-309.

Choi, S.K., Oh, H.M., Lee, S.K., Jeong, D.G., Ryu, S.E., Son, K.H., Han, D.C., Sung, N.D., Baek, N.I., and Kwon, B.M. (2006). Biflavonoids inhibited phosphatase of regenerating liver-3 (PRL-3). Nat Prod Res *20*, 341-346.

Chong, P.S., Zhou, J., Cheong, L.L., Liu, S.C., Qian, J., Guo, T., Sze, S.K., Zeng, Q., and Chng, W.J. (2014). LEO1 is regulated by PRL-3 and mediates its oncogenic properties in acute myelogenous leukemia. Cancer Res *74*, 3043-3053.

Cobb, M.H., Hepler, J.E., Cheng, M., and Robbins, D. (1994). The mitogen-activated protein kinases, ERK1 and ERK2. Semin Cancer Biol *5*, 261-268.

Cohen, P. (2002). The origins of protein phosphorylation. Nat Cell Biol *4*, E127-130.

Corradetti, M.N., Inoki, K., Bardeesy, N., DePinho, R.A., and Guan, K.L. (2004). Regulation of the TSC pathway by LKB1: evidence of a molecular link between tuberous sclerosis complex and Peutz-Jeghers syndrome. Genes Dev *18*, 1533-1538.

Cowan, K.J., and Storey, K.B. (2003). Mitogen-activated protein kinases: new signaling pathways functioning in cellular responses to environmental stress. J Exp Biol *206*, 1107-1115.

Cuadrado, A., and Nebreda, A.R. (2010). Mechanisms and functions of p38 MAPK signalling. Biochem J *429*, 403-417.

Cuenda, A., and Rousseau, S. (2007). p38 MAP-kinases pathway regulation, function and role in human diseases. Biochim Biophys Acta *1773*, 1358-1375.

D'Souza-Schorey, C., and Chavrier, P. (2006). ARF proteins: roles in membrane traffic and beyond. Nat Rev Mol Cell Biol *7*, 347-358.

Daouti, S., Li, W.H., Qian, H., Huang, K.S., Holmgren, J., Levin, W., Reik, L., McGady, D.L., Gillespie, P., Perrotta, A., *et al.* (2008). A selective phosphatase of regenerating liver phosphatase inhibitor suppresses tumor cell anchorage-independent growth by a novel mechanism involving p130Cas cleavage. Cancer Res *68*, 1162-1169.

Dazert, E., and Hall, M.N. (2011). mTOR signaling in disease. Curr Opin Cell Biol *23*, 744-755.

Demetriades, C., Doumpas, N., and Teleman, A.A. (2014). Regulation of TORC1 in response to amino acid starvation via lysosomal recruitment of TSC2. Cell *156*, 786-799.

Depowski, P.L., Rosenthal, S.I., and Ross, J.S. (2001). Loss of expression of the PTEN gene protein product is associated with poor outcome in breast cancer. Mod Pathol *14*, 672-676.

Dewang, P.M., Hsu, N.M., Peng, S.Z., and Li, W.R. (2005). Protein tyrosine phosphatases and their inhibitors. Curr Med Chem *12*, 1-22.

Diamond, R.H., Cressman, D.E., Laz, T.M., Abrams, C.S., and Taub, R. (1994). PRL-1, a unique nuclear protein tyrosine phosphatase, affects cell growth. Mol Cell Biol *14*, 3752-3762.

Diamond, R.H., Peters, C., Jung, S.P., Greenbaum, L.E., Haber, B.A., Silberg, D.G., Traber, P.G., and Taub, R. (1996). Expression of PRL-1 nuclear PTPase is associated with proliferation in liver but with differentiation in intestine. Am J Physiol *271*, G121-129.

Dibble, C.C., Elis, W., Menon, S., Qin, W., Klekota, J., Asara, J.M., Finan, P.M., Kwiatkowski, D.J., Murphy, L.O., and Manning, B.D. (2012). TBC1D7 is a third subunit of the TSC1-TSC2 complex upstream of mTORC1. Mol Cell *47*, 535-546.

Dong, Y., Yin, S., Song, X., Huo, Y., Fan, L., Ye, M., and Hu, H. (2015). Involvement of ROS-p38-H2AX axis in novel curcumin analogues-induced apoptosis in breast cancer cells. Mol Carcinog.

Dumaual, C.M., Sandusky, G.E., Crowell, P.L., and Randall, S.K. (2006). Cellular localization of PRL-1 and PRL-2 gene expression in normal adult human tissues. J Histochem Cytochem *54*, 1401-1412.

Eke, I., and Cordes, N. (2015). Focal adhesion signaling and therapy resistance in cancer. Semin Cancer Biol *31*, 65-75.

Enslen, H., Brancho, D.M., and Davis, R.J. (2000). Molecular determinants that mediate selective activation of p38 MAP kinase isoforms. EMBO J *19*, 1301-1311.

Fagerli, U.M., Holt, R.U., Holien, T., Vaatsveen, T.K., Zhan, F., Egeberg, K.W., Barlogie, B., Waage, A., Aarset, H., Dai, H.Y., *et al.* (2008). Overexpression and involvement in migration by the metastasis-associated phosphatase PRL-3 in human myeloma cells. Blood *111*, 806-815.

Fiordalisi, J.J., Keller, P.J., and Cox, A.D. (2006). PRL tyrosine phosphatases regulate rho family GTPases to promote invasion and motility. Cancer Res *66*, 3153-3161.

Forte, E., Orsatti, L., Talamo, F., Barbato, G., De Francesco, R., and Tomei, L. (2008). Ezrin is a specific and direct target of protein tyrosine phosphatase PRL-3. Biochim Biophys Acta *1783*, 334-344.

Frias, M.A., Thoreen, C.C., Jaffe, J.D., Schroder, W., Sculley, T., Carr, S.A., and Sabatini, D.M. (2006). mSin1 is necessary for Akt/PKB phosphorylation, and its isoforms define three distinct mTORC2s. Curr Biol *16*, 1865-1870.

Fulda, S., Gorman, A.M., Hori, O., and Samali, A. (2010). Cellular stress responses: cell survival and cell death. Int J Cell Biol *2010*, 214074.

Gao, J., Liao, J., and Yang, G.Y. (2009). CAAX-box protein, prenylation process and carcinogenesis. Am J Transl Res *1*, 312-325.

Gialeli, C., Theocharis, A.D., and Karamanos, N.K. (2011). Roles of matrix metalloproteinases in cancer progression and their pharmacological targeting. FEBS J *278*, 16-27.

Guo, K., Li, J., Tang, J.P., Koh, V., Gan, B.Q., and Zeng, Q. (2004). Catalytic domain of PRL-3 plays an essential role in tumor metastasis: formation of PRL-3 tumors inside the blood vessels. Cancer Biol Ther *3*, 945-951.

Guo, K., Li, J., Tang, J.P., Tan, C.P., Hong, C.W., Al-Aidaroos, A.Q., Varghese, L., Huang, C., and Zeng, Q. (2011). Targeting intracellular oncoproteins with antibody therapy or vaccination. Sci Transl Med *3*, 99ra85.

Guo, K., Li, J., Wang, H., Osato, M., Tang, J.P., Quah, S.Y., Gan, B.Q., and Zeng, Q. (2006). PRL-3 initiates tumor angiogenesis by recruiting endothelial cells in vitro and in vivo. Cancer Res *66*, 9625-9635.

Guo, K., Tang, J.P., Jie, L., Al-Aidaroos, A.Q., Hong, C.W., Tan, C.P., Park, J.E., Varghese, L., Feng, Z., Zhou, J., *et al.* (2012). Engineering the first chimeric antibody in targeting intracellular PRL-3 oncoprotein for cancer therapy in mice. Oncotarget *3*, 158-171.

Guo, K., Tang, J.P., Tan, C.P., Wang, H., and Zeng, Q. (2008). Monoclonal antibodies target intracellular PRL phosphatases to inhibit cancer metastases in mice. Cancer Biol Ther *7*, 750-757.

Gupta, G.P., and Massague, J. (2006). Cancer metastasis: building a framework. Cell *127*, 679-695.

Guy, C.T., Cardiff, R.D., and Muller, W.J. (1992). Induction of mammary tumors by expression of polyomavirus middle T oncogene: a transgenic mouse model for metastatic disease. Mol Cell Biol *12*, 954-961.

Guzinska-Ustymowicz, K., Kisluk, J., Terlikowski, S.J., Pryczynicz, A., Niewiarowska, K., Ustymowicz, M., Hawryluk, M., Poludniewski, M., and Kemona, A. (2013). Expression of phosphatase of regenerating liver-3 (PRL-3) in endometrioid cancer and lymph nodes metastases. Advances in medical sciences *58*, 221-226.

Gwinn, D.M., Shackelford, D.B., Egan, D.F., Mihaylova, M.M., Mery, A., Vasquez, D.S., Turk, B.E., and Shaw, R.J. (2008). AMPK phosphorylation of raptor mediates a metabolic checkpoint. Mol Cell *30*, 214-226.

Han, D.S., Huang, H.P., Wang, T.G., Hung, M.Y., Ke, J.Y., Chang, K.T., Chang, H.Y., Ho, Y.P., Hsieh, W.Y., and Yang, W.S. (2010). Transcription activation of myostatin by trichostatin A in differentiated C2C12 myocytes via ASK1-MKK3/4/6-JNK and p38 mitogen-activated protein kinase pathways. J Cell Biochem *111*, 564-573.

Han, Y.M., Lee, S.K., Jeong, D.G., Ryu, S.E., Han, D.C., Kim, D.K., and Kwon, B.M. (2012). Emodin inhibits migration and invasion of DLD-1 (PRL-3) cells via inhibition of PRL-3 phosphatase activity. Bioorg Med Chem Lett *22*, 323-326.

Hanahan, D., and Weinberg, R.A. (2011). Hallmarks of cancer: the next generation. Cell *144*, 646-674.

Hao, R.T., Zhang, X.H., Pan, Y.F., Liu, H.G., Xiang, Y.Q., Wan, L., and Wu, X.L. (2010). Prognostic and metastatic value of phosphatase of regenerating liver-3 in invasive breast cancer. J Cancer Res Clin Oncol *136*, 1349-1357.

Hara, K., Maruki, Y., Long, X., Yoshino, K., Oshiro, N., Hidayat, S., Tokunaga, C., Avruch, J., and Yonezawa, K. (2002). Raptor, a binding partner of target of rapamycin (TOR), mediates TOR action. Cell *110*, 177-189.

Hardie, D.G. (1990). Roles of protein kinases and phosphatases in signal transduction. Symp Soc Exp Biol *44*, 241-255.

Hassan, N.M., Hamada, J., Kameyama, T., Tada, M., Nakagawa, K., Yoshida, S., Kashiwazaki, H., Yamazaki, Y., Suzuki, Y., Sasaki, A., *et al.* (2011). Increased expression of the PRL-3 gene in human oral squamous cell carcinoma and dysplasia tissues. Asian Pacific journal of cancer prevention : APJCP *12*, 947-951.

Hatate, K., Yamashita, K., Hirai, K., Kumamoto, H., Sato, T., Ozawa, H., Nakamura, T., Onozato, W., Kokuba, Y., Ihara, A., *et al.* (2008). Liver metastasis of colorectal cancer by protein-tyrosine phosphatase type 4A, 3 (PRL-3) is mediated through lymph node

metastasis and elevated serum tumor markers such as CEA and CA19-9. Oncol Rep *20*, 737-743.

Hazin, J., Moldenhauer, G., Altevogt, P., and Brady, N.R. (2015). A novel method for measuring cellular antibody uptake using imaging flow cytometry reveals distinct uptake rates for two different monoclonal antibodies targeting L1. J Immunol Methods.

He, C., and Levine, B. (2010). The Beclin 1 interactome. Curr Opin Cell Biol *22*, 140-149.

Hemmings, B.A., and Restuccia, D.F. (2015). The PI3K-PKB/Akt pathway. Cold Spring Harb Perspect Biol *7*.

Hoeffer, C.A., and Klann, E. (2010). mTOR signaling: at the crossroads of plasticity, memory and disease. Trends Neurosci *33*, 67-75.

Holz, M.K., and Blenis, J. (2005). Identification of S6 kinase 1 as a novel mammalian target of rapamycin (mTOR)-phosphorylating kinase. J Biol Chem *280*, 26089-26093.

Hsieh, C.C., and Papaconstantinou, J. (2006). Thioredoxin-ASK1 complex levels regulate ROS-mediated p38 MAPK pathway activity in livers of aged and long-lived Snell dwarf mice. FASEB J *20*, 259-268.

Hu, L., Luo, H., Wang, W., Li, H., and He, T. (2013). Poor prognosis of phosphatase of regenerating liver 3 expression in gastric cancer: a meta-analysis. PloS one *8*, e76927.

Huang, J., and Manning, B.D. (2008). The TSC1-TSC2 complex: a molecular switchboard controlling cell growth. Biochem J *412*, 179-190.

Huang, Y.H., Al-Aidaroos, A.Q., Yuen, H.F., Zhang, S.D., Shen, H.M., Rozycka, E., McCrudden, C.M., Tergaonkar, V., Gupta, A., Lin, Y.B., *et al.* (2014). A role of autophagy in PTP4A3-driven cancer progression. Autophagy *10*, 1787-1800.

Ikenoue, T., Inoki, K., Yang, Q., Zhou, X., and Guan, K.L. (2008). Essential function of TORC2 in PKC and Akt turn motif phosphorylation, maturation and signalling. EMBO J *27*, 1919-1931.

Inoki, K., Li, Y., Xu, T., and Guan, K.L. (2003a). Rheb GTPase is a direct target of TSC2 GAP activity and regulates mTOR signaling. Genes Dev *17*, 1829-1834.

Inoki, K., Li, Y., Zhu, T., Wu, J., and Guan, K.L. (2002). TSC2 is phosphorylated and inhibited by Akt and suppresses mTOR signalling. Nat Cell Biol *4*, 648-657.

Inoki, K., Zhu, T., and Guan, K.L. (2003b). TSC2 mediates cellular energy response to control cell growth and survival. Cell *115*, 577-590.

Ishii, T., Funato, Y., and Miki, H. (2013). Thioredoxin-related protein 32 (TRP32) specifically reduces oxidized phosphatase of regenerating liver (PRL). J Biol Chem *288*, 7263-7270.

Jacinto, E. (2008). What controls TOR? IUBMB Life *60*, 483-496.

Jacinto, E., Loewith, R., Schmidt, A., Lin, S., Ruegg, M.A., Hall, A., and Hall, M.N. (2004). Mammalian TOR complex 2 controls the actin cytoskeleton and is rapamycin insensitive. Nat Cell Biol *6*, 1122-1128.

Janus, A., Robak, T., and Smolewski, P. (2005). The mammalian target of the rapamycin (mTOR) kinase pathway: its role in tumourigenesis and targeted antitumour therapy. Cell Mol Biol Lett *10*, 479-498.

Jewell, J.L., Russell, R.C., and Guan, K.-L. (2013). Amino acid signalling upstream of mTOR. Nat Rev Mol Cell Biol *14*, 133-139.

Jian, M., Nan, L., Guocheng, J., Qingfu, Z., Xueshan, Q., and Enhua, W. (2012). Downregulating PRL-3 inhibit migration and invasion of lung cancer cell via RhoA and mDia1. Tumori *98*, 370-376.

Jiang, Y., Liu, X.Q., Rajput, A., Geng, L., Ongchin, M., Zeng, Q., Taylor, G.S., and Wang, J. (2011). Phosphatase PRL-3 is a direct regulatory target of TGFbeta in colon cancer metastasis. Cancer Res *71*, 234-244.

Jing, H., and Lee, S. (2014). NF-kappaB in cellular senescence and cancer treatment. Mol Cells *37*, 189-195.

Jinlian, L., Yingbin, Z., and Chunbo, W. (2007). p38 MAPK in regulating cellular responses to ultraviolet radiation. J Biomed Sci *14*, 303-312.

Johnson, G.L., and Lapadat, R. (2002). Mitogen-activated protein kinase pathways mediated by ERK, JNK, and p38 protein kinases. Science *298*, 1911-1912.

Jung, C.H., Ro, S.H., Cao, J., Otto, N.M., and Kim, D.H. (2010). mTOR regulation of autophagy. FEBS Lett *584*, 1287-1295.

Jung, J.Y., Roh, K.H., Jeong, Y.J., Kim, S.H., Lee, E.J., Kim, M.S., Oh, W.M., Oh, H.K., and Kim, W.J. (2008). Estradiol protects PC12 cells against CoCl2-induced apoptosis. Brain Res Bull *76*, 579-585.

Kaizuka, T., Hara, T., Oshiro, N., Kikkawa, U., Yonezawa, K., Takehana, K., Iemura, S., Natsume, T., and Mizushima, N. (2010). Tti1 and Tel2 are critical factors in mammalian target of rapamycin complex assembly. J Biol Chem *285*, 20109-20116.

Kalluri, R., and Weinberg, R.A. (2009). The basics of epithelial-mesenchymal transition. J Clin Invest *119*, 1420-1428.

Kantidakis, T., Ramsbottom, B.A., Birch, J.L., Dowding, S.N., and White, R.J. (2010). mTOR associates with TFIIIC, is found at tRNA and 5S rRNA genes, and targets their repressor Maf1. Proc Natl Acad Sci U S A *107*, 11823-11828.

Kato, H., Semba, S., Miskad, U.A., Seo, Y., Kasuga, M., and Yokozaki, H. (2004). High expression of PRL-3 promotes cancer cell motility and liver metastasis in human colorectal cancer: a predictive molecular marker of metachronous liver and lung metastases. Clin Cancer Res *10*, 7318-7328.

Kaul, G., Pattan, G., and Rafeequi, T. (2011). Eukaryotic elongation factor-2 (eEF2): its regulation and peptide chain elongation. Cell Biochem Funct *29*, 227-234.

Khapare, N., Kundu, S.T., Sehgal, L., Sawant, M., Priya, R., Gosavi, P., Gupta, N., Alam, H., Karkhanis, M., Naik, N., *et al.* (2012). Plakophilin3 loss leads to an increase in PRL3 levels promoting K8 dephosphorylation, which is required for transformation and metastasis. PLoS One *7*, e38561.

Kim, D.H., Sarbassov, D.D., Ali, S.M., King, J.E., Latek, R.R., Erdjument-Bromage, H., Tempst, P., and Sabatini, D.M. (2002). mTOR interacts with raptor to form a nutrient-sensitive complex that signals to the cell growth machinery. Cell *110*, 163-175.

Kim, D.H., Sarbassov, D.D., Ali, S.M., Latek, R.R., Guntur, K.V., Erdjument-Bromage, H., Tempst, P., and Sabatini, D.M. (2003). GbetaL, a positive regulator of the rapamycin-sensitive pathway required for the nutrient-sensitive interaction between raptor and mTOR. Mol Cell *11*, 895-904.

Kim, E., Goraksha-Hicks, P., Li, L., Neufeld, T.P., and Guan, K.L. (2008). Regulation of TORC1 by Rag GTPases in nutrient response. Nat Cell Biol *10*, 935-945.

Kirkegaard, T., Witton, C.J., McGlynn, L.M., Tovey, S.M., Dunne, B., Lyon, A., and Bartlett, J.M. (2005). AKT activation predicts outcome in breast cancer patients treated with tamoxifen. J Pathol *207*, 139-146.

Kong, W., Swain, G.P., Li, S., and Diamond, R.H. (2000). PRL-1 PTPase expression is developmentally regulated with tissue-specific patterns in epithelial tissues. Am J Physiol Gastrointest Liver Physiol *279*, G613-621.

Kotake-Nara, E., and Saida, K. (2007). Characterization of CoCl2-induced reactive oxygen species (ROS): Inductions of neurite outgrowth and endothelin-2/vasoactive intestinal contractor in PC12 cells by CoCl2 are ROS dependent, but those by MnCl2 are not. Neurosci Lett *422*, 223-227.

Kozlov, G., Cheng, J., Lievre, C., Banville, D., Gehring, K., and Ekiel, I. (2002). 1H, 13C and 15N resonance assignments of the human phosphatase PRL-3. J Biomol NMR *24*, 169-170.

Kozlov, G., Cheng, J., Ziomek, E., Banville, D., Gehring, K., and Ekiel, I. (2004). Structural insights into molecular function of the metastasis-associated phosphatase PRL-3. J Biol Chem *279*, 11882-11889.

Krebs, E.G., and Fischer, E.H. (1955). Phosphorylase activity of skeletal muscle extracts. J Biol Chem *216*, 113-120.

Krndija, D., Munzberg, C., Maass, U., Hafner, M., Adler, G., Kestler, H.A., Seufferlein, T., Oswald, F., and von Wichert, G. (2012). The phosphatase of regenerating liver 3 (PRL-3) promotes cell migration through Arf-activity-dependent stimulation of integrin alpha5 recycling. J Cell Sci *125*, 3883-3892.

Kurschat, P., Wickenhauser, C., Groth, W., Krieg, T., and Mauch, C. (2002). Identification of activated matrix metalloproteinase-2 (MMP-2) as the main gelatinolytic enzyme in malignant melanoma by in situ zymography. J Pathol *197*, 179-187.

Lai, W., Chen, S., Wu, H., Guan, Y., Liu, L., Zeng, Y., Zhao, H., Jiang, J., and Chu, Z. (2011). PRL-3 promotes the proliferation of LoVo cells via the upregulation of KCNN4 channels. Oncol Rep *26*, 909-917.

Lai, W., Liu, L., Zeng, Y., Wu, H., Xu, H., Chen, S., and Chu, Z. (2013). KCNN4 channels participate in the EMT induced by PRL-3 in colorectal cancer. Med Oncol *30*, 566.

Lan, A., Liao, X., Mo, L., Yang, C., Yang, Z., Wang, X., Hu, F., Chen, P., Feng, J., Zheng, D., *et al.* (2011). Hydrogen sulfide protects against chemical hypoxia-induced injury by inhibiting ROS-activated ERK1/2 and p38MAPK signaling pathways in PC12 cells. PLoS One *6*, e25921.

Laplante, M., and Sabatini, D.M. (2012). mTOR signaling in growth control and disease. Cell *149*, 274-293.

Laurent, C., Valet, F., Planque, N., Silveri, L., Maacha, S., Anezo, O., Hupe, P., Plancher, C., Reyes, C., Albaud, B., *et al.* (2011). High PTP4A3 phosphatase expression correlates with metastatic risk in uveal melanoma patients. Cancer Res *71*, 666-674.

Lee, S.K., Han, Y.M., Yun, J., Lee, C.W., Shin, D.S., Ha, Y.R., Kim, J., Koh, J.S., Hong, S.H., Han, D.C., *et al.* (2012). Phosphatase of regenerating liver-3 promotes migration and invasion by upregulating matrix metalloproteinases-7 in human colorectal cancer cells. Int J Cancer *131*, E190-203.

Li, J., Guo, K., Koh, V.W., Tang, J.P., Gan, B.Q., Shi, H., Li, H.X., and Zeng, Q. (2005). Generation of PRL-3- and PRL-1-specific monoclonal antibodies as potential diagnostic markers for cancer metastases. Clin Cancer Res *11*, 2195-2204.

Li, Z., Zhan, W., Wang, Z., Zhu, B., He, Y., Peng, J., Cai, S., and Ma, J. (2006). Inhibition of PRL-3 gene expression in gastric cancer cell line SGC7901 via microRNA suppressed reduces peritoneal metastasis. Biochem Biophys Res Commun *348*, 229-237.

Li, Z.R., Wang, Z., Zhu, B.H., He, Y.L., Peng, J.S., Cai, S.R., Ma, J.P., and Zhan, W.H. (2007). Association of tyrosine PRL-3 phosphatase protein expression with peritoneal metastasis of gastric carcinoma and prognosis. Surg Today *37*, 646-651.

Lian, S., Meng, L., Liu, C., Xing, X., Song, Q., Dong, B., Han, Y., Yang, Y., Peng, L., Qu, L., *et al.* (2013). PRL-3 activates NF-kappaB signaling pathway by interacting with RAP1. Biochem Biophys Res Commun *430*, 196-201.

Lian, Y.X., Chen, R., Xu, Y.H., Peng, C.L., and Hu, H.C. (2012). Effect of protein-tyrosine phosphatase 4A3 by small interfering RNA on the proliferation of lung cancer. Gene *511*, 169-176.

Liang, F., Liang, J., Wang, W.Q., Sun, J.P., Udho, E., and Zhang, Z.Y. (2007). PRL3 promotes cell invasion and proliferation by down-regulation of Csk leading to Src activation. J Biol Chem *282*, 5413-5419.

Liang, F., Luo, Y., Dong, Y., Walls, C.D., Liang, J., Jiang, H.Y., Sanford, J.R., Wek, R.C., and Zhang, Z.Y. (2008). Translational control of C-terminal Src kinase (Csk) expression by PRL3 phosphatase. J Biol Chem *283*, 10339-10346.

Lin, K.R., Lee, S.F., Hung, C.M., Li, C.L., Yang-Yen, H.F., and Yen, J.J. (2007). Survival factor withdrawal-induced apoptosis of TF-1 cells involves a TRB2-Mcl-1 axis-dependent pathway. J Biol Chem *282*, 21962-21972.

Lin, X.X., Yang, X.F., Jiang, J.X., Zhang, S.J., Guan, Y., Liu, Y.N., Sun, Y.H., and Xie, Q.M. (2014). Cigarette smoke extract-induced BEAS-2B cell apoptosis and anti-oxidative Nrf-2 up-regulation are mediated by ROS-stimulated p38 activation. Toxicol Mech Methods *24*, 575-583.

Liu, B., Chen, Y., and St Clair, D.K. (2008a). ROS and p53: a versatile partnership. Free Radic Biol Med *44*, 1529-1535.

Liu, H., Lv, L., and Yang, K. (2015). Chemotherapy targeting cancer stem cells. Am J Cancer Res *5*, 880-893.

Liu, Y., Zheng, P., Liu, Y., Ji, T., Liu, X., Yao, S., Cheng, X., Li, Y., Chen, L., Xiao, Z., *et al.* (2013). An epigenetic role for PRL-3 as a regulator of H3K9 methylation in colorectal cancer. Gut *62*, 571-581.

Liu, Y., Zhou, J., Chen, J., Gao, W., Le, Y., Ding, Y., and Li, J. (2009). PRL-3 promotes epithelial mesenchymal transition by regulating cadherin directly. Cancer Biol Ther *8*, 1352-1359.

Liu, Y.Q., Li, H.X., Lou, X., and Lei, J.Y. (2008b). Expression of phosphatase of regenerating liver 1 and 3 mRNA in esophageal squamous cell carcinoma. Arch Pathol Lab Med *132*, 1307-1312.

Lou, X., Liu, Y., Lei, J.Y., and Li, H. (2012). Overexpression of phosphatase regenerating liver 3 in oesophageal squamous cell carcinoma associated with metastasis and its comparison with phosphatase regenerating liver 1. Cell Biol Int *36*, 759-763.

Lowe, S.W., and Lin, A.W. (2000). Apoptosis in cancer. Carcinogenesis *21*, 485-495.

Ma, L., Chen, Z., Erdjument-Bromage, H., Tempst, P., and Pandolfi, P.P. (2005). Phosphorylation and functional inactivation of TSC2 by Erk implications for tuberous sclerosis and cancer pathogenesis. Cell *121*, 179-193.

Ma, X.M., and Blenis, J. (2009). Molecular mechanisms of mTOR-mediated translational control. Nat Rev Mol Cell Biol *10*, 307-318.

Makkouk, A., and Weiner, G.J. (2015). Cancer immunotherapy and breaking immune tolerance: new approaches to an old challenge. Cancer Res *75*, 5-10.

Matsukawa, Y., Semba, S., Kato, H., Koma, Y., Yanagihara, K., and Yokozaki, H. (2010). Constitutive suppression of PRL-3 inhibits invasion and proliferation of gastric cancer cell in vitro and in vivo. Pathobiology *77*, 155-162.

Matter, W.F., Estridge, T., Zhang, C., Belagaje, R., Stancato, L., Dixon, J., Johnson, B., Bloem, L., Pickard, T., Donaghue, M., *et al.* (2001). Role of PRL-3, a human muscle-specific tyrosine phosphatase, in angiotensin-II signaling. Biochem Biophys Res Commun *283*, 1061-1068.

McParland, V., Varsano, G., Li, X., Thornton, J., Baby, J., Aravind, A., Meyer, C., Pavic, K., Rios, P., and Kohn, M. (2011). The metastasis-promoting phosphatase PRL-3 shows activity toward phosphoinositides. Biochemistry *50*, 7579-7590.

Mendoza, M.C., Er, E.E., and Blenis, J. (2011). The Ras-ERK and PI3K-mTOR pathways: cross-talk and compensation. Trends Biochem Sci *36*, 320-328.

Menon, S., Dibble, C.C., Talbott, G., Hoxhaj, G., Valvezan, A.J., Takahashi, H., Cantley, L.C., and Manning, B.D. (2014). Spatial control of the TSC complex integrates insulin and nutrient regulation of mTORC1 at the lysosome. Cell *156*, 771-785.

Min, G., Lee, S.K., Kim, H.N., Han, Y.M., Lee, R.H., Jeong, D.G., Han, D.C., and Kwon, B.M. (2013). Rhodanine-based PRL-3 inhibitors blocked the migration and invasion of metastatic cancer cells. Bioorg Med Chem Lett *23*, 3769-3774.

Min, S.H., Kim, D.M., Heo, Y.S., Kim, H.M., Kim, I.C., and Yoo, O.J. (2010). Downregulation of p53 by phosphatase of regenerating liver 3 is mediated by MDM2 and PIRH2. Life Sci *86*, 66-72.

Ming, J., Jiang, Y., Jiang, G., and Zheng, H. (2014). Phosphatase of regenerating liver-3 induces angiogenesis by increasing extracellular signal-regulated kinase phosphorylation in endometrial adenocarcinoma. Pathobiology *81*, 1-7.

Ming, J., Liu, N., Gu, Y., Qiu, X., and Wang, E.H. (2009). PRL-3 facilitates angiogenesis and metastasis by increasing ERK phosphorylation and up-regulating the levels and activities of Rho-A/C in lung cancer. Pathology *41*, 118-126.

Miskad, U.A., Semba, S., Kato, H., Matsukawa, Y., Kodama, Y., Mizuuchi, E., Maeda, N., Yanagihara, K., and Yokozaki, H. (2007). High PRL-3 expression in human gastric cancer is a marker of metastasis and grades of malignancies: an in situ hybridization study. Virchows Arch *450*, 303-310.

Miskad, U.A., Semba, S., Kato, H., and Yokozaki, H. (2004). Expression of PRL-3 phosphatase in human gastric carcinomas: close correlation with invasion and metastasis. Pathobiology *71*, 176-184.

Mitra, S.K., and Schlaepfer, D.D. (2006). Integrin-regulated FAK-Src signaling in normal and cancer cells. Curr Opin Cell Biol *18*, 516-523.

Mittal, K., Ebos, J., and Rini, B. (2014). Angiogenesis and the tumor microenvironment: vascular endothelial growth factor and beyond. Semin Oncol *41*, 235-251.

Mizuuchi, E., Semba, S., Kodama, Y., and Yokozaki, H. (2009). Down-modulation of keratin 8 phosphorylation levels by PRL-3 contributes to colorectal carcinoma progression. Int J Cancer *124*, 1802-1810.

Mohn, K.L., Laz, T.M., Hsu, J.C., Melby, A.E., Bravo, R., and Taub, R. (1991). The immediate-early growth response in regenerating liver and insulin-stimulated H-35 cells: comparison with serum-stimulated 3T3 cells and identification of 41 novel immediate-early genes. Mol Cell Biol *11*, 381-390.

Mollevi, D.G., Aytes, A., Berdiel, M., Padulles, L., Martinez-Iniesta, M., Sanjuan, X., Salazar, R., and Villanueva, A. (2009). PRL-3 overexpression in epithelial cells is induced by surrounding stromal fibroblasts. Mol Cancer *8*, 46.

Mollevi, D.G., Aytes, A., Padulles, L., Martinez-Iniesta, M., Baixeras, N., Salazar, R., Ramos, E., Figueras, J., Capella, G., and Villanueva, A. (2008). PRL-3 is essentially overexpressed in primary colorectal tumours and associates with tumour aggressiveness. Br J Cancer *99*, 1718-1725.

Moon, M.K., Han, Y.M., Lee, Y.J., Lee, L.H., Yang, J.H., Kwon, B.M., and Kim, D.K. (2010). Inhibitory activities of anthraquinones from Rubia akane on phosphatase regenerating liver-3. Arch Pharm Res *33*, 1747-1751.

Muda, M., Theodosiou, A., Rodrigues, N., Boschert, U., Camps, M., Gillieron, C., Davies, K., Ashworth, A., and Arkinstall, S. (1996). The dual specificity phosphatases M3/6 and MKP-3 are highly selective for inactivation of distinct mitogen-activated protein kinases. J Biol Chem *271*, 27205-27208.

Nakamoto, T., Sakai, R., Honda, H., Ogawa, S., Ueno, H., Suzuki, T., Aizawa, S., Yazaki, Y., and Hirai, H. (1997). Requirements for localization of p130cas to focal adhesions. Mol Cell Biol *17*, 3884-3897.

Neshat, M.S., Mellinghoff, I.K., Tran, C., Stiles, B., Thomas, G., Petersen, R., Frost, P., Gibbons, J.J., Wu, H., and Sawyers, C.L. (2001). Enhanced sensitivity of PTEN-deficient tumors to inhibition of FRAP/mTOR. Proc Natl Acad Sci U S A *98*, 10314-10319.

Nicholson, D.W., Ali, A., Thornberry, N.A., Vaillancourt, J.P., Ding, C.K., Gallant, M., Gareau, Y., Griffin, P.R., Labelle, M., Lazebnik, Y.A., *et al.* (1995). Identification and inhibition of the ICE/CED-3 protease necessary for mammalian apoptosis. Nature *376*, 37-43.

Nishimura, A., and Linder, M.E. (2013). Identification of a novel prenyl and palmitoyl modification at the CaaX motif of Cdc42 that regulates RhoGDI binding. Mol Cell Biol *33*, 1417-1429.

Noonan, D.M., Benelli, R., and Albini, A. (2007). Angiogenesis and cancer prevention: a vision. Recent Results Cancer Res *174*, 219-224.

Oh, W.J., and Jacinto, E. (2011). mTOR complex 2 signaling and functions. Cell Cycle *10*, 2305-2316.

Ono, K., and Han, J. (2000). The p38 signal transduction pathway: activation and function. Cell Signal *12*, 1-13.

Ooki, A., Yamashita, K., Kikuchi, S., Sakuramoto, S., Katada, N., Waraya, M., Kawamata, H., Nishimiya, H., Nakamura, K., and Watanabe, M. (2011). Therapeutic potential of PRL-3 targeting and clinical significance of PRL-3 genomic amplification in gastric cancer. BMC Cancer *11*, 122.

Ooki, A., Yamashita, K., Kikuchi, S., Sakuramoto, S., Katada, N., and Watanabe, M. (2010). Phosphatase of regenerating liver-3 as a convergent therapeutic target for lymph node metastasis in esophageal squamous cell carcinoma. Int J Cancer *127*, 543-554.

Orsatti, L., Forte, E., Tomei, L., Caterino, M., Pessi, A., and Talamo, F. (2009). 2-D Difference in gel electrophoresis combined with Pro-Q Diamond staining: a successful approach for the identification of kinase/phosphatase targets. Electrophoresis *30*, 2469-2476.

Park, H., Jung, S.K., Jeong, D.G., Ryu, S.E., and Kim, S.J. (2008). Discovery of novel PRL-3 inhibitors based on the structure-based virtual screening. Bioorg Med Chem Lett *18*, 2250-2255.

Park, J.E., Yuen, H.F., Zhou, J.B., Al-Aidaroos, A.Q., Guo, K., Valk, P.J., Zhang, S.D., Chng, W.J., Hong, C.W., Mills, K., *et al.* (2013a). Oncogenic roles of PRL-3 in FLT3-ITD induced acute myeloid leukaemia. EMBO Mol Med *5*, 1351-1366.

Park, J.E., Yuen, H.F., Zhou, J.B., Al-Aidaroos, A.Q., Guo, K., Valk, P.J., Zhang, S.D., Chng, W.J., Hong, C.W., Mills, K., *et al.* (2013b). Oncogenic roles of PRL-3 in FLT3-ITD induced acute myeloid leukaemia. EMBO Mol Med *5*, 1351-1366.

Parker, B.S., Argani, P., Cook, B.P., Liangfeng, H., Chartrand, S.D., Zhang, M., Saha, S., Bardelli, A., Jiang, Y., St Martin, T.B., *et al.* (2004). Alterations in vascular gene expression in invasive breast carcinoma. Cancer Res *64*, 7857-7866.

Parsons, J.T., Horwitz, A.R., and Schwartz, M.A. (2010). Cell adhesion: integrating cytoskeletal dynamics and cellular tension. Nat Rev Mol Cell Biol *11*, 633-643.

Pathak, M.K., Dhawan, D., Lindner, D.J., Borden, E.C., Farver, C., and Yi, T. (2002). Pentamidine is an inhibitor of PRL phosphatases with anticancer activity. Mol Cancer Ther *1*, 1255-1264.

Pearce, L.R., Huang, X., Boudeau, J., Pawlowski, R., Wullschleger, S., Deak, M., Ibrahim, A.F., Gourlay, R., Magnuson, M.A., and Alessi, D.R. (2007). Identification of Protor as a novel Rictor-binding component of mTOR complex-2. Biochem J *405*, 513-522.

Peng, L., Jin, G., Wang, L., Guo, J., Meng, L., and Shou, C. (2006). Identification of integrin alpha1 as an interacting protein of protein tyrosine phosphatase PRL-3. Biochem Biophys Res Commun *342*, 179-183.

Peng, L., Ning, J., Meng, L., and Shou, C. (2004). The association of the expression level of protein tyrosine phosphatase PRL-3 protein with liver metastasis and prognosis of patients with colorectal cancer. J Cancer Res Clin Oncol *130*, 521-526.

Peng, L., Xing, X., Li, W., Qu, L., Meng, L., Lian, S., Jiang, B., Wu, J., and Shou, C. (2009). PRL-3 promotes the motility, invasion, and metastasis of LoVo colon cancer cells through PRL-3-integrin beta1-ERK1/2 and-MMP2 signaling. Mol Cancer *8*, 110.

Peter, A.T., and Dhanasekaran, N. (2003). Apoptosis of granulosa cells: a review on the role of MAPK-signalling modules. Reprod Domest Anim *38*, 209-213.

Peterson, T.R., Laplante, M., Thoreen, C.C., Sancak, Y., Kang, S.A., Kuehl, W.M., Gray, N.S., and Sabatini, D.M. (2009). DEPTOR is an mTOR inhibitor frequently overexpressed in multiple myeloma cells and required for their survival. Cell *137*, 873-886.

Playford, M.P., and Schaller, M.D. (2004). The interplay between Src and integrins in normal and tumor biology. Oncogene *23*, 7928-7946.

Polato, F., Codegoni, A., Fruscio, R., Perego, P., Mangioni, C., Saha, S., Bardelli, A., and Broggini, M. (2005). PRL-3 phosphatase is implicated in ovarian cancer growth. Clin Cancer Res *11*, 6835-6839.

Pratheeshkumar, P., Son, Y.O., Budhraja, A., Wang, X., Ding, S., Wang, L., Hitron, A., Lee, J.C., Kim, D., Divya, S.P., *et al.* (2012). Luteolin inhibits human prostate tumor growth by suppressing vascular endothelial growth factor receptor 2-mediated angiogenesis. PLoS One *7*, e52279.

Proud, C.G. (2002). Regulation of mammalian translation factors by nutrients. Eur J Biochem *269*, 5338-5349.

Qian, F., Li, Y.P., Sheng, X., Zhang, Z.C., Song, R., Dong, W., Cao, S.X., Hua, Z.C., and Xu, Q. (2007). PRL-3 siRNA inhibits the metastasis of B16-BL6 mouse melanoma cells in vitro and in vivo. Mol Med *13*, 151-159.

Qu, S., Liu, B., Guo, X., Shi, H., Zhou, M., Li, L., Yang, S., Tong, X., and Wang, H. (2014). Independent oncogenic and therapeutic significance of phosphatase PRL-3 in FLT3-ITD-negative acute myeloid leukemia. Cancer *120*, 2130-2141.

Radke, I., Gotte, M., Kersting, C., Mattsson, B., Kiesel, L., and Wulfing, P. (2006). Expression and prognostic impact of the protein tyrosine phosphatases PRL-1, PRL-2, and PRL-3 in breast cancer. Br J Cancer *95*, 347-354.

Ren, T., Jiang, B., Xing, X., Dong, B., Peng, L., Meng, L., Xu, H., and Shou, C. (2009). Prognostic significance of phosphatase of regenerating liver-3 expression in ovarian cancer. Pathology oncology research : POR *15*, 555-560.

Reynolds, T.H.t., Bodine, S.C., and Lawrence, J.C., Jr. (2002). Control of Ser2448 phosphorylation in the mammalian target of rapamycin by insulin and skeletal muscle load. J Biol Chem *277*, 17657-17662.

Rios, P., Li, X., and Kohn, M. (2013). Molecular mechanisms of the PRL phosphatases. FEBS J *280*, 505-524.

Rouleau, C., Roy, A., St Martin, T., Dufault, M.R., Boutin, P., Liu, D., Zhang, M., Puorro-Radzwill, K., Rulli, L., Reczek, D., *et al.* (2006). Protein tyrosine phosphatase PRL-3 in malignant cells and endothelial cells: expression and function. Mol Cancer Ther *5*, 219-229.

Roux, P.P., Ballif, B.A., Anjum, R., Gygi, S.P., and Blenis, J. (2004). Tumor-promoting phorbol esters and activated Ras inactivate the tuberous sclerosis tumor suppressor complex via p90 ribosomal S6 kinase. Proc Natl Acad Sci U S A *101*, 13489-13494.

Roux, P.P., and Blenis, J. (2004). ERK and p38 MAPK-activated protein kinases: a family of protein kinases with diverse biological functions. Microbiol Mol Biol Rev *68*, 320-344.

Rovetta, F., Stacchiotti, A., Faggi, F., Catalani, S., Apostoli, P., Fanzani, A., and Aleo, M.F. (2013). Cobalt triggers necrotic cell death and atrophy in skeletal C2C12 myotubes. Toxicol Appl Pharmacol *271*, 196-205.

Sabatini, D.M., Erdjument-Bromage, H., Lui, M., Tempst, P., and Snyder, S.H. (1994). RAFT1: a mammalian protein that binds to FKBP12 in a rapamycin-dependent fashion and is homologous to yeast TORs. Cell *78*, 35-43.

Sabers, C.J., Martin, M.M., Brunn, G.J., Williams, J.M., Dumont, F.J., Wiederrecht, G., and Abraham, R.T. (1995). Isolation of a protein target of the FKBP12-rapamycin complex in mammalian cells. J Biol Chem *270*, 815-822.

Sabio, G., Arthur, J.S., Kuma, Y., Peggie, M., Carr, J., Murray-Tait, V., Centeno, F., Goedert, M., Morrice, N.A., and Cuenda, A. (2005). p38gamma regulates the localisation of SAP97 in the cytoskeleton by modulating its interaction with GKAP. EMBO J *24*, 1134-1145.

Saha, S., Bardelli, A., Buckhaults, P., Velculescu, V.E., Rago, C., St Croix, B., Romans, K.E., Choti, M.A., Lengauer, C., Kinzler, K.W., *et al.* (2001). A phosphatase associated with metastasis of colorectal cancer. Science *294*, 1343-1346.

Sahai, E. (2007). Illuminating the metastatic process. Nat Rev Cancer *7*, 737-749.

Sancak, Y., Bar-Peled, L., Zoncu, R., Markhard, A.L., Nada, S., and Sabatini, D.M. (2010). Ragulator-Rag complex targets mTORC1 to the lysosomal surface and is necessary for its activation by amino acids. Cell *141*, 290-303.

Sancak, Y., Peterson, T.R., Shaul, Y.D., Lindquist, R.A., Thoreen, C.C., Bar-Peled, L., and Sabatini, D.M. (2008). The Rag GTPases bind raptor and mediate amino acid signaling to mTORC1. Science *320*, 1496-1501.

Sancak, Y., Thoreen, C.C., Peterson, T.R., Lindquist, R.A., Kang, S.A., Spooner, E., Carr, S.A., and Sabatini, D.M. (2007). PRAS40 is an insulin-regulated inhibitor of the mTORC1 protein kinase. Mol Cell *25*, 903-915.

Saraste, A., and Pulkki, K. (2000). Morphologic and biochemical hallmarks of apoptosis. Cardiovasc Res *45*, 528-537.

Sarbassov, D.D., Ali, S.M., Kim, D.H., Guertin, D.A., Latek, R.R., Erdjument-Bromage, H., Tempst, P., and Sabatini, D.M. (2004). Rictor, a novel binding partner of mTOR, defines a rapamycin-insensitive and raptor-independent pathway that regulates the cytoskeleton. Curr Biol *14*, 1296-1302.

Sarbassov, D.D., Ali, S.M., and Sabatini, D.M. (2005a). Growing roles for the mTOR pathway. Curr Opin Cell Biol *17*, 596-603.

Sarbassov, D.D., Ali, S.M., Sengupta, S., Sheen, J.H., Hsu, P.P., Bagley, A.F., Markhard, A.L., and Sabatini, D.M. (2006). Prolonged rapamycin treatment inhibits mTORC2 assembly and Akt/PKB. Mol Cell *22*, 159-168.

Sarbassov, D.D., Guertin, D.A., Ali, S.M., and Sabatini, D.M. (2005b). Phosphorylation and regulation of Akt/PKB by the rictor-mTOR complex. Science *307*, 1098-1101.

Scanlon, E.F., and Murthy, S. (1991). The process of metastasis. CA Cancer J Clin *41*, 301-305.

Sekulic, A., Hudson, C.C., Homme, J.L., Yin, P., Otterness, D.M., Karnitz, L.M., and Abraham, R.T. (2000). A direct linkage between the phosphoinositide 3-kinase-AKT signaling pathway and the mammalian target of rapamycin in mitogen-stimulated and transformed cells. Cancer Res *60*, 3504-3513.

Semba, S., Mizuuchi, E., and Yokozaki, H. (2010). Requirement of phosphatase of regenerating liver-3 for the nucleolar localization of nucleolin during the progression of colorectal carcinoma. Cancer Sci *101*, 2254-2261.

Sharma, S.V., and Settleman, J. (2007). Oncogene addiction: setting the stage for molecularly targeted cancer therapy. Genes Dev *21*, 3214-3231.

Shaw, R.J. (2009). LKB1 and AMP-activated protein kinase control of mTOR signalling and growth. Acta Physiol (Oxf) *196*, 65-80.

Shi, Y. (2009). Serine/threonine phosphatases: mechanism through structure. Cell *139*, 468-484.

Simon, H.U., Haj-Yehia, A., and Levi-Schaffer, F. (2000). Role of reactive oxygen species (ROS) in apoptosis induction. Apoptosis *5*, 415-418.

Steelman, L.S., Chappell, W.H., Abrams, S.L., Kempf, R.C., Long, J., Laidler, P., Mijatovic, S., Maksimovic-Ivanic, D., Stivala, F., Mazzarino, M.C., *et al.* (2011). Roles of the Raf/MEK/ERK and PI3K/PTEN/Akt/mTOR pathways in controlling growth and sensitivity to therapy-implications for cancer and aging. Aging (Albany NY) *3*, 192-222.

Sui, X., Kong, N., Ye, L., Han, W., Zhou, J., Zhang, Q., He, C., and Pan, H. (2014). p38 and JNK MAPK pathways control the balance of apoptosis and autophagy in response to chemotherapeutic agents. Cancer Lett *344*, 174-179.

Sun, J.P., Luo, Y., Yu, X., Wang, W.Q., Zhou, B., Liang, F., and Zhang, Z.Y. (2007). Phosphatase activity, trimerization, and the C-terminal polybasic region are all required for PRL1-mediated cell growth and migration. J Biol Chem *282*, 29043-29051.

Sun, Z.H., and Bu, P. (2012). Downregulation of phosphatase of regenerating liver-3 is involved in the inhibition of proliferation and apoptosis induced by emodin in the SGC-7901 human gastric carcinoma cell line. Exp Ther Med *3*, 1077-1081.

Sundaram, M.V. (2006). RTK/Ras/MAPK signaling. WormBook, 1-19.

Tabernero, L., Aricescu, A.R., Jones, E.Y., and Szedlacsek, S.E. (2008). Protein tyrosine phosphatases: structure-function relationships. FEBS J *275*, 867-882.

Tajrishi, M.M., Tuteja, R., and Tuteja, N. (2011). Nucleolin: The most abundant multifunctional phosphoprotein of nucleolus. Commun Integr Biol *4*, 267-275.

Tamura, K., Sudo, T., Senftleben, U., Dadak, A.M., Johnson, R., and Karin, M. (2000). Requirement for p38alpha in erythropoietin expression: a role for stress kinases in erythropoiesis. Cell *102*, 221-231.

Tanoue, T., Yamamoto, T., Maeda, R., and Nishida, E. (2001). A Novel MAPK phosphatase MKP-7 acts preferentially on JNK/SAPK and p38 alpha and beta MAPKs. J Biol Chem *276*, 26629-26639.

Tee, A.R., Manning, B.D., Roux, P.P., Cantley, L.C., and Blenis, J. (2003). Tuberous sclerosis complex gene products, Tuberin and Hamartin, control mTOR signaling by acting as a GTPase-activating protein complex toward Rheb. Curr Biol *13*, 1259-1268.

Thedieck, K., Polak, P., Kim, M.L., Molle, K.D., Cohen, A., Jeno, P., Arrieumerlou, C., and Hall, M.N. (2007). PRAS40 and PRR5-like protein are new mTOR interactors that regulate apoptosis. PLoS One *2*, e1217.

Theodosiou, A., and Ashworth, A. (2002). MAP kinase phosphatases. Genome Biol *3*, REVIEWS3009.

Theodosiou, A., Smith, A., Gillieron, C., Arkinstall, S., and Ashworth, A. (1999). MKP5, a new member of the MAP kinase phosphatase family, which selectively dephosphorylates stress-activated kinases. Oncogene *18*, 6981-6988.

Tian, W., Qu, L., Meng, L., Liu, C., Wu, J., and Shou, C. (2012). Phosphatase of regenerating liver-3 directly interacts with integrin beta1 and regulates its phosphorylation at tyrosine 783. BMC Biochem *13*, 22.

Tonks, N.K., Diltz, C.D., and Fischer, E.H. (1988). Purification of the major protein-tyrosine-phosphatases of human placenta. J Biol Chem *263*, 6722-6730.

Towler, M.C., and Hardie, D.G. (2007). AMP-activated protein kinase in metabolic control and insulin signaling. Circ Res *100*, 328-341.

Ubersax, J.A., and Ferrell, J.E., Jr. (2007). Mechanisms of specificity in protein phosphorylation. Nat Rev Mol Cell Biol *8*, 530-541.

Ustaalioglu, B.B., Bilici, A., Barisik, N.O., Aliustaoglu, M., Vardar, F.A., Yilmaz, B.E., Seker, M., and Gumus, M. (2012). Clinical importance of phosphatase of regenerating liver-3 expression in breast cancer. Clinical & translational oncology : official publication of the Federation of Spanish Oncology Societies and of the National Cancer Institute of Mexico *14*, 911-922.

van Kempen, L.C., and Coussens, L.M. (2002). MMP9 potentiates pulmonary metastasis formation. Cancer Cell *2*, 251-252.

van Zijl, F., Krupitza, G., and Mikulits, W. (2011). Initial steps of metastasis: cell invasion and endothelial transmigration. Mutat Res *728*, 23-34.

Vanhaesebroeck, B., and Alessi, D.R. (2000). The PI3K-PDK1 connection: more than just a road to PKB. Biochem J *346 Pt 3*, 561-576.

Volpert, O.V., Fong, T., Koch, A.E., Peterson, J.D., Waltenbaugh, C., Tepper, R.I., and Bouck, N.P. (1998). Inhibition of angiogenesis by interleukin 4. J Exp Med *188*, 1039-1046.

Walls, C.D., Iliuk, A., Bai, Y., Wang, M., Tao, W.A., and Zhang, Z.Y. (2013). Phosphatase of regenerating liver 3 (PRL3) provokes a tyrosine phosphoproteome to drive prometastatic signal transduction. Mol Cell Proteomics *12*, 3759-3777.

Wang, H., Quah, S.Y., Dong, J.M., Manser, E., Tang, J.P., and Zeng, Q. (2007a). PRL-3 down-regulates PTEN expression and signals through PI3K to promote epithelial-mesenchymal transition. Cancer Res *67*, 2922-2926.

Wang, H., Vardy, L.A., Tan, C.P., Loo, J.M., Guo, K., Li, J., Lim, S.G., Zhou, J., Chng, W.J., Ng, S.B., *et al.* (2010). PCBP1 suppresses the translation of metastasis-associated PRL-3 phosphatase. Cancer Cell *18*, 52-62.

Wang, J., Kirby, C.E., and Herbst, R. (2002). The tyrosine phosphatase PRL-1 localizes to the endoplasmic reticulum and the mitotic spindle and is required for normal mitosis. J Biol Chem *277*, 46659-46668.

Wang, L., Harris, T.E., Roth, R.A., and Lawrence, J.C., Jr. (2007b). PRAS40 regulates mTORC1 kinase activity by functioning as a direct inhibitor of substrate binding. J Biol Chem *282*, 20036-20044.

Wang, L., Peng, L., Dong, B., Kong, L., Meng, L., Yan, L., Xie, Y., and Shou, C. (2006). Overexpression of phosphatase of regenerating liver-3 in breast cancer: association with a poor clinical outcome. Ann Oncol *17*, 1517-1522.

Wang, L., Shen, Y., Song, R., Sun, Y., Xu, J., and Xu, Q. (2009). An anticancer effect of curcumin mediated by down-regulating phosphatase of regenerating liver-3 expression on highly metastatic melanoma cells. Mol Pharmacol *76*, 1238-1245.

Wang, Y., Li, Z.F., He, J., Li, Y.L., Zhu, G.B., Zhang, L.H., and Li, Y.L. (2007c). Expression of the human phosphatases of regenerating liver (PRLs) in colonic adenocarcinoma and its correlation with lymph node metastasis. Int J Colorectal Dis *22*, 1179-1184.

Wang, Z., He, Y.L., Cai, S.R., Zhan, W.H., Li, Z.R., Zhu, B.H., Chen, C.Q., Ma, J.P., Chen, Z.X., Li, W., *et al.* (2008). Expression and prognostic impact of PRL-3 in lymph node metastasis of gastric cancer: its molecular mechanism was investigated using artificial microRNA interference. Int J Cancer *123*, 1439-1447.

Wani, W.Y., Boyer-Guittaut, M., Dodson, M., Chatham, J., Darley-Usmar, V., and Zhang, J. (2015). Regulation of autophagy by protein post-translational modification. Lab Invest *95*, 14-25.

Weinstein, I.B., and Joe, A. (2008). Oncogene addiction. Cancer Res *68*, 3077-3080; discussion 3080.

Wu, X., Zeng, H., Zhang, X., Zhao, Y., Sha, H., Ge, X., Zhang, M., Gao, X., and Xu, Q. (2004). Phosphatase of regenerating liver-3 promotes motility and metastasis of mouse melanoma cells. Am J Pathol *164*, 2039-2054.

Xing, X., Lian, S., Hu, Y., Li, Z., Zhang, L., Wen, X., Du, H., Jia, Y., Zheng, Z., Meng, L., *et al.* (2013). Phosphatase of regenerating liver-3 (PRL-3) is associated with metastasis and poor prognosis in gastric carcinoma. Journal of translational medicine *11*, 309.

Xu, J., Cao, S., Wang, L., Xu, R., Chen, G., and Xu, Q. (2011). VEGF promotes the transcription of the human PRL-3 gene in HUVEC through transcription factor MEF2C. PLoS One *6*, e27165.

Xu, Y., Zhu, M., Zhang, S., Liu, H., Li, T., and Qin, C. (2010). Expression and prognostic value of PRL-3 in human intrahepatic cholangiocarcinoma. Pathol Oncol Res *16*, 169-175.

Yip, C.K., Murata, K., Walz, T., Sabatini, D.M., and Kang, S.A. (2010). Structure of the human mTOR complex I and its implications for rapamycin inhibition. Mol Cell *38*, 768-774.

Yu, H., Lee, H., Herrmann, A., Buettner, R., and Jove, R. (2014). Revisiting STAT3 signalling in cancer: new and unexpected biological functions. Nat Rev Cancer *14*, 736-746.

Zarubin, T., and Han, J. (2005). Activation and signaling of the p38 MAP kinase pathway. Cell Res *15*, 11-18.

Zeng, Q., Dong, J.M., Guo, K., Li, J., Tan, H.X., Koh, V., Pallen, C.J., Manser, E., and Hong, W. (2003). PRL-3 and PRL-1 promote cell migration, invasion, and metastasis. Cancer Res *63*, 2716-2722.

Zeng, Q., Hong, W., and Tan, Y.H. (1998). Mouse PRL-2 and PRL-3, two potentially prenylated protein tyrosine phosphatases homologous to PRL-1. Biochem Biophys Res Commun *244*, 421-427.

Zeng, Q., Si, X., Horstmann, H., Xu, Y., Hong, W., and Pallen, C.J. (2000). Prenylation-dependent association of protein-tyrosine phosphatases PRL-1, -2, and -3 with the plasma membrane and the early endosome. J Biol Chem *275*, 21444-21452.

Zhang, D., Bar-Eli, M., Meloche, S., and Brodt, P. (2004). Dual regulation of MMP-2 expression by the type 1 insulin-like growth factor receptor: the phosphatidylinositol 3-kinase/Akt and Raf/ERK pathways transmit opposing signals. J Biol Chem *279*, 19683-19690.

Zhang, F., Lazorchak, A.S., Liu, D., Chen, F., and Su, B. (2012a). Inhibition of the mTORC2 and chaperone pathways to treat leukemia. Blood *119*, 6080-6088.

Zhang, J., Xiao, Z., Lai, D., Sun, J., He, C., Chu, Z., Ye, H., Chen, S., and Wang, J. (2012b). miR-21, miR-17 and miR-19a induced by phosphatase of regenerating liver-3 promote the proliferation and metastasis of colon cancer. Br J Cancer *107*, 352-359.

Zhang, J., Yu, X.H., Yan, Y.G., Wang, C., and Wang, W.J. (2015). PI3K/Akt signaling in osteosarcoma. Clin Chim Acta *444*, 182-192.

Zhang, X.Y., and Bishop, A.C. (2008). Engineered inhibitor sensitivity in the WPD loop of a protein tyrosine phosphatase. Biochemistry *47*, 4491-4500.

Zhang, Z.Y. (2003). Chemical and mechanistic approaches to the study of protein tyrosine phosphatases. Acc Chem Res *36*, 385-392.

Zhang, Z.Y. (2005). Functional studies of protein tyrosine phosphatases with chemical approaches. Biochim Biophys Acta *1754*, 100-107.

Zhao, W.B., Li, Y., Liu, X., Zhang, L.Y., and Wang, X. (2008). Evaluation of PRL-3 expression, and its correlation with angiogenesis and invasion in hepatocellular carcinoma. Int J Mol Med *22*, 187-192.

Zheng, P., Liu, Y.X., Chen, L., Liu, X.H., Xiao, Z.Q., Zhao, L., Li, G.Q., Zhou, J., Ding, Y.Q., and Li, J.M. (2010). Stathmin, a new target of PRL-3 identified by proteomic methods, plays a key role in progression and metastasis of colorectal cancer. J Proteome Res *9*, 4897-4905.

Zheng, P., Meng, H.M., Gao, W.Z., Chen, L., Liu, X.H., Xiao, Z.Q., Liu, Y.X., Sui, H.M., Zhou, J., Liu, Y.H., *et al.* (2011). Snail as a key regulator of PRL-3 gene in colorectal cancer. Cancer Biol Ther *12*, 742-749.

Zhou, H., and Huang, S. (2010). mTOR signaling in cancer cell motility and tumor metastasis. Crit Rev Eukaryot Gene Expr *20*, 1-16.

Zhou, J., Bi, C., Chng, W.J., Cheong, L.L., Liu, S.C., Mahara, S., Tay, K.G., Zeng, Q., Li, J., Guo, K., *et al.* (2011). PRL-3, a metastasis associated tyrosine phosphatase, is involved in FLT3-ITD signaling and implicated in anti-AML therapy. PLoS One *6*, e19798.

Zhou, J., Cheong, L.L., Liu, S.C., Chong, P.S., Mahara, S., Bi, C., Ong, K.O., Zeng, Q., and Chng, W.J. (2012a). The pro-metastasis tyrosine phosphatase, PRL-3 (PTP4A3), is a novel mediator of oncogenic function of BCR-ABL in human chronic myeloid leukemia. Mol Cancer *11*, 72.

Zhou, J., Wang, S., Lu, J., Li, J., and Ding, Y. (2009). Over-expression of phosphatase of regenerating liver-3 correlates with tumor progression and poor prognosis in nasopharyngeal carcinoma. Int J Cancer *124*, 1879-1886.

Zhou, Z., Han, V., and Han, J. (2012b). New components of the necroptotic pathway. Protein Cell *3*, 811-817.

Zimmerman, M.W., Homanics, G.E., and Lazo, J.S. (2013). Targeted deletion of the metastasis-associated phosphatase Ptp4a3 (PRL-3) suppresses murine colon cancer. PLoS One *8*, e58300.

Zimmerman, M.W., McQueeney, K.E., Isenberg, J.S., Pitt, B.R., Wasserloos, K.A., Homanics, G.E., and Lazo, J.S. (2014). Protein-tyrosine phosphatase 4A3 (PTP4A3) promotes vascular endothelial growth factor signaling and enables endothelial cell motility. J Biol Chem *289*, 5904-5913.

Zoncu, R., Efeyan, A., and Sabatini, D.M. (2011). mTOR: from growth signal integration to cancer, diabetes and ageing. Nat Rev Mol Cell Biol *12*, 21-35.

Zou, W., Zeng, J., Zhuo, M., Xu, W., Sun, L., Wang, J., and Liu, X. (2002). Involvement of caspase-3 and p38 mitogen-activated protein kinase in cobalt chloride-induced apoptosis in PC12 cells. J Neurosci Res *67*, 837-843.